ENDOTHELIN-1-INDUCED CALCIUM SIGNALING IN ARTERIES AND VEINS

By

Nathan R. Tykocki

A DISSERTATION

Submitted to
Michigan State University
in partial fulfillment of the requirements
for the degree of

DOCTOR OF PHILOSOPHY

Pharmacology and Toxicology

2012

ABSTRACT

ENDOTHELIN-1-INDUCED CALCIUM SIGNALING IN ARTERIES AND VEINS

By

Nathan R. Tykocki

Due to the high volume of blood contained in the venous circulation, a small increase in venous contraction can have a profound impact on systemic blood distribution and blood pressure. The endogenous vasoconstrictor peptide Endothelin-1 (ET-1) has been identified as a regulator of venous tone, since veins desensitize less than arteries to ET-1 and maintain contractility to ET-1 in hypertension. However, relatively little is known about the mechanisms regulating venous contraction. This project was designed to explore how increases in intracellular Ca^{2+} relate to venous contractility, and test the hypothesis that Ca^{2+} signaling induced by ET-1 differs between veins and arteries.

Although contraction to ET-1 in rat aorta (RA) and rat vena cava (RVC) requires Ca^{2+}, inhibition of voltage-gated calcium channels or nonselective cation channels did not significantly inhibit ET-1-induced contraction in either tissue. However, inhibition of the reverse-mode Na^{+}/Ca^{2+} exchanger (NCX) by KB-R7943 (10 μM) significantly attenuated ET-1-induced contraction in RVC but not RA, suggesting that calcium influx by reverse-mode NCX is an important mechanism of Ca^{2+} influx during ET-1-induced contraction of RVC (chapter 3).

We next investigated the mechanisms of intracellular Ca^{2+} stores release activated by ET-1 by examining the presence and function of ryanodine receptors (RyR) (chapter 4)

and IP_3 receptors (IP_3R) (chapter 5) in RA and RVC. RA expressed mRNA for all 3 RyR subtypes, and the RyR activator caffeine (20 mM) caused a prolonged increase in intracellular Ca^{2+} associated with a rapid contraction. While RVC also expressed RyR mRNA, caffeine caused a small, transient increase in intracellular Ca^{2+} that was not associated with contraction. These data suggest that RyR, while present in both RA and RVC, are unable to release sufficient Ca^{2+} to cause contraction in RVC.

RA and RVC express protein for all 3 IP_3R subtypes, and the membrane-permeable IP_3 analogue, Bt-IP_3, caused contraction in both tissues. To measure ET-1-induced IP_3R activation, Ca^{2+} wave characteristics were measured in RVC during exposure to ET-1 (100 nM). ET-1 increased Ca^{2+} wave frequency, occurrence and velocity in RVC, suggesting IP_3-mediated Ca^{2+} release. However, ET-1-induced contraction was unchanged by the IP_3R inhibitor 2-APB (100 μM), suggesting IP_3-mediated Ca^{2+} release was not a significant source of Ca^{2+} during RVC contraction. To test if phospholipase-C (PLC) was activated by ET-1, isometric contraction was measured in RA and RVC rings exposed to vehicle, the PLC inhibitor U-73122 or its inactive analog U-73343 (1 μM). While U-73343 did not significantly inhibit contraction to ET-1, U-73122 significantly reduced maximum contraction to ET-1 in both tissues. These findings suggest that ET-1 activates PLC in RA and RVC, but DAG – and not IP_3 – may regulate contraction to ET-1 in RVC.

Taken together, these findings suggest that mechanisms of both extracellular Ca^{2+} influx and intracellular Ca^{2+} release are different in RVC than in RA, and that this may account for the differences in ET-1-induced contraction between RA and RVC.

ACKNOWLEDGEMENTS

I would first like to acknowledge my parents, David and Carol Tykocki, for their unwavering support of me during my entire education, both before and after college. It is because of your love and commitment that I have been able to succeed, even when faced with adversity I did not think I could overcome alone. Thank you for expecting the best from me, and for helping me realize my true potential.

Secondly, I would like to acknowledge my mentors. When many others had given me the cold shoulder while applying for graduate school, Dr. Stephanie Watts believed in me and helped me believe I could be a scientist. Her enthusiasm and determination are infectious, and have kept me going through many failures and setbacks. Thank you so much for taking a chance on me all those years ago. Dr. Bill Jackson has helped me gain the self-confidence I have needed to become a better scientist. His trust in my abilities has truly helped me find my niche in science, and I am forever grateful. Thank you also to my committee members, Dr. Jim Galligan, Dr. Greg Fink and Dr. Bob Wiseman, for challenging me to push past my comfort zone as a scientist.

Lastly, I want to thank my wife, Abigail, for so many things I could not list them all here. I could not be here without your support, your patience, your love, and your understanding. I know it's not always been easy, but you have helped me stay grounded and maintain perspective through some very difficult decisions. You are an amazing woman, and I am proud to be your husband.

TABLE OF CONTENTS

LIST OF TABLES

LIST OF FIGURES

LIST OF ABBREVIATIONS

(+/+)	Homozygous littermate to (sl/sl) rat
2-APB	2-aminoethoxydiphenyl borate
AA	Arachidonic acid
AT	Angiotensin
AT_1	Angiotensin II receptor type 1
BK channel	Large-conductance calcium-activated potassium channel
Bt-IP_3	2,3,6-tri-O-butyryl-myo-inositol-1,4,5-trisphosphate-hexakis (acetoxymethyl) ester
CA	Carotid artery
CaM	Calmodulin
Ca^{2+}/CaM/CaMK	Calcium/calmodulin/calmodulin kinase
cGMP	Cyclic guanosine monophosphate
CICR	Calcium-induced calcium release
DAG	Diacylglycerol
DGK	Diacylglycerol kinase
DGL	Diacylglycerol lipase
DβH	Dopamine β-hydroxylase
eNOS	Endothelial nitric oxide synthase
ET-1	Endothelin-1
GPCR	G protein-coupled receptor
IP_3	Inositol 1,4,5-trisphosphate
JV	Jugular vein

KB-R7943	2-(2-(4-(4-nitrobenzyloxy)phenyl)ethyl)-isothiourea methanesulfonate
LNNA	N-(ω)-nitro-L-arginine
LGCC	Ligand-gated calcium channel
MAPK	Mitogen-activated protein kinase
MLC	Myosin light chain
MLCK	Myosin light chain kinase
MLCP	Myosin light chain phosphatase
NCX	Na^+/Ca^{2+} exchanger
NKA	Na^+/K^+ ATPase
NE	Norepinephrine
NO	Nitric oxide
NSCC	Nonselective cation channel
OAG	1-oleoyl-2-acetyl-*sn*-glycerol
PA	Phosphatidic acid
PE	Phenylephrine
PGF-2α	Prostaglandin F-2α
PIP_2	Phosphatidylinositol 4,5-bisphosphate
PKA	Protein kinase A
PKC	Protein kinase C
PKG	Protein kinase G
PLC	Phospholipase C
ppET-1	Preproendothelin-1

RA	Rat thoracic aorta
ROS	Reactive oxygen species
RVC	Rat vena cava
RyR	Ryanodine receptor
S6c	Sarafotoxin 6c
SD	Sprague-Dawley
SER	Sarcoplasmic/endoplasmic reticulum
(sl/sl)	Homozygous spotting lethal ET_B receptor-deficient rat
SMA	Superior mesenteric artery
SMV	Superior mesenteric vein
SOCC	Store-operated calcium channel
SOCE	Store-operated calcium entry
SR	Sarcoplasmic reticulum
TEA	Tetraethylammonium
TRP	Transient receptor potential cation channel
VGCC	Voltage-gated calcium channel
VICC	Voltage-independent calcium channel
VSM	Vascular smooth muscle

CHAPTER 1: INTRODUCTION

Due to the high volume of blood contained in the venous circulation, a small increase in venous contraction can have a profound impact on systemic blood distribution and ultimately blood pressure regulation [1]. While changes in the venous circulation seem to be an essential part of the pathophysiology of hypertension, little is currently known about the mechanisms regulating venous contraction. Recent evidence identifies the endogenous vasoconstrictor peptide endothelin-1 (ET-1) as a possible regulator of venous tone. Specifically, veins desensitize less than arteries to ET-1 and maintain contractility to ET-1 in hypertension [2,3]. These findings also suggest that ET-1-induced venous and arterial contraction is regulated by distinct and different mechanisms.

Even with the breadth of research into Ca^{2+} signaling in smooth muscle, the mechanisms responsible for Ca^{2+} mobilization by ET-1 (particularly in terms of ET-1-induced venous contraction) remain unclear. While changes in venous capacitance are linked to increased blood pressure, relatively little is known about the mechanisms that govern contraction in venous smooth muscle as compared to arterial smooth muscle. Since ET receptors are linked to multiple hypertensive research models and human vascular pathologies, understanding the mechanisms that regulate venous contractility may help clarify the role of the veins in hypertension and other vascular diseases where venous dysfunction is evident.

The goal of this project was to elucidate the differences between ET-1-mediated Ca^{2+}

signaling in veins and arteries by investigating how ET-1 regulates changes in cytosolic Ca^{2+} in venous smooth muscle, and what effects these changes in Ca^{2+} have on venous contractility. More specifically, this research explores the mechanisms by which ET-1 causes extracellular Ca^{2+} influx and sarcoplasmic Ca^{2+} stores release in veins, and compares them to ET-1-mediated Ca^{2+} signaling in arteries.

1. The Endothelin System

1.1 Endothelin and Endothelin Receptors

Of the three, 21-amino acid endothelin isoforms (ET-1, ET-2, and ET-3), ET-1 is the predominant isoform in the human vasculature [4]. ET-1 also affects a host of tissues outside of the cardiovascular system, including brain, kidney, intestine and adrenal gland [5]. As shown in **Figure 1**, the biosynthesis of ET-1 begins with the transcription of a 203-amino acid preproendothelin-1 (ppET-1) peptide. Furin, a dibasic-pair-specific endopeptidase, cleaves ppET-1 into the 39-amino acid peptide precursor of ET-1, Big-ET-1 [6]. Big-ET-1 is then further cleaved by the membrane-bound metallopeptidase Endothelin Converting Enzyme-1 (ECE-1) to form ET-1 [7]. ET-1 is not stored, but produced and released *de novo*, and its synthesis is a tightly regulated process. Stimuli such as wall stretch, ischemia, and angiotensin II can increase endothelial ET-1 synthesis [8-10].

Two G protein-coupled receptors (GPCR's), the ET_A and ET_B receptor, are activated by ET-1. While other splice variants of ET receptors have been characterized, only the

ET_A and ET_B receptor have been cloned and recognized by the International Union of Pharmacology Committee on Receptor Nomenclature and Drug Classification (NC-IUPHAR). Both subtypes are heptahelical receptors belonging to the G-protein coupled rhodopsin-type receptor superfamily, and have 59% sequence homology between them [11]. ET_A receptors can be distinguished from ET_B receptors pharmacologically, based on their relative affinities for each of the three endothelin isopeptides. ET_A is modestly selective for ET-1 (ET-1 ≈ ET-2 >> ET-3), while ET_B is non-selective (ET-1 = ET-2 = ET-3) [11]. Depending on the cell type in which they are expressed, ET receptors can couple to several different types of G protein, including $G\alpha_s$, $G\alpha_i$, $G\alpha_q$ and $G\alpha_{12/13}$ [12,13]. Thus, the array of physiological responses and signaling mechanisms activated by ET-1 can vary between cell types, and depends on ET receptor subtype expression as well as G protein coupling.

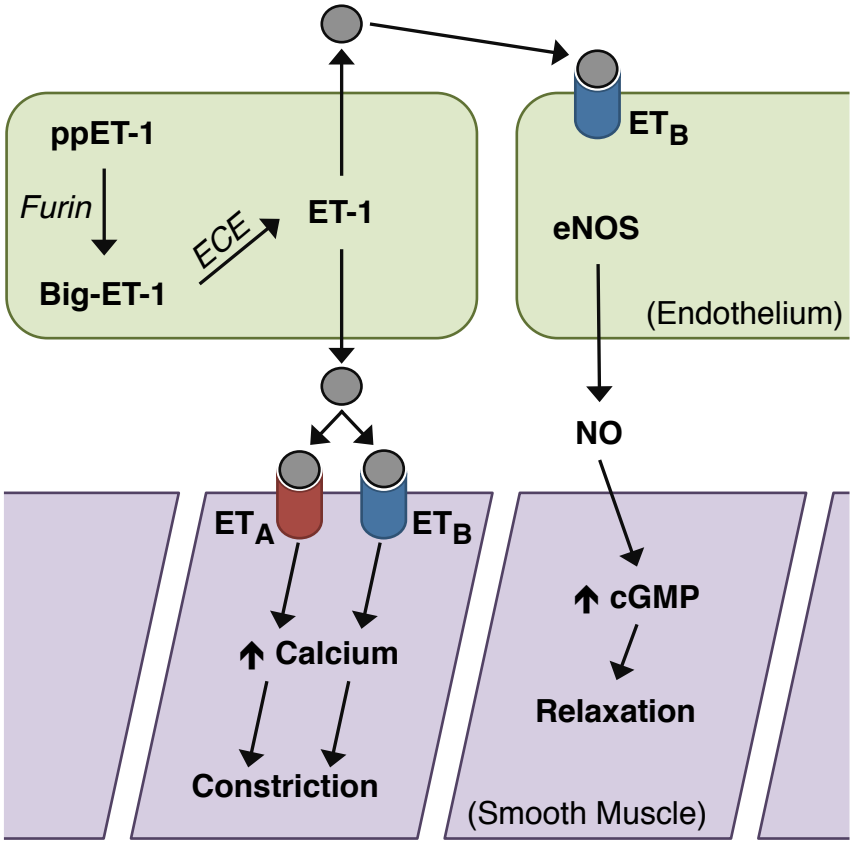

Figure 1. The synthesis of Endothelin-1 in the vasculature. After transcription, prepro-Endothelin-1 (ppET-1) is cleaved by the endopeptidase Furin to form Big-ET-1. Big-ET-1 is then cleaved by endothelin-converting-enzyme (ECE) to form the 21-amino acid peptide ET-1. Once released, ET-1 binds to ET receptors on smooth muscle cells to cause vasoconstriction, but can also bind to endothelial cell ET receptors to cause vasodilation. Adapted from Kawanabe *et al* 2010 [7]. **For interpretation of the references to color in this and all other figures, the reader is referred to the electronic version of this dissertation.**

1.2. Functions of Endothelin-1

Physiological responses to ET-1 can be attributed to ET_A receptors, ET_B receptors, or both. ET-1 is not solely a vasoconstrictor; it stimulates angiogenesis, induces astrocyte proliferation, activates nociceptive neurons, constricts bronchi, and stimulates the production of several inflammatory mediators in neutrophils and macrophages [11,14-16]. Dysfunction or dysregulation in the endothelin (ET) system is present in chronic pain, acute renal failure, asthma, colorectal cancer, and stroke, but dysfunction is most apparent in vascular diseases like hypertension [17-20]. Plasma ET-1 levels are elevated in humans with salt-sensitive essential hypertension, and vascular ET-1 expression is increased in severe hypertension [21]. In types of human hypertension where plasma ET-1 remains steady, vascular tissues from hypertensive humans exhibit exaggerated reactivity to ET-1 [22]. In the DOCA-salt model of hypertension, vascular contraction to ET-1 is decreased even though plasma ET-1 concentrations are increased [23]. This implies that the tissue responses to ET-1 are altered due to dysfunctional ET receptor signaling and not concentration-dependent activation of ET-1-mediated pathways [24].

As the number of biological responses affected by ET-1 grows, one tenet remains unchanged: many, if not most, of the responses to ET-1 are Ca^{2+}-dependent. Whether ET receptors increase intracellular Ca^{2+} by activating extracellular Ca^{2+} influx or intracellular Ca^{2+} release depends on the tissue, ET receptor subtype expression and the response being measured [25-27]. As summarized in **Figure 2**, these increases in intracellular Ca^{2+} can be due to voltage-dependent Ca^{2+} influx, voltage-independent

Ca^{2+} influx (*e.g.* store-operated Ca^{2+} entry and nonselective cation channel activation), release of one of several intracellular Ca^{2+} stores, or any combination thereof [28-30]. These Ca^{2+} increases are transient in some cells. In others, ET-1 causes a slow and prolonged increase in intracellular Ca^{2+}. Subtle changes to these Ca^{2+} signals can cause major alterations in cellular function and ultimately lead to the pathogenesis of disease. As such, the complex mechanisms by which ET-1 can modulate intracellular Ca^{2+} to alter cellular function remain a novel and intriguing area of investigation.

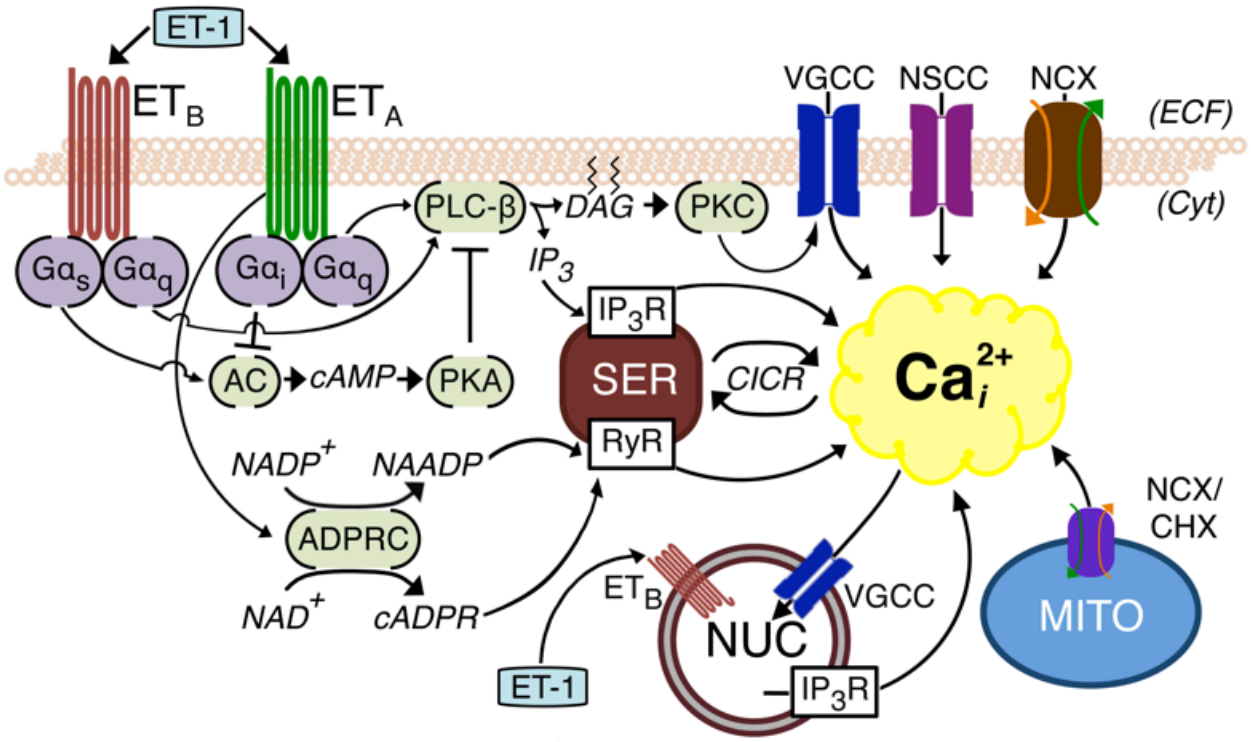

Figure 2. Mechanisms linked to ET re ceptor-dependent increases in $[Ca^{2+}]_i$. This cartoon illustrates mechanisms that are linked to ET receptor-dependent increases in $[Ca^{2+}]_i$. Arrows represent activation; teed lines represent inhibition. From Tykocki and Watts (2010) [31]. Abbreviations: AC, adenylate cyclase; ADPRC, ADP-ribosyl cyclase; cADPR, cyclic ADP ribose; cAMP, cyclic adenosine monophosphate; CHX, Ca^{2+}/H^+ antiporter; CICR, Ca^{2+}-induced Ca^{2+} release; Cyt, cytosol; DAG, diacylglycerol; ECF, extracellular fluid; ET-1, endothelin-1; IP_3, inositol triphosphate; IP_3R, inositol triphosphate receptor; MITO, mitochondria; NAADP, nicotinic acid adenine dinucleotide phosphate; NAD^+, nicotinamide adenine dinucleotide; NADP, nicotinamide adenine dinucleotide phosphate; NCX, Na^+/Ca^{2+} exchanger; NSCC, non-selective cation channel; NUC, nucleus; PKA, protein kinase A; PKCα, protein kinase C-α; PLC-β,

phospholipase C-β; RyR, ryanodine receptor; SER, smooth endoplasmic reticulum; SOCC, store-operated Ca^{2+} channel; VGCC, voltage-gated Ca^{2+} channel**.**

2. Calcium Signaling

Responses regulated by ET-1 have been associated with increases in intracellular Ca^{2+} ($[Ca^{2+}]_i$) either by influx of Ca^{2+} or release of intracellular Ca^{2+} stores. $[Ca^{2+}]_i$ is tightly regulated by a multitude of ion channels and exchangers that control influx, efflux, sequestration, and release of Ca^{2+} [32-34]. **Table 1** outlines the different types of plasma membrane Ca^{2+} channels and the receptors/channels that modulate intracellular Ca^{2+} release. Included is a description of their characteristics, known pharmacological activators, and known pharmacological inhibitors.

Increases in $[Ca^{2+}]_i$ can be due to influx only, stores release only, or a portion of both – and the contribution of each source of Ca^{2+} varies between receptors. This complex regulatory mechanism exists to control $[Ca^{2+}]_i$, since small changes in amplitude, duration and location of Ca^{2+} influx are sufficient to cause a wide variety of physiological responses [35]. The pathways for Ca^{2+} influx and Ca^{2+} stores release are multi-faceted and tightly controlled because small changes in intracellular Ca^{2+} can be the difference between cell survival and cell death [36].

Table 1. Calcium channel characteristics, activators and inhibitors

Voltage-Gated Calcium Channels (VGCC's)

Common Name	Official Name	Characteristics	Specific Activators	Specific Inhibitors	Ref.
L-type	$Ca_V1.2$	Cardiac and smooth muscle Ca^{2+} Channel. Regulates contraction. Moderate activation threshold ($V_{0.5}$= -10 mV). Relatively slow inactivation rate.	BAYK-8644	nifedipine, verapamil	[37]
N-type	Ca_V 2.2	Neuronal Ca^{2+} Channel. Regulates neurotransmitter release. High activation threshold ($V_{0.5}$= +10 mV). Moderate inactivation rate (100-800 msec).	--	ω-conotoxin CVIA, ω-gramma-toxin SIA	[37]
P/Q-type	Ca_V 2.1	Neuronal Ca^{2+} Channel. Regulates neurotransmitter release. Moderate activation threshold ($V_{0.5}$= -10 mV). Inactivation rate varies by β subunit (0.09-1000 msec).	--	ω-conotoxin MVIIC, ω-agatoxin IIIA	[37]
R-type	Ca_V 2.3	Neuronal Ca^{2+} Channel. Regulates Ca^{2+}-dependent gene expression and enzyme activity. High activation threshold ($V_{0.5}$= +5 mV). Fast inactivation rate (2.1-2.4 msec).	--	SNX-482, ω-PnTx3-3	[37]
T-type	Ca_V 3.1	Dendritic Ca^{2+} Channel. Regulates action potentials and subthreshold oscillations. Low activation threshold ($V_{0.5}$= -45 mV). Moderate inactivation rate (20-50 msec).	--	kurtoxin, mibefradil	[37]

Table 1 (cont'd)

Voltage-Independent Calcium Channels (VICC's)

Abbr.	Full Name	Characteristics	Activators	Inhibitors	Ref.
NSCC's	Non-selective cation channels	Ion channels that lack specificity for a specific cation. Examples: NSCC-1 and NSCC-2; most TRP channels.	maitotoxin	LOE-908	[28]
LGCC's	Ligand-gated calcium channels	Ion channels activated by binding of a ligand to the channel. Examples: P2X, 5-HT_3, and NACh receptors.	Varies by type	Varies by type	[38-40]
SOCC's	Store-operated calcium channels	Ca^{2+} channel activated by depletion of sarcoplasmic Ca^{2+} stores. Examples: STIM1/Orai complexes and TRPC channels.	SR Ca^{2+} depletion	SKF-96365	[41]

Receptors Mediating Intracellular Calcium Release

Abbr.	Full Name	Characteristics	Activators	Inhibitors	Ref.
IP_3R	Inositol 1,4,5-trisphosphate Receptor	Tetrameric receptor in the endoplasmic reticular membrane that functions as a low-conductance cation channel. Activated by IP_3.	IP_3	Xesto-spongin C, 2-APB	[42]
RyR	Ryanodine Receptor	Tetrameric receptor in the endoplasmic reticular membrane that functions as a high-conductance cation channel. Activated by increased intracellular calcium.	Caffeine	Tetracaine, Ryanodine	[43]

2.1. Calcium Influx

Generally, Ca^{2+} enters a cell by passing through Ca^{2+} channels that open in response to any number of stimuli. The Ca^{2+} concentration within a cell is much lower than the Ca^{2+} concentration in the extracellular fluid (100 nM *vs.* 2.5 mM, respectively) [44]. This Ca^{2+} concentration gradient allows Ca^{2+} ions to move through the channels and into a cell by passive diffusion. Membrane depolarization, ligand binding, and release of intracellular stores are all capable of causing plasma membrane Ca^{2+} channels to open [45]. Those that open due to membrane depolarization are the voltage-gated Ca^{2+} channels (VGCC's) and any others are considered voltage-independent Ca^{2+} channels (VICC's). The VICC's can be further broken down into store-operated Ca^{2+} channels (SOCC's), ligand-gated Ca^{2+} channels (LGCC's) and non-selective cation channels (NSCC's).

2.2. Release of Calcium Stores

The major store of intracellular Ca^{2+} is the endoplasmic reticulum, or the sarcoplasmic reticulum in muscle cells [33]. Ca^{2+} is liberated from sarcoplasmic/endoplasmic reticulum (SER) stores through two Ca^{2+} channels: inositol 1,4,5-trisphosphate (IP_3) receptors and ryanodine receptors [46,47]. These receptors are actually tetrameric ion channels, roughly ~255 kDa (IP_3 receptors) and ~550 kDa (ryanodine receptors) in size [48,49]. As shown in **Figure 3**, IP_3 receptors and ryanodine receptors share a similar structure, consisting of central pores through which Ca^{2+} can pass and allosteric binding sites on their respective N-terminal domains that regulate channel opening [50].

IP_3 is produced when phospholipase C (PLC) hydrolyzes phosphatidylinositol 4,5-bisphosphate (PIP_2) to generate both IP_3 and diacylglycerol (DAG) [51]. IP_3 activates IP_3 receptors on the SER membrane, causing them open and allow Ca^{2+} to leave the SER and enter the cytoplasm [52]. These Ca^{2+} release events can remain localized (Ca^{2+} "puffs"), or combine and propagate along the entire cell (Ca^{2+} "waves") [53]. DAG activates protein kinase-C (PKC), which then can inhibit IP_3 production by PLC [54]. PKC also phosphorylates NSCC's and VGCC's, which alters their function to either inhibit or sustain calcium influx [30]. DAG can also activate several types of NSCC's to activate Ca^{2+} influx [55].

Ryanodine receptors, when activated by local increases in intracellular Ca^{2+}, cause additional Ca^{2+} release from SER stores [56]. As such, ryanodine receptors can amplify small Ca^{2+} signals caused by Ca^{2+} influx or Ca^{2+} release [57]. In addition to amplification of Ca^{2+} signals, ryanodine receptors are involved in the termination of Ca^{2+} influx across the plasma membrane. Ryanodine receptors are on the SER membrane closest to the plasma membrane, whereby a "spark" of Ca^{2+} from ryanodine receptors can activate Ca^{2+}-sensitive potassium channels and close VGCC's as the membrane hyperpolarizes [58]. RyR-mediated Ca^{2+} sparks can be distinguished from IP_3-mediated Ca^{2+} puffs by their magnitude, kinetics and spatial spread [53]. Ryanodine receptors serve to amplify Ca^{2+} signals rapidly, but then to also terminate voltage-dependent Ca^{2+} influx.

Thus, IP_3 receptors and ryanodine receptors activate pathways that tightly regulate Ca^{2+} release from SER stores, and regulate voltage-dependent Ca^{2+} entry both

spatially and temporally. The interplay between PLC, IP_3, DAG, and PKC also keeps intracellular Ca^{2+} concentration precisely controlled while still allowing for rapid release of minute amounts of Ca^{2+} in response to a stimulus.

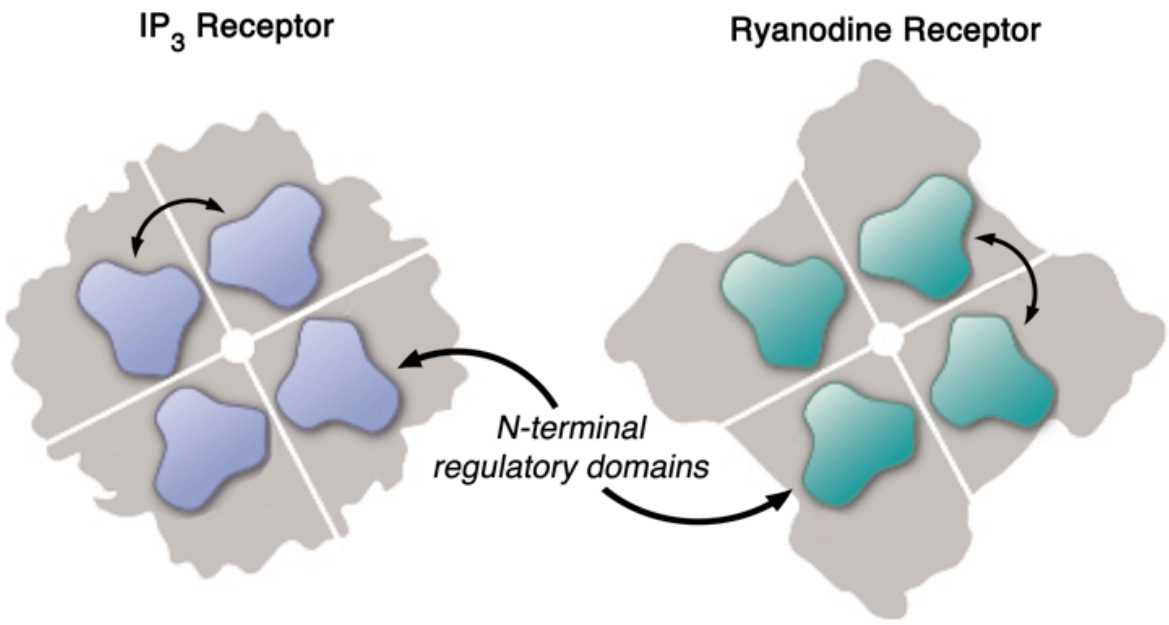

Figure 3. Structural similarities between ryanodine receptors and IP_3 receptors. Both IP_3 receptors (*left*) and ryanodine receptors (*right*) consist of four subunits arranged to form a tetrameric ion channel. The N-terminus domains of both receptors consist of regulatory domains (shown in blue and green) that interact with one another to allosterically modulate channel opening. Adapted from Hamada *et al* (2012) [50].

2.3. Calcium Sensitization

Ca2+-dependent regulation of smooth muscle tone is a balancing act between opposing mechanisms that cause contraction and relaxation. Ca^{2+} causes smooth muscle contraction by activating myosin light chain kinase (MLCK), which then phosphorylates myosin light chain (MLC) and ultimately causes contraction [59]. The sensitivity of MLC to Ca^{2+} is regulated by activation of myosin light chain phosphatase (MLCP) by proteins like telokin, which opposes the actions of MLCK and causes MLC dephosphorylation and relaxation [60]. The balance between MLCK-dependent phosphorylation and MLCP-dependent de-phosphorylation of MLC regulates the balance between contraction and relaxation in smooth muscle. As shown in **Figure 4**, Ca^{2+} binds to calmodulin, which activates MLCK. MLCK then phosphorylates MLC, which increases the ATPase activity of MLC and thus increases cross bridge cycling and leads to contraction [61]. MLCP activity is regulated by several proteins, including CPI-17 and Rho kinase (RhoK), which inhibit MLCP activity through both Ca^{2+}-dependent and Ca^{2+}-independent mechanisms [62]. Inhibition of MLCP increases smooth muscle contraction without changing MLCK activity, and thus increases the sensitivity of the contractile machinery to Ca^{2+}

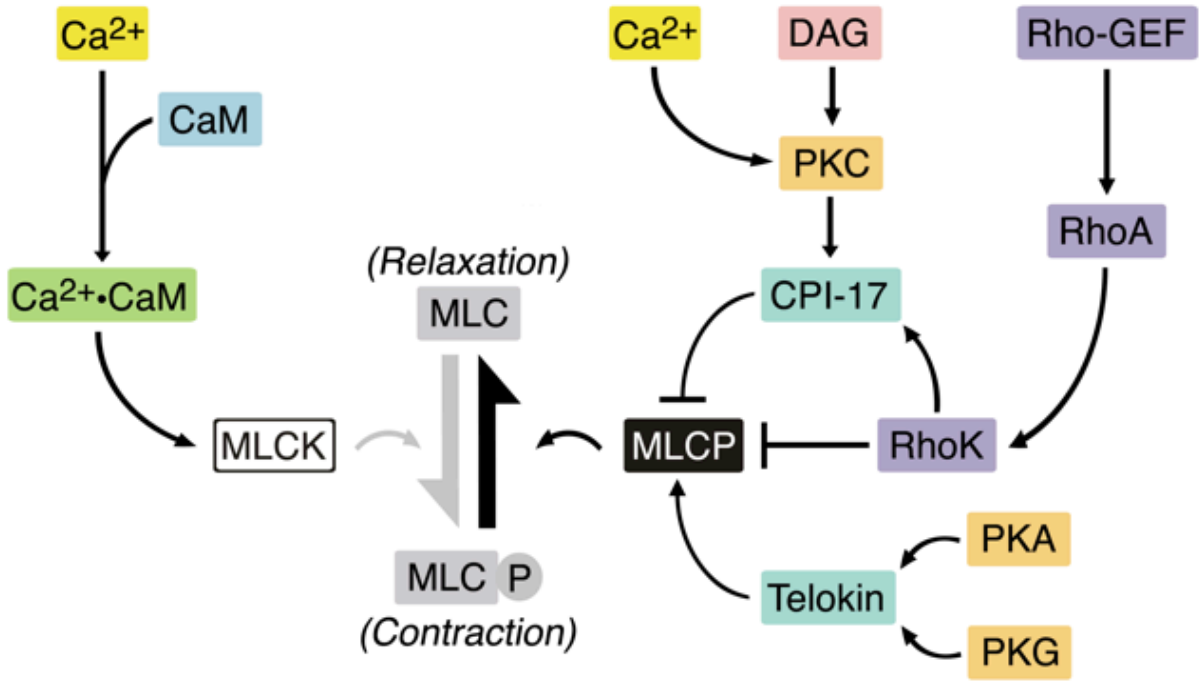

Figure 4. Regulation of smooth muscle calcium sensitivity and contraction. This cartoon illustrates how Ca^{2+} regulates myosin light chain kinase (MLCK) and myosin light chain phosphatase (MLCP) to alter myosin light chain phosphorylation to cause relaxation and contraction. Arrows represent activation; teed lines represent inhibition. Abbreviations: MLC, myosin light chain; CaM, calmodulin; DAG, diacylglycerol; PKA, protein kinase A; PKC, protein kinase C; PKG, protein kinase G; RhoK, RhoA-dependent protein kinases; GEF, guanine nucleotide exchange factor. Adapted from Somlyo *et al* (2003) and Eto *et al* (2009) [59,60]

3. The Relationship between ET-1 and Calcium

The interdependence between ET-1 and Ca^{2+} is apparent when examining both the physiological effects of ET receptor activation and ET-1 synthesis. Although multiple cell types synthesize ET-1, the predominant source of ET-1 is the vascular endothelial cell [63]. Molecules that increase endothelial cell intracellular Ca^{2+} augment expression of preproendothelin-1 (ppET-1) mRNA *via* a Ca^{2+}/calmodulin/calmodulin kinase (Ca^{2+}/CaM/CaM-K) pathway [64,65]. The physiological responses elicited by ET-1 can be both Ca^{2+}-dependent and Ca^{2+}-independent [25,66,67]. Some examples of Ca^{2+}-dependent processes regulated by ET-1 can be found in **Table 2**. Table 2 also separates ET_A receptor-dependent responses from ET_B receptor responses, and notes the specific Ca^{2+} sources activated by each receptor. In some responses, ET_A receptors regulate Ca^{2+} stores release and ET_B receptors regulate Ca^{2+} influx (*e.g.* bronchoconstriction). In others, ET_A or ET_B receptors regulate both Ca^{2+} influx and stores release. No correlation exists between ET receptor subtype and the source of Ca^{2+} governing the response. Thus, Ca^{2+} influx and mobilization by ET-1 is cell type-specific, with regard to which ET receptor subtypes are involved.

Some of the most-studied effects of ET-1 are those in the vasculature, where ET-1 acts as a potent vasoconstrictor [68]. ET-1-induced increases in intracellular Ca^{2+} are similar in pattern to those caused by other Ca^{2+}-dependent vasoconstrictors, where Ca^{2+} increases in two stages. First, there is an initial increase in intracellular Ca^{2+} from SER Ca^{2+} stores, which is followed by a sustained increase in intracellular Ca^{2+} due to the influx of Ca^{2+} from the extracellular space [29]. This pattern of initial release/sustained

influx is evident in non-vascular cells as well, whereby ET-1 can induce neutrophil migration, attenuate cGMP formation in astrocytes, stimulate diuresis and natriuresis, and cause vasorelaxation [69-72]. What differs between cells and tissues are the *specific* mechanisms that regulate the initial extracellular calcium influx and the sustained intracellular Ca^{2+} mobilization in response to ET receptor activation.

Table 2. Examples of physiological processes mediated by ET receptors that are calcium-dependent.

Calcium-Dependent Physiological Responses Mediated by ET_A Receptors				
Tissue/Cell Type:	**Response(s):**	**Calcium Influx**	**$[Ca^{2+}]_i$ Release**	**Ref.**
Neutrophils	Activation and degranulation	✔		[73]
Cardiac myocytes	Inhibition of C-type Natriuretic Peptide (CNP) signaling	✔	✔	[74]
Human bronchus	Release of intracellular Ca^{2+} stores, causing bronchoconstriction		✔	[69]
Thin limb, loop of Henle	Unknown; thought to regulate sodium and water reabsorption	✔	✔	[75]
Aortic smooth muscle	Vasoconstriction	✔	✔	[67]
Venous smooth muscle	Wave-like Ca^{2+} signals, ultimately causing venoconstriction	✔	✔	[76]
Human optic nerve head	Ca^{2+}-dependent proliferation	✔	✔	[77]
Mouse osteoblasts	Induces bone formation	✔	✔	[78]
Rat carotid body	Hypoxia up-regulates ET_A receptors, which increases mitogenesis	✔		[79]
Olfactory mucosa non-neuronal cells	Unknown; both transient and sustained Ca^{2+} entry	✔	✔	[80]

Table 2 (cont'd)

Calcium-Dependent Physiological Responses Mediated by ET_B Receptors				
Tissue/Cell Type:	**Response(s):**	**Calcium Influx**	**$[Ca^{2+}]_i$ Release**	**Ref.**
Neutrophils	Chemotactic neutrophil migration		✔	[68]
Human bronchus	Ca^{2+} influx followed by Ca^{2+} stores release, causing bronchoconstriction	✔	✔	[64]
Collecting duct	Inhibition of water reabsorption and Na^+-K^+-ATPase activity	✔	✔	[81]
Guinea pig gall bladder	Constriction		✔	[82]
Human umbilical vein	Ca^{2+} influx, causing venoconstriction	✔		[83]
Endothelial cells	Increased NO production and vasodilatation	✔	✔	[84]
Olfactory mucosa sensory neurons	Unknown; both transient and sustained Ca^{2+} entry	✔	✔	[75]

3.1. Voltage-Dependent Calcium Influx

The specific VGCC's implicated in ET-1-induced calcium entry vary, which is not surprising due to the range of responses influenced by ET-1 (*see* **Figure 1**). L-type, T-type, and R-type calcium channels have all been associated with voltage-dependent calcium influx caused by ET-1, and the relative involvement of each channel type depends on the species and cell type being studied [85,86]. The activation of multiple Ca^{2+} channels during voltage-dependent Ca^{2+} influx is not unique to ET-1; what is interesting is that ET-1 may regulate VGCC's directly as well as indirectly. The idea that ET-1 can act as a Ca^{2+} channel opener was proposed as early as 1988, but it is also possible that ET receptor activation alters the voltage-gating properties of VGCC's indirectly, to increase Ca^{2+} influx through them [87,88]. Several researchers published compelling evidence against the theory that ET-1 was a direct agonist of L-type VGCC's, instead postulating that ET-1 altered VGCC function through second messengers like PLC and PKC [89-91].

Neither the ET_A receptor nor the ET_B receptor regulates voltage-dependent Ca^{2+} entry exclusively. Depending on the cell, tissue, and experimental conditions, activation of either or both ET receptors can regulate voltage-dependent Ca^{2+} influx. In cardiac myocytes, for example, ET_A receptors as well as ET_B receptors regulate specific voltage-dependent Ca^{2+} currents [92]. ET_A receptors mediate ET-1-dependent inhibition of voltage-dependent Ca^{2+} currents caused by isoproterenol. In the same cells, ET-1-dependent stimulation of Ca^{2+} currents after exposure to atrial natriuretic peptide (ANP) is mediated by ET_B receptors. Cell, tissue, and conditional variability has

made it difficult to characterize the exact mechanisms by which each ET receptor causes voltage-dependent Ca^{2+} influx, as well as the relative contribution and importance of voltage-dependent Ca^{2+} influx to ET-1-mediated responses. Nevertheless, ET receptor-mediated membrane depolarization and voltage-dependent Ca^{2+} influx are important mechanisms by which ET-1 can increase intracellular Ca^{2+} [93-95].

Pharmacological inhibition of voltage-dependent calcium influx is a well-established and often-used treatment for hypertension, as calcium channel blockers (*e.g.* nifedipine) decrease blood pressure by inhibiting calcium influx and reducing vasoconstriction [96]. These drugs have cardio-protective benefits as well; prolonged treatment with nifedipine not only lowers blood pressure, but also improves endothelium-dependent vasorelaxation and reduces ET-1-dependent contraction [97]. Another calcium channel blocker, lacidipine, decreases ventricular hypertrophy and prepro-ET-1 expression in spontaneously-hypertensive rats [98]. These findings reinforce the importance of calcium mobilization in the vasculature, and show that the relationship between ET-1 and calcium is not a one-way street – ET-1 mobilizes calcium, but increases in calcium also augment the synthesis of ET-1. So, inhibition of voltage-dependent calcium influx decreases ET-1's deleterious effects on vascular function during hypertension, while simultaneously decreasing transcription of ET-1 precursors and ultimately reducing ET-1 production in other tissues.

3.2. Voltage-Independent Calcium Influx

Regardless of the type of VGCC's associated with ET-1-induced Ca^{2+} influx or the direct/indirect activation of VGCC's by ET-1, inhibition of all voltage-dependent Ca^{2+} channels does not abolish the inward Ca^{2+} currents caused by ET-1 [99]. In some excitable tissues, VGCC's are not activated in response to ET-1 [100]. Therefore, the remaining ET-1-induced Ca^{2+} influx is through any of several voltage-independent Ca^{2+} entry pathways (*see* **Figure 2**). As previously defined, voltage-independent Ca^{2+} channels (VICC's) include Ca^{2+} channels that are activated by a ligand directly (LGCC's), activated by intracellular Ca^{2+} release (SOCC's), or by indirect activation through G-protein-dependent signaling pathways (NSCC's) (*see* **Table 1**). Although no LGCC that is directly activated by ET-1 is known currently, pharmacological investigation shows SOCC's and NSCC's are important influx pathways in ET-1-induced smooth muscle contraction, MAP Kinase phosphorylation, and arachidonic acid release [101-103]. The relative contribution of SOCC's and NSCC's to ET-1-mediated Ca^{2+} influx is dependent on the concentrations of ET-1 used. Inhibition of NSCC's or SOCC's by SKF-96365 or LOE-908, respectively, abolished the calcium currents caused by low concentrations of ET-1 ($\leq$ 0.1 nM) [104]. In the same study, however, Ca^{2+} currents caused by higher concentrations of ET-1 were only abolished by a combination of SKF-96365 and LOE-908. Since the opening of both SOCC's and NSCC's could be stimulated by release of intracellular Ca^{2+} stores, differentiating ET-1-induced extracellular Ca^{2+} influx from Ca^{2+}-induced Ca^{2+} influx has proven difficult [41]. Similar to voltage-dependent Ca^{2+} entry, voltage-independent Ca^{2+} entry can be regulated by either ET_A receptors or ET_B receptors, depending on the cell or tissue type [101].

Neither ET receptor is associated with Ca^{2+} influx through only one type of VICC in all cell types.

Changes to voltage-independent Ca^{2+} entry in hypertension are not well described, but Ca^{2+} influx through VICC's appears to have little affect on systemic blood pressure. Treatment with Ginoside-Rd, a purported VICC inhibitor, did not lower systemic blood pressure in hypertensive rats [4,105]. In the same experiment, however, VICC inhibition decreased vascular remodeling and ET-1-induced smooth muscle cell proliferation [4]. So, while there is little evidence that voltage-independent Ca^{2+} influx is involved in the pathogenesis of hypertension, both ET-1 and VICC's are implicated in the progression of hypertension-induced vascular hypertrophy.

3.3. Release of Intracellular Calcium Stores

ET receptors cause intracellular Ca^{2+} stores release by activating PLC and increasing IP_3 production [29,106]. Similar to ET-1's effects on Ca^{2+} influx pathways, the Ca^{2+} released from IP_3-sensitive stores does not account for the increase in $[Ca^{2+}]_i$ entirely [30]. Intracellular Ca^{2+} must also come from other reticular stores (*e.g.* ryanodine-sensitive stores) or an atypical intracellular Ca^{2+} store (*e.g.* mitochondrial stores and lysosomal stores) that ET-1 can mobilize. In peritubular smooth muscle cells and renal afferent arterioles, ET-1 alters cyclic-ADP ribose production to sensitize ryanodine-activated SER stores [107-109]. Neither IP_3-sensitive stores nor atypical Ca^{2+} stores, however, account for ET-1-induced increases in intracellular Ca^{2+} entirely, consistently, and across cell types.

While many studies confirm that ET-1 causes intracellular Ca^{2+} release, none provide evidence that ET_A receptors and ET_B receptors mobilize different intracellular Ca^{2+} stores. The intracellular Ca^{2+} stores mobilized by ET-1 depend upon the cell type, and not the ET receptor subtype.

Smooth muscle cells from hypertensive rats maintain increased intracellular Ca^{2+} after depolarization, which implies intracellular Ca^{2+} storage and mobilization are altered during hypertension [110]. However, IP_3-mediated Ca^{2+} released by ET-1 stimulation is blunted in DOCA-salt hypertension and unchanged in spontaneously-hypertensive rats [111]. Thus, even though basal intracellular Ca^{2+} is increased in hypertension, the ability of ET-1 to mobilize Ca^{2+} directly may be impaired or unchanged.

3.4. Calcium Signaling in the Nucleus

Traditionally, ET receptors are thought to be plasma membrane receptors, where they can be activated by extracellular ET-1 to initiate a G-protein-dependent intracellular signaling cascade. Recently, Bkaily *et al* showed the presence of ET_B receptors and R-type VGCC's in the nuclear membrane (*see* **Figure 2**). They further postulate that internalization of plasma-membrane ET receptors frees ET-1 from the receptor, and this cytosolic ET-1 activates ET_B receptors in the nuclear membrane [112]. The activation of nuclear ET_B receptors causes an increase in nuclear Ca^{2+} by opening R-type Ca^{2+} channels and Na^+/Ca^{2+} exchangers (NCX) on the nuclear membrane, as well as indirectly activating IP_3 receptors and ryanodine receptors located in the nucleoplasmic reticulum [113]. The sequestration of Ca^{2+} within the nucleus may serve as a regulatory

element for maintaining Ca^{2+} homeostasis within the cell, much like sarcoplasmic reticular or mitochondrial uptake of Ca^{2+}. It also may regulate the expression of Ca^{2+}-sensitive genes, or act as a protective mechanism to buffer the nucleus against Ca^{2+} depletion or overload [114,115]. If Ca^{2+} can enter the nucleus, it is likely that it can leave the nucleus as well. What remains to be seen is if nuclear ET receptors signal differently than membrane ET receptors, and how intracellular ET-1 can regulate both intra-nuclear and intracellular Ca^{2+} mobilization.

Understanding of the function of nuclear GPCR's is a work-in-progress. Much of this research has focused on the angiotensin (AT) AT_1 receptor. Binding sites for angiotensin-II on the nuclei of rat hepatocytes turned out to be AT_1 receptors that regulate reactive oxygen species (ROS) production [116,117]. Further investigation will explain the function of nuclear ET receptors and their role in maintaining Ca^{2+} homeostasis.

3.5. Calcium Efflux and Calcium Exchange

In addition to Ca^{2+} influx mechanisms that increase intracellular Ca^{2+}, there are Ca^{2+} efflux mechanisms that lower the concentration of intracellular Ca^{2+} back to basal levels. Due to its large inward electrochemical gradient, Ca^{2+} efflux usually requires the use of energy (in the form of ATP) to push Ca^{2+} out of the cell and back into the extracellular space [44]. If these mechanisms were inhibited by ET-1, the net result would be prolonged elevations of intracellular Ca^{2+} concentration due to retention of Ca^{2+} [118]. ET-1 suppresses plasma membrane Ca^{2+}-ATPase function and expression in hepatic

sinusoidal endothelial fenestrae, leading to contraction [119]. Thus, inhibition of active transport of Ca^{2+} out of the cell represents another means by which ET-1 can modify intracellular Ca^{2+}.

An important mechanism also exists to extrude Ca^{2+} from the cytosol, but without the use of ATP. The Na^{+}/Ca^{2+} exchanger (NCX) (**Figure 5**) has been characterized as a unique mechanism that is capable of both efflux and influx of Ca^{2+}. The NCX is a bi-directional antiporter of Ca^{2+} and Na^{+}, the directionality of which is primarily regulated by the electrochemical gradients for Ca^{2+} and Na^{+} [120]. When operating in forward mode, the NCX transports three Na^{+} ions into the cell for each Ca^{2+} ion transported out. In reverse mode, three Na^{+} ions are transported out for each Ca^{2+} ion transported in. An increase in intracellular Ca^{2+} favors forward-mode NCX function, whereas an increase in intracellular Na^{+} favors reverse-mode function [121]. Membrane depolarization can also regulate the NCX but the extent of which depends on the NCX isoforms and splice variants present [122].

Poburko *et al* have published compelling evidence that the NCX is part of an important Ca^{2+} regulatory system, whereby localized increases in Na^{+} within the cytoplasm drive NCX-mediated Ca^{2+} influx and oscillations in cytosolic Ca^{2+} during contraction [123]. This is usually associated with agonist-induced activation of Na^{+} influx through NSCC's, such as several members of the canonical transient receptor potential (TRPC) family [124,125]. If ET-1 were to activate Na^{+} influx, this could subsequently cause NCX-mediated Ca^{2+} influx and contraction. This appears possible in ventricular myocytes, where ET-1 causes the NCX in the plasma membrane to operate in reverse mode,

causing the NCX to become Ca^{2+} influx pumps instead of acting as Ca^{2+} efflux pumps [126]. Interestingly, ET-1 may also regulate Ca^{2+} influx *via* reverse-mode NCX in a manner independent of Na^{+} influx by causing phosphorylation of the NCX the favors function in reverse mode over forward mode [127]. Thus, the interaction between ET-1 and the NCX could be an important regulatory mechanism, even in cells where Na^{+} influx is not caused by ET-1 directly.

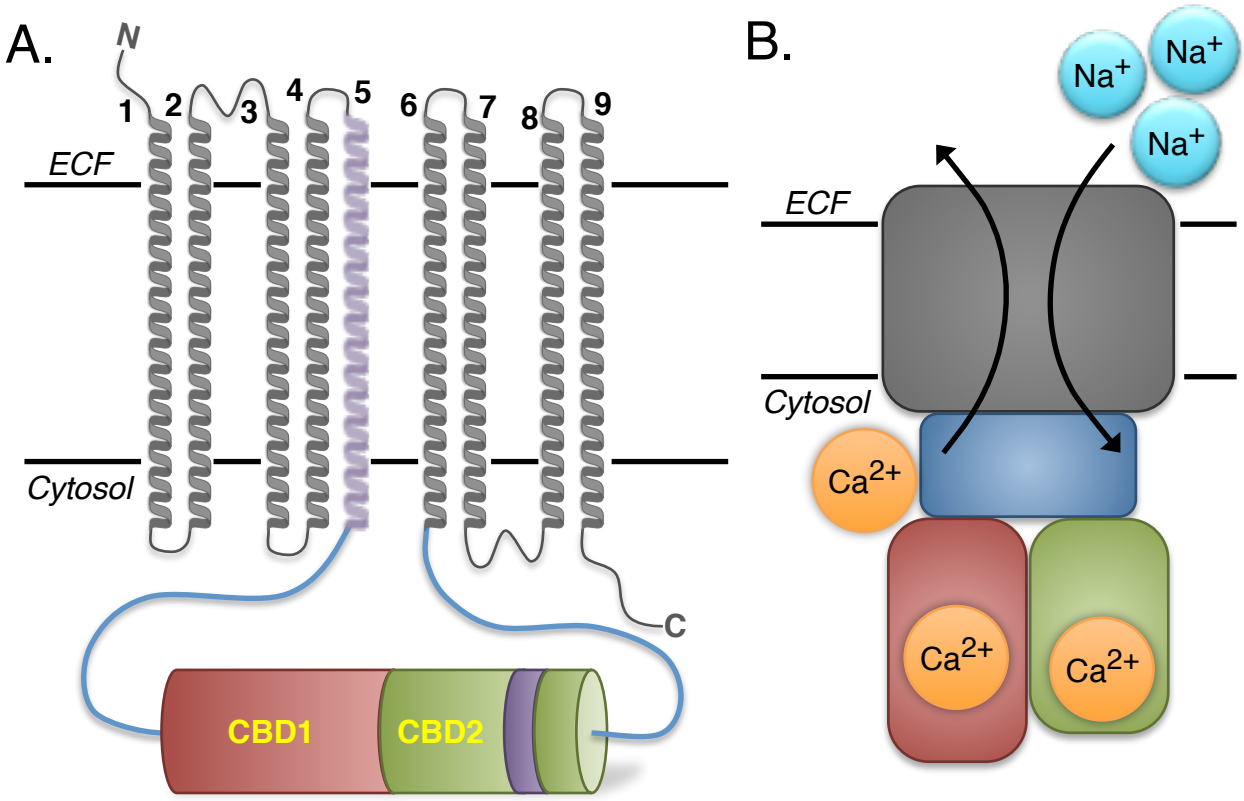

Figure 5. Structure and function of the Na^+/Ca^{2+} Exchanger (NCX). (Adapted from Hilge *et al* (2006) [128]). (A) The NCX contains nine transmembrane domains (grey), with two Ca^{2+} binding domains: CBD1 (red) and CBD2 (green). The CBD's are linked to the transmembrane domains by an α-catenin-like domain (CLD; blue), linking domains 5 and 6. Sites of alternative slicing are shown in violet. (B) Schematic of NCX operation, showing Ca^{2+} binding to CBD1 (red) and CBD2 (green).

4. The Functions of Veins and Arteries

4.1. Structure and Function

Differences in the structure of arteries and veins are indicative of their interconnected physiological functions. A summary of the important differences between arteries and veins can be found in **Table 3**. Arteries serve to deliver oxygen and nutrients to tissues, while veins serve the critical function of bringing deoxygenated and waste-filled blood back to the heart and lungs for re-oxygenation and purification. As they contain substantially more elastin and smooth muscle than veins, arteries are vessels with low compliance and high resistance (**Figure 6**). In comparison to arteries, veins are extremely compliant and distensible, making their resistance low. Because of this ability to stretch and expand easily, the venous system can store approximately 70% of the body's total blood volume at a given moment [129].

While not as forceful as arteries, veins do exhibit significant vasoreactivity to many agonists [130]. Adrenergic agonists, prostaglandins, and ET-1 all cause prolonged venous contraction. Furthermore, veins desensitize less than arteries to ET-1 and maintain contractility to ET-1 in hypertension, while arteries do not [2]. Sustained venous contraction (*i.e.* a sustained decrease in venous capacitance, as could be instigated by ET-1) could lead to increased venous return to the heart, increased cardiac filling, increased cardiac output into arterial circulation, and thus increases in blood pressure [1]. There is evidence that changes in arterial blood volume are the major determinant of long-term blood pressure, even though total blood volume is

generally not increased in human essential hypertension [131-134]. For arterial blood volume to increase without a change in total blood volume, blood volume elsewhere in the circulatory system must decrease. Since the venous system stores approximately 70% of total blood volume at a given moment, a small decrease in venous blood storage could force a large amount of blood into the arterial circulation [135]. Impaired venous distensibility and decreased venous capacitance are seen in hypertensive patients, which can increase arterial blood volume by decreasing the storage capacity of veins [136,137]. Thus, veins may play an important role in blood pressure regulation.

Table 3. Important differences between arteries and veins.

Arteries	Veins	Reference
High BAYK8644 sensitivity	Low BAYK8644 sensitivity	[138]
Low α_1 adrenoreceptor expression	high α_1 adrenoreceptor expression	[139]
α_1 adrenoreceptors only	α_1 and α_2 adrenoreceptors	[140]
Substance P relaxation	Substance P contraction	[141]
Low hydrogen peroxide	high hydrogen peroxide	[142]
Low xanthine oxidase and catalase	high xanthine oxidase and catalase	[143]
Slow myosin heavy chain expression	fast myosin heavy chain expression	[144]
Slow contractile kinetics to agonists	fast contractile kinetics to agonists	[2]
Chymase-dependent Big-ET-1 processing	chymase-independent Big-ET-1 processing	[145]
No ET_A-ET_B receptor interaction	ET_A-ET_B receptor interaction	[146]
No S6c-induced contraction	S6c-induced contraction	[148]

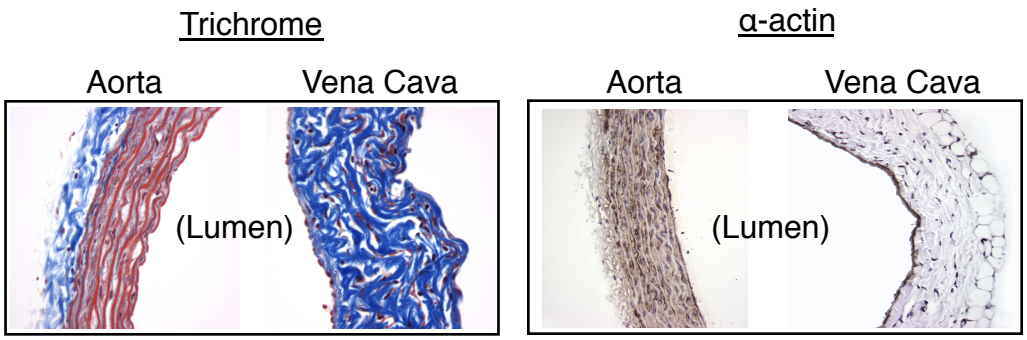

Figure 6. Structure of the rat aorta and vena cava. Masson Trichrome (left) and smooth muscle α-actin staining (right) of aorta and vena cava from a normotensive rat. *Left:* elastin (red); muscle (pink); collagen (blue). *Right:* positive smooth muscle α-actin staining (brown). L = lumen. Adapted from Rondelli *et al* (2007) [144].

4.2. Venous Contraction and Calcium Dependence

While ET-1-induced contraction of aorta requires both extracellular Ca^{2+} influx and intracellular Ca^{2+} release, little is known about Ca^{2+} signaling by ET-1 in vena cava. Thus, several preliminary experiments were performed to assess the Ca^{2+} dependence of ET-1-induced venous contraction, and measure the changes in intracellular Ca^{2+} in vena cava in response to ET-1.

When extracellular Ca^{2+} is removed and intracellular Ca^{2+} stores are depleted, contraction to ET-1 is markedly attenuated in both aorta and vena cava (**Figure 7**). This suggests that ET-1-induced contraction is Ca^{2+}-dependent in vena cava, just as it is in aorta. Also, different Ca^{2+} signaling mechanisms appear to be activated by ET-1 during the development of contraction in both tissues. As shown in **Figure 8**, ET-1 initially causes a transient spike in global cytosolic Ca^{2+}, which is followed by a maintained and prolonged elevation in cytosolic Ca^{2+} as contraction continues. The biphasic nature of these changes in cytosolic Ca^{2+} suggests that Ca^{2+} release and Ca^{2+} influx by ET-1 occur sequentially: first, ET-1 activates the release of intracellular Ca^{2+} stores, causing the transient spike in cytosolic Ca^{2+}. Subsequently, ET-1 causes the influx of extracellular Ca^{2+}, which causes an elevated cytosolic Ca^{2+} concentration to be maintained during the course of contraction.

Considering these data alone, Ca^{2+} signaling during contraction by ET-1 appears very similar in aorta and vena cava, in that both require Ca^{2+} for contraction, both exhibit similar Ca^{2+} kinetics, and both utilize mechanisms of extracellular Ca^{2+} influx as well as

intracellular Ca^{2+} release during ET-1-induced contraction. However, these findings, as well as our findings presented in **Figure 7** and **Figure 8** do little to distinguish between the specific mechanisms that regulate changes in intracellular Ca^{2+}. In subsequent chapters, I will provide compelling evidence that aorta and vena cava utilize markedly different extracellular Ca^{2+} influx and intracellular Ca^{2+} release mechanisms to regulate changes in cytosolic Ca^{2+} during ET-1-induced contraction.

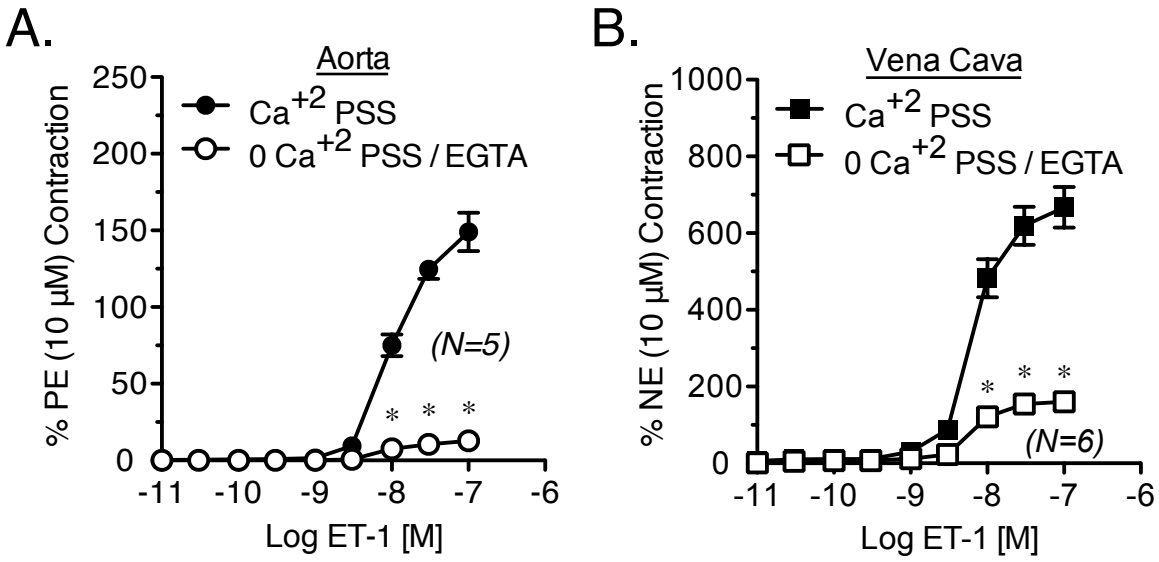

Figure 7. ET-1-induced contraction requires Ca^{2+}. ET-1 concentration response curves in aorta and vena cava, either incubated in Ca^{2+}-replete buffer (Ca^{2+} PSS) or Ca^{2+}-free buffer with 1 mM EGTA (0 Ca^{2+}/EGTA). (A): Ca^{2+}-replete aorta (solid circles) and aorta incubated in Ca^{2+} free/ 1mM EGTA (open circles). (B): Ca^{2+}-replete vena cava (solid squares) and vena cava incubated in Ca^{2+} free/ 1mM EGTA (open squares). PE = phenylephrine; NE = norepinephrine; N = 5-6; * = $p < 0.05$ *vs.* vehicle.

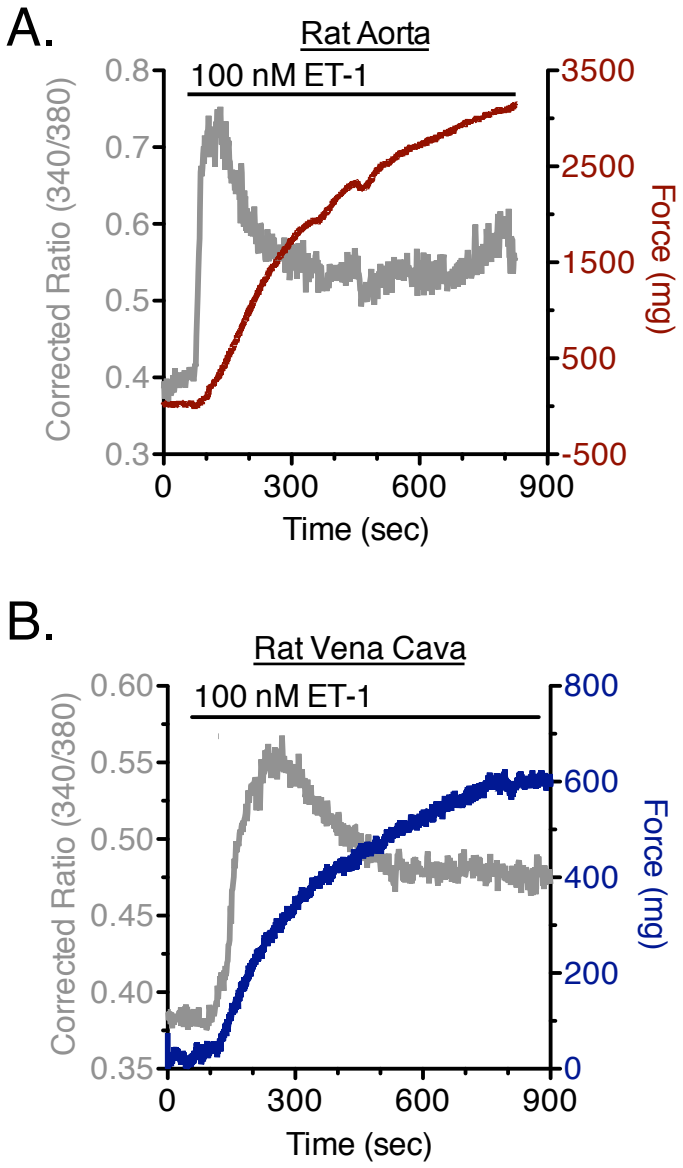

Figure 8. ET-1 increases intracellular Ca^{2+} during contraction. Fluorescence ratio (grey, left axis) and contraction (blue/red, right axis) in rat aorta (A) and vena cava (B), during ET-1-induced contraction. Tissues were loaded with Fura-2 fluorescent Ca^{2+} indicator for 30 minutes. After initial baseline recording, the tissue was then exposed to 100 nM ET-1. Representative of greater than 4 experiments.

4.3. ET-1-Mediated Calcium Influx

As mentioned in **Section 4.1** above, much of the current research into ET-1-mediated Ca^{2+} signaling suggests that a reasonable portion of the vascular smooth muscle contractions caused by ET-1 were regulated through the influx of Ca^{2+} through voltage-dependent and voltage-independent Ca^{2+} channels. My own preliminary research also suggests that this was true, since removal of extracellular Ca^{2+} nearly abolished contraction to ET-1 (**Figure 7**), and ET-1 caused a prolonged and steady increase in cytosolic Ca^{2+} (**Figure 8**) suggested a prolonged influx of Ca^{2+}. However, in both aorta and vena cava, a multitude of inhibitors that blocked VGCC's (1 μM nifedipine, 10 μM diltiazem) and NSCC's (10 μM SKF-96365, 10 μM LOE-908) had no significant effect on ET-1-induced contraction in aorta or vena cava. In fact, only a combination of nifedipine, SKF96365 and LOE908 significantly attenuated the maximal contraction in aorta and vena cava (**Table 4**). These data suggest that no single Ca^{2+} channel is responsible for extracellular Ca^{2+} influx during ET-1-mediated contraction in aorta and vena cava. Furthermore, they suggest that an important Ca^{2+} influx mechanism during ET-1-induced contraction remains uncharacterized in both aorta and vena cava.

Table 4. Measurement of ET-1 potency and efficacy, as derived from isometric contractility concentration response data. Maximum response to ET-1 is shown as percent of phenylephrine contraction (aorta, %PE) or norepinephrine contraction (vena cava, %NE). Potency (EC_{50}[M]) data are given as log(EC_{50}) to allow for standard error calculation and statistical comparison. L-VGCC = L-type voltage-gated Ca^{2+} channel; NSCC = non-selective cation channel; SOCC = store-operated Ca^{2+} channel. For each experiment, N > 5. Yellow = p<0.05 *versus* control.

AORTA

		Maximum (% PE)		*log(EC50)*	
Drug	**Conc. (μM)**	**Vehicle**	**Exposed**	**Vehicle**	**Exposed**
Nifedipine	1	140±7%	132±25%	-8.46±0.06	-8.29±0.14
Diltiazem	10	149±13%	114±12%	-7.97±0.05	-8.02±0.04
SKF-96365	10	144±14%	113±20%	-7.92±0.11	-7.75±0.42
LOE-908	10	160±3%	142±13%	-8.15±0.03	-8.28±0.05
Nif/SKF/LOE	0.05/10/10	171±30%	111±15%	-8.06±0.05	-8.21±0.06

VENA CAVA

		Maximum (% NE)		*log(EC50)*	
Drug	**Conc. (μM)**	**Vehicle**	**Exposed**	**Vehicle**	**Exposed**
Nifedipine	1	303±33%	307±90%	-8.87±0.11	-8.83±0.25
Diltiazem	10	612±96%	581±33%	-8.14±0.08	-8.13±0.06
SKF-96365	10	538±108%	438±77%	-8.01±0.18	-8.03±0.13
LOE-908	10	551±71%	478±75%	-8.18±0.09	-8.36±0.09
Nif/SKF/LOE	0.05/10/10	748±41%	516±93%	-8.29±0.03	-8.36±0.09

5. Hypotheses

While changes in venous capacitance are linked to increased blood pressure, relatively little is known about the mechanisms that govern contraction in venous smooth muscle as compared to arterial smooth muscle. Even with the breadth of research into Ca^{2+} signaling in smooth muscle, the mechanisms responsible for Ca^{2+} mobilization by ET-1 (particularly in terms of ET-1-induced venous contraction) also remain unclear. Our preliminary data suggest that the differences in Ca^{2+} signaling between aorta and vena cava may be due to differences in Ca^{2+} influx mechanisms, but these data also do not investigate any differences in sarcoplasmic Ca^{2+} release mechanisms. As such, this project was designed to test the global hypothesis that Ca^{2+} signaling induced by ET-1 differs between veins and arteries, and to fill the gap in knowledge about how venous contraction could contribute to the pathogenesis of hypertension. This global hypothesis is divided into three sub-hypotheses:

Sub-hypothesis 1: Ca^{2+} influx through alternative mechanisms, such as reverse-mode Na^{+}/Ca^{2+} exchange, is a significant mechanism of Ca^{2+} entry activated by ET-1 in vena cava and aorta. Since Ca^{2+} influx through plasma membrane Ca^{2+} channels could not account for Ca^{2+} influx during ET-1-induced contraction, I expect that ET-1 causes the Na^{+}/Ca^{2+} exchanger (NCX) to function in reverse-mode to move Ca^{2+} into venous and arterial smooth muscle cells.

Sub-hypothesis 2: *Ca^{2+} released through ryanodine receptors contribute to ET-1-induced Ca^{2+} signaling and contraction.* I expect that ET-1 mobilizes intracellular Ca^{2+} from ryanodine receptor-dependent Ca^{2+} stores in the aorta and vena cava.

Sub-hypothesis 3: *ET-1-induced contraction of aorta and vena cava depends on IP_3-mediated release of intracellular Ca^{2+} stores.* I expect that ET-1 mobilizes intracellular Ca^{2+} from IP_3 receptor-dependent Ca^{2+} stores in the aorta and vena cava.

6. Experimental Model

All experiments were performed on aorta and vena cava from male rats. While we recognize the role of smaller vessels at maintaining total peripheral resistance and regulating venous capacitance, we believe that aorta and vena cava are an appropriate model for interpreting the effects of ET-1 since the vena cava is important in controlling central blood volume and circulatory dynamics [1,135]. Aorta and vena cava express both ET receptors, and ETA receptors are coupled to contraction in both tissues [147]. However, ET_B receptors are coupled to contraction in vena cava as well [148]. Finally, important differences exist between aorta and vena cava in terms of their respective responses to ET-1. Vena cava desensitize less than aorta to ET-1 and vena cava maintain sensitivity to ET-1 in hypertension [2,149]. The considerable amount of prior research with these tissues also allows for a broad range of comparisons between these findings and prior results.

CHAPTER 2: MATERIALS AND METHODS

1. Animals and Euthanasia

Experiments were conducted in laboratory facilities in the Department of Pharmacology and Toxicology at Michigan State University. All procedures that involve animals were performed in accordance with the Institutional Animal Care and Use Committee at Michigan State University and the *Guide for the Care and Use of Laboratory Animals* of the National Research Council (USA) [150]. Normal male Sprague-Dawley rats (Charles River Laboratories, Portage, MI, USA), DβH-ET_B:$ET_B^{(sl/sl)}$ male rats, and their DβH-ET_B:$ET_B^{(+/+)}$ male littermates (250-300 g) were used. All animals were genotyped prior to experimentation. Euthanasia was performed by I.P. injection of FatalPlus (80-100 mg/kg), followed by a bilateral pneumothorax. Pentobarbital, the active ingredient in FatalPlus, is a well-known anesthetic and its use for euthanasia is consistent with the recommendations of the Panel on Euthanasia of the American Veterinary Medical Association. Significant measures were taken to minimize discomfort and expedite euthanasia of all research animals used.

2. Smooth Muscle Cell Dissociation and Immunofluorescence

Rat aorta (RA) and vena cava (RVC) were dissected and cleaned of outer adipose tissue in physiological salt solution (PSS) containing (mM): NaCl, 130; KCl, 4.7; KH_2PO_4, 1.18; $MgSO_4$-$7H_2O$, 1.17; $NaHCO_3$, 14.8; dextrose, 5.5; Na_2EDTA-$2H_2O$, 0.03; $CaCl_2$, 1.6; (pH=7.2). Cleaned tissues were cut into ~1 mm rings and then

transferred to 1.5 ml microcentrifuge tubes and incubated with dissociation solution (80 mM NaCl, 80 mM monosodium glutamate, 5.6 mM KCl, 20 mM $MgCl_2$, 10 mM HEPES, 10 mM glucose, and 1 mg/mL BSA, pH 7.3) with 1 mg/mL dithiothreitol and 0.3 mg/mL papain for 18 min in a 37°C water bath. The solution was removed and replaced with fresh dissociation solution containing 100 µM $CaCl_2$ and 1 mg/mL collagenase and incubated 9 min in a 37°C tissue bath. The solution was removed and cells were re-suspended in dissociation solution by gentle trituration. Cells were transferred to coverslips using a Shandon Cytospin 4 Centrifuge (Thermo Scientific, Waltham, MA, USA). Cells were then fixed in Zamboni's fixative for 20 min, permeabilized with 1% Triton X-100 in PBS for 20 min, and blocked with goat serum (1% diluted in PBS) for 1 h at 37°C. Primary antibodies were diluted in blocker, added to the coverslips, and cells were incubated at 37°C for 1 h. Primary antibodies used included: mouse anti-RyR1/2, (1:500; Life Technologies, Grand Island, NY USA); mouse anti-IP_3R1 (1:1000; Neuromab, Davis, CA, USA); rabbit anti-IP_3R2 (1:1000; Millipore, Billerica, MD USA); rabbit anti-IP_3R3, (1:1000; Millipore); rabbit anti-α-actin (1:100; Abcam, Cambridge, MA, USA); and FITC-conjugated mouse anti-α-actin (1:1000; Sigma-Aldrich, St. Louis, MO USA). Coverslips were washed briefly 3 times with PBS, before incubation in secondary antibodies (goat anti-mouse Alexa Fluor 568, 1:1000; goat anti-rabbit 568, 1:1000; and goat anti-rabbit 488, 1:1000; Life Technologies, Carlsbad, CA, USA) for 1 h at 37°C. Coverslips were washed 3 times with PBS and placed face down onto slides in Prolong Gold with DAPI (Life Technologies). Cells were then imaged using an Olympus® FV1000 confocal system mounted on an Olympus® inverted microscope.

3. Whole Tissue Immunofluorescence

Freshly dissected vena cava were cleaned of adipose tissue in physiological salt solution (PSS). The vessel was then cut length-wise and pinned with lumen facing up. Tissues were fixed for 10 minutes in 4° C methanol, and taken through a standard protocol. Primary antibodies used were: anti-ET_B antibody (rabbit polyclonal, 1 µg/ml, Alomone Labs, Jerusalem, Israel); anti-PECAM antibody (goat polyclonal, 1 µg/ml, Santa Cruz, CA, USA) in 1.5% blocking serum, or both combined in 1.5% blocking serum. Secondary antibodies used were: donkey anti-rabbit Cy-5 (1:400, Jackson Immunoresearch, West Grove, PA, USA); mouse anti-goat FITC (1:800, Jackson Immunoresearch, West Grove, PA, USA) in 1.5% blocking serum or both combined in 1.5% blocking serum. Tissues were then mounted on slides using Prolong Gold Medium with DAPI (Invitrogen, Carlsbad, CA, USA) and viewed using fluorescence microscopy.

4. Whole Tissue Immunohistochemistry

Cleaned aorta and vena cava rings were formalin-fixed (10%) overnight. Tissues were then paraffin-embedded, sliced into 5 micron-thick sections and placed on glass coverslips. Tissue sections were dewaxed, unmasked using Unmasking Reagent (Vector Laboratories, Burlingame, CA, USA), and taken through a standard protocol. Primary antibody used was anti-ET_B antibody (rabbit polyclonal, 1:200, Alomone Labs, Jerusalem, Israel) in 1.5% blocking serum in phosphate buffered saline or 1.5% blocking serum as a control. Development of slides proceeded according to the

manufacturer's kit using 3,3'-diaminobenzidine as the developing substrate (Vector Laboratories, Burlingame, CA, USA) and slides were counterstained with Vector Hematoxylin. After air-drying, coverslips were affixed and slides were examined using a Nikon inverted microscope.

5. Western Blot Analysis

Endothelium-intact and endothelium-denuded tissues were ground with mortar and pestle under liquid nitrogen in 1 ml of ice-cold homogenation buffer (50 mM Tris (pH 7.4), 4% SDS, 20% glycerol, 0.5 mM phenylmethylsulfonyl fluoride, 1 mM orthovanadate, 10 µg/ml aprotinin, 10 µg/ml leupeptin). Homogenate was vortexed, sonicated, transferred to a plastic centrifuge tube, and spun at 4° C to pellet debris; the supernatant was then kept. A Bicinchoninic Acid (BCA) assay was used to determine protein concentration. Due to the high molecular weight of RyR and IP_3R protein (560 kDa and 310 kDa, respectively), Western blotting was performed using techniques for high molecular weight proteins as outlined in current literature [48,151,152]. Samples (4:1 in denaturing sample buffer, boiled for 5 minutes) were separated on gradient (8-15%) SDS-polyacrylamide gels. Proteins were then wet-transferred to PVDF membrane at 60 V for one hour at 4° C. Membranes were blocked for 3-4 hours (Tris-buffer saline, 4% chick egg ovalbumin, 2.5% sodium azide; Licor® Odyssey blocker or 5% Bio-Rad® milk). Blots were probed for between one hour to overnight with primary antibody (rocking, at 4° C), rinsed three times in Tris-buffered saline (TBS) + Tween (0.1%) with a final rinse in TBS and incubated with the appropriate secondary antibody for 1 hour at 4° C

(rocking). Methods of detection included standard ECL capturing images on film or Licor® Odyssey. Band density was quantified using ImageJ software (NIH, USA).

6. Immunoprecipitation

NCX-1 antibody (2 µg, Swant, Switzerland) was added to 200 µg of rat aorta and rat vena cava tissue homogenate. Two hours after addition, protein A/G agarose beads (30 µl, Santa Cruz Biotechnology, USA) were then added to each sample and tumbled overnight at 4° C. Samples were then centrifuged (2500 rpm for 1 min), after which the supernatant was removed and replaced with fresh phosphate buffered saline (PBS) before re-suspension of precipitate. This process was repeated 3 times. After the final centrifugation, the supernatant was removed and replaced with 35 µl of denaturing sample buffer, boiled for 5 minutes, and centrifuged (2500 rpm for 1 min). The resulting supernatant was separated on a 7.5% SDS-polyacrylamide gel and wet-transferred to PVDF membrane for standard Western analysis using NCX-1 antibody (1:1000; Swant, Switzerland). Positive control for NCX-1 was rat heart homogenate (Santa Cruz Biotechnology, Santa Cruz, CA USA). Band density was quantified using ImageJ software (NIH, USA).

7. Isometric Smooth Muscle Contraction

Rat thoracic aorta, vena cava, jugular vein (JV), carotid artery (CA), superior mesenteric artery (SMA) and superior mesenteric vein (SMV) were first cleaned of external adipose tissue in PSS. In experiments where endothelium-denuded tissues were used, the

endothelium was mechanically denuded with a small brush, fashioned from size 1 braided silk suture and an 18-gauge needle. Tissue rings were then mounted in warmed, aerated PSS (37°C; 95/5% O_2/CO_2) in isolated tissue baths (20 ml) for measurement of isometric contractile force using a 750 TOBS Tissue Organ Bath System (Danish Myo Technology, Aarhus, Denmark) and PowerLab for Windows (ADInstruments, Colorado Springs, CO, USA). The tissues were placed under optimum resting tension (4g for RA; 1g for RVC, CA and JV; 1.5g for SMA; and 0.1g for SMV), as previously determined. Tissues were allowed to equilibrate for one hour in PSS prior to initial challenge with 10 µM phenylephrine (PE) (RA), 10 µM norepinephrine (NE) (RVC, SMA, and SMV) or 60 mM KCl (CA and JV) to test for tissue viability. Endothelium viability was then confirmed by the presence of relaxation to 1 µM acetylcholine after contraction by the adrenergic agonists. In experiments using endothelium-denuded tissues, abolition of acetylcholine-induced relaxation was used to confirm endothelial denudation. Tissues were then washed every 15 minutes until they returned to resting tension. Cumulative concentration response curves or responses to single concentrations of agonists were then recorded. Antagonists, inhibitors, or their vehicles were incubated with the tissues for 1h prior to addition of agonists.

8. Extracellular Calcium

Calcium influx during ET-1-induced contraction was measured as previously described [153]. Briefly, aorta and vena cava were first incubated in Ca^{2+}-replete PSS and initially challenged with 10 µM NE (vena cava) or PE (aorta) to test for tissue viability. After

washout and upon return to resting tension, tissues were incubated for 30 min in Ca^{2+}-free PSS with 1 mM EGTA. Tissues were then switched to nominally Ca^{2+}-free PSS (no EGTA) for 10 minutes before the addition of a maximum concentration of ET-1 (100 nM). After plateau of any ET-1-induced contraction, cumulative concentration response curves to Ca^{2+} (1 μM – 3 mM $CaCl_2$) were performed in the presence of ET-1.

9. Reverse-mode NCX Function

While no specific agonist of reverse-mode NCX is available currently, removal of extracellular sodium will cause NCX-dependent calcium influx and elicit a transient contraction of vascular smooth muscle [154]. As such, isometric contractility was used to determine if NCX could function in reverse-mode in aorta and vena cava to cause calcium influx. Aorta and vena cava were hung in a custom-fabricated wire myograph, and tissue viability was confirmed by challenge with 10 μM norepinephrine (vena cava) or phenylephrine (aorta). Tissues were then exposed to vehicle (dimethyl sulfoxide) for 30 minutes before exposure to low-Na^+ (15 mM) PSS for 10 min. To control for changes in osmolarity, N-methyl D-glucamine was substituted for NaCl in low-Na^+ PSS. Tissues then recovered in normal-Na^+ (145 mM) PSS for 30 minutes. After recovery, tissues were incubated with KB-R7943 (10 μM) for 30 minutes before a second exposure to low-Na^+ PSS for 10 minutes.

10. Calcium Imaging

We designed and fabricated a custom imaging apparatus that allows for the simultaneous measurement of calcium fluorescence and isometric contraction of aorta and vena cava rings. As such, correlations between temporal changes in intracellular calcium and contractile force development were made that were not possible in independent experiments. This apparatus also reduced the quantity of animals needed to complete our studies, as well as increased the power of our data analyses. Measurements of intracellular calcium were performed using both intensiometric (Fluo 4) and ratiometric (Fura 2) imaging dyes. Ratiometric measurements with Fura 2 correct for differences in cell thickness and dye concentration, thus quantification of global changes in intracellular calcium concentration can be made with greater consistency and certainty [155]. Fura 2, however, does not respond rapidly enough to measure calcium waves within individual cells in whole tissue. In contrast to Fura 2, Fluo 4 shows rapid changes in calcium as a change in fluorescence intensity. While the use of confocal microscopy compensates partially for variations in tissue thickness, variations in dye concentration do not allow for the consistent quantification of $[Ca^{2+}]_i$ [156]. In order to measure quantifiable changes in global calcium as well as rapid changes in Calcium in individual cells within tissues, we used both types of calcium indicators in our experiments. Aorta and vena cava smooth muscle cells were loaded with the intensiometric calcium indicator Fluo 4-AM or the ratiometric calcium indicator Fura 2-AM by bath incubation. The dye solutions were made in calcium-replete PSS, and contained: 10 μM Fluo 4-AM or Fura 2-AM dye (Invitrogen, Carlsbad CA, USA), 0.5% dimethyl sulfoxide (DMSO), and 0.01% Pluronic (Invitrogen, Carlsbad CA, USA). The

dye solution was applied to vena cava for 1 hour and aorta for 1.5 hours at room temperature, and exchanged for fresh dye solution once during that time. Before imaging, a 30-minute superfusion with aerated PSS (95/5% O_2/CO_2) was performed to wash any extracellular dye from the bath and allow for dye de-esterification and gradual temperature increase to 37^{o} C. Resting tension (1g for RVC and 4g for RA) was then applied, and tissues were allowed to reach steady-state resting tension before continuing the experiments. Isometric contraction was measured using a custom-made Wheatstone bridge force transducer connected to a bridge amplifier and PowerLab interface (ADInstruments, Colorado Springs, CO, USA), and recorded using Chart software (ADInstruments, USA). In experiments using Fluo 4-AM, all vessels were imaged using a long working distance 63x water-immersion objective (N.A. 0.8, W.D. 3 mm; Leica, Wetzlar, Germany). Fluo 4-AM fluorescence at 526 nm was acquired at 30 frames per second using the CSU-10B spinning-disc confocal system (Solamere, Salt Lake City UT, USA) with 488 nm laser illumination (Solamere, Salt Lake City UT, USA) and an intensified CCD camera (XR Mega-10, Stanford Photonics, Palo Alto, CA). Images were recorded using Piper software (Stanford Photonics, Palo Alto, CA). In experiments using Fura 2-AM, all vessels were imaged using a photometry system (Photon Technologies Int'l (PTI), Birmingham NJ, USA) mounted on a Nikon TE-300 inverted microscope (Nikon Instruments, Melville NY, USA) equipped with a 40x (N.A. 0.75) Plan-Fluor long working-distance objective. Fura 2-AM was excited with 340 and 380 nm wavelength light, as controlled by a DeltaRam-X multi-wavelength illuminator, and emission was measures at 510 nm with a D-104 photomultiplier system (PTI) at 0.8

Hz. FeliX software (PTI) was used to control the illuminator and photometer, and record all acquired data.

11. Real-Time RT-PCR

Real-time RT-PCR was performed as previously described [157]. Briefly, rat aorta and vena cava were removed and placed in sterile water, then cleaned of fat and blood. Total RNA was isolated using the MELT Total Nucleic Acid Isolation System and reverse transcribed with Superscript II reverse transcriptase (Invitrogen, Carlsbad, CA). Standard real-time RT-PCR was done using a GeneAMP 7500 Real-Time PCR machine (Applied Biosystems, Carlsbad, CA) and SYBR Green PCR Fast Master Mix (Applied Biosystems). Rat primers were purchased from Qiagen (Valencia, CA): RyR-1 (RefSeq Accession #: XM_001078539; 131 bp amplicon), RyR-2 (RefSeq Accession #: NM_001191043; 66 bp amplicon), and RyR-3 (RefSeq Accession #: XM_001080527; 141 bp amplicon). Calibrator control was beta-2 microglobulin (RefSeq Accession #: NM_012512, 128 bp amplicon) (SABiosciences, Frederick, MD USA). PCR conditions were: 95°C for 10 minutes followed by 40 cycles of (95°C, 15 sec; 60°C, 60 sec). A standard dissociation curve was run following the above cycle conditions. Each sample was run in duplicate.

12. Data Quantification

To quantify calcium fluorescence intensity from Fluo 4 experiments, global and ROI intensity were calculated using *ImageJ* software (Nat'l Institutes of Health, USA). To

analyze frequency and amplitude of calcium waves from Fluo 4 experiments, SparkAn software (courtesy of Drs. M.T. Nelson and A.D. Bonev, University of Vermont) was used. Only increases in fluorescence that were at least 20% above basal levels for each cell were considered, and measurements were taken from 10, randomly selected cells. To quantify ratiometric changes in smooth muscle cell calcium from Fura 2 experiments, data were analyzed using Microsoft Excel (Microsoft, Redmond WA, USA). Contractility data were recorded in milligrams and normalized to an initial challenge with adrenergic agonist (norepinephrine for vein, phenylephrine for artery). All contraction data is thus reported as a percent of adrenergic response, to account for variations in tissue size and viability. Data resulting from all experiments were assessed for homogeneity of variance, which determined the appropriate parametric or non-parametric test for statistical comparisons. Comparisons where $p < 0.05$ are considered significant.

13. Statistical Analysis

Three to five replicates are generally the smallest indicator of significance in our statistical models. Even so, we verified that the sample sizes were sufficient to give a statistical power of ≥80% (α=0.05, $\beta \leq 0.2$). Preliminary data for each experiment were used to estimate effect size (standardized mean difference between groups), as required for power analysis and sample size estimation. Calculated effect sizes were also verified by comparison to similar published findings.

Mean, standard error and variance was calculated for all data sets. For comparisons of two samples of equal variance, statistical significance between groups was established using two-tailed, unpaired Student's t-tests (α=0.05). For samples of unequal variance, the Mann-Whitney U test was used (α=0.05). For multiple sample comparisons, two-way ANOVA was used to assess treatment effects, followed by Bonferroni's post hoc analysis to compare individual means.

CHAPTER 3: REVERSE-MODE Na^+/Ca^{2+} EXCHANGE IS AN IMPORTANT MEDIATOR OF VENOUS CONTRACTION

1. Rationale

The Na^+/Ca^{2+} exchanger (NCX) is a bi-directional regulator of cytosolic Ca^{2+}, capable of both Ca^{2+} influx and Ca^{2+} efflux [120]. As the NCX does not hydrolyze ATP to provide energy for ion transport, the direction of Ca^{2+} movement through the NCX depends on the net electrochemical gradients for Na^+ and Ca^{2+} [158]. In forward mode, the NCX transports Ca^{2+} out of cells; in reverse mode, NCX takes up extracellular Ca^{2+}. Ion transport by the NCX is also electrogenic, with a stoichiometry of 3 Na^+ ions exchanged for each Ca^{2+} ion [159]. Thus, both the function and regulation of the NCX are highly complex as they depend on the ionic concentration, membrane potential, and electrogenic nature of the Na^+/Ca^{2+} exchange.

Ca^{2+} regulation by the NCX is believed to be important in the maintenance of arterial tone and blood pressure [160]. Animals overexpressing smooth muscle NCX have elevated blood pressure and salt-sensitive hypertension [161]. Likewise, knockout of smooth muscle NCX decreases vasoconstriction and lowers blood pressure [154]. The relationship between increased NCX expression and increased arterial tone implies that Ca^{2+} influx through the reverse-mode NCX is an important determinant of arterial smooth muscle tone [162].

While a growing body of evidence suggests that venous tone contributes to blood pressure maintenance [1], little is known about the mechanisms regulating venous smooth muscle calcium handling and contraction. Two mathematical models, based upon research conducted using rabbit inferior vena cava, predict that Na^+ influx and reverse-mode NCX activation are required for sarcoplasmic stores refilling during vascular smooth muscle contraction [163,164]. It remains unclear if the reverse-mode NCX is an important regulator of venous smooth muscle tone.

In this study, we used the reverse-mode NCX inhibitor 2-(2-(4-(4-nitrobenzyloxy)phenyl)ethyl)-isothiourea methanesulfonate (KB-R7943) to test the hypothesis that reverse-mode NCX is a means of Ca^{2+} entry in rat aorta (RA) and vena cava (RVC). We also performed additional experiments to assess the specificity of KB-R7943 for the reverse-mode NCX in RA and RVC, since KB-R7943 was known to have off-target effects that may influence the interpretation of our results.

2. Results

2.1. Presence of NCX-1 Protein

Immunoprecipitation, followed by Western blotting, was used to confirm the presence of NCX1 protein in RA and RVC whole-tissue homogenate. A distinct band was visible in all immunoprecipitates at ~110 kDa, which corresponds to the expected molecular weight of the NCX1 protein (**Figure 9a**). An identical band was also present in the positive control (rat heart lysate) and absent in samples from which NCX1 antibody was omitted. Densitometry was then used to quantify NCX1 protein expression in a total of 6 aorta and vena cava samples from two different experiments (**Figure 9b**). Data were normalized to the density of their respective positive control samples. Neither normalized band density nor raw band density were significantly different between aorta and vena cava immunoprecipitates, indicating that aorta and vena cava express NCX1 protein similarly.

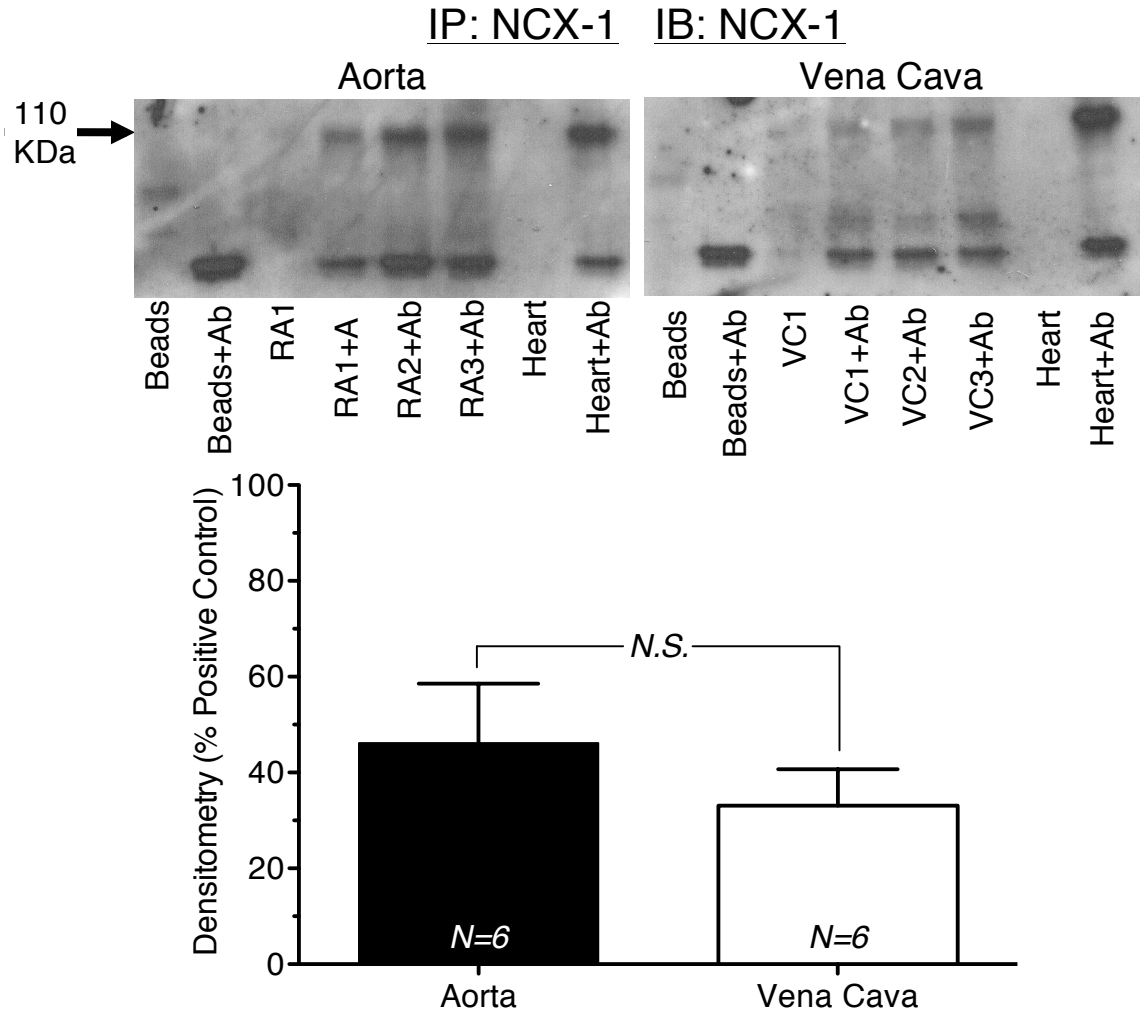

Figure 9. NCX-1 protein expression in aorta and vena cava. (*Top*) Representative Western blot analysis of immunoprecipitation of NCX1 from 200 µg of whole-tissue protein homogenate from aorta (RA1-3) and vena cava (VC1-3), isolated from Sprague-Dawley rats. NCX1 protein was immunoprecipitated using protein A/G beads (Santa Cruz Biotechnology, CA USA) and NCX1 antibody (Ab) (Swant, Switzerland). Blots were probed with antibody against NCX1. (*Bottom*) Densitometry of NCX western blot analysis shows no significant difference in NCX expression between aorta (black) and vena cava (white). N.S. = $p>0.05$; N=6.

2.2. Reverse-mode NCX function

Having established the presence of NCX-1 protein, we proceeded to measure reverse-mode NCX function in RA and RVC using isometric contractility. Rapid reduction of extracellular Na^+ (Na^+_O) is a common test of NCX function, as NCX function is regulated by the Na^+ electrochemical gradient [165]. In RA, exposure to low-Na^+ PSS (14 mM) for 10 minutes caused a small relaxation followed by a small, transient contraction in aorta that was not inhibited by the reverse-mode NCX inhibitor KB-R7943 at either concentration tested (1 μM or 10 μM) (**Figure 10a-e**). However, low-Na^+ PSS exposure caused a sustained contraction in vena cava that was not attenuated by KB-R7943 (1 μM), but was significantly reduced by KB-R7943 (10 μM) (**Figure 11a-e**). Simultaneous measurement of contraction and Fura 2 fluorescence ratio showed that contraction during low-Na^+ PSS exposure was accompanied by an increase in intracellular Ca^{2+}, which was attenuated by KB-R7943 (10 μM) (**Figure 12a-e**). Thus, contraction of vena cava due to low-Na^+ exposure is mediated, in part, by Ca^{2+} influx through KB-R7943-sensitive Ca^{2+} influx.

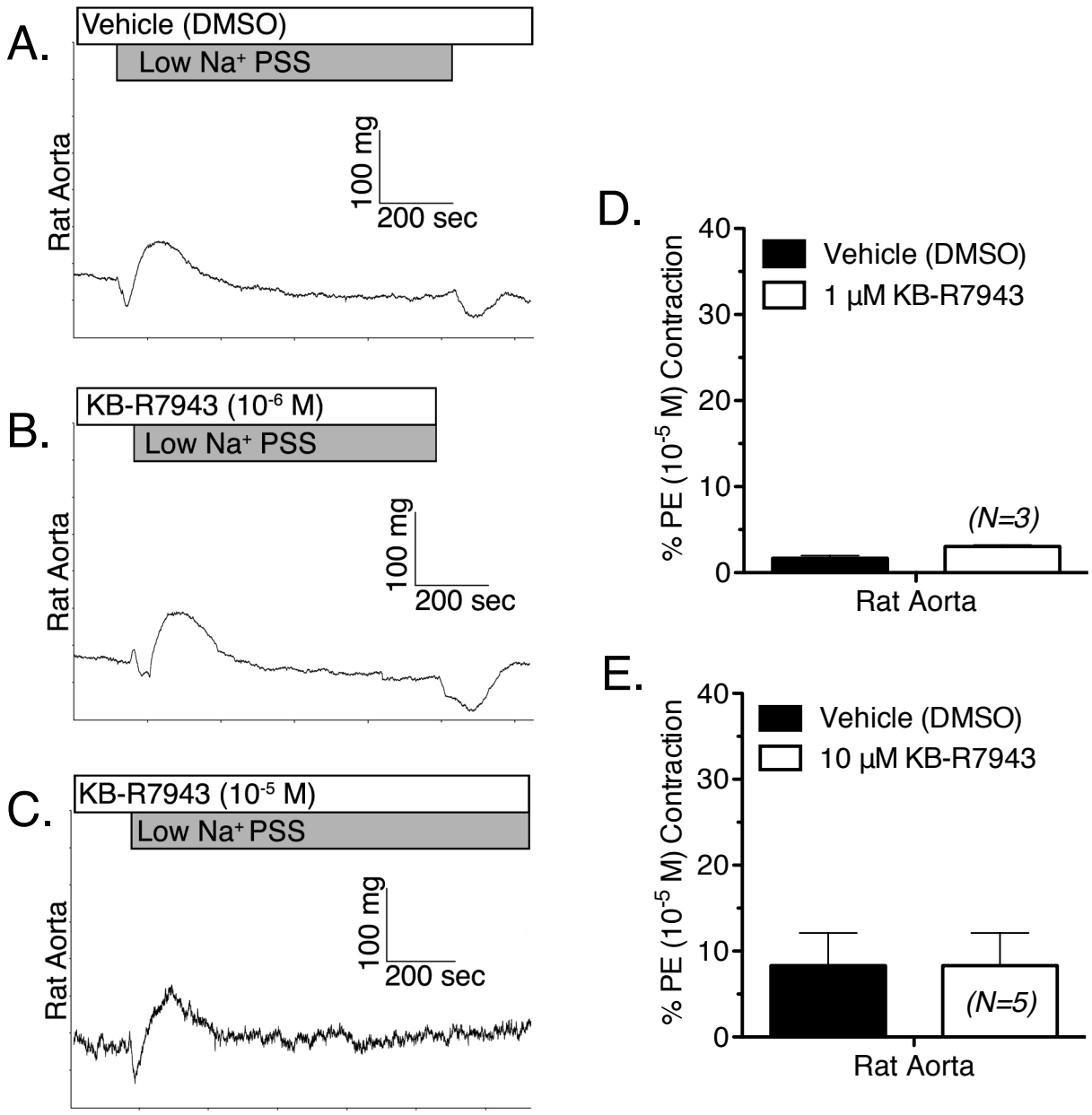

Figure 10. Representative tracings of rat aorta contraction, in response to rapid exposure to low-Na^+ (~15 mM) physiological salt solution. Shown are responses from tissues incubated with vehicle (DMSO) (A), 1 μM KB-R7943 (B) and 10 μM KB-R7943 (C). Arrows indicate the baseline and maximal contraction used to measure the responses. Summary graphs of low-Na^+-induced contraction in aorta, in the presence or absence of KB-R7943 (1 μM and 10 μM). All bars represent mean ± SEM for the

number of animals indicated. Black bars represent vehicle-exposed tissues. White bars represent exposed to 1 μM KB-R7943 (D) or 10 μM KB-R7943 (E). Results are shown as percentages of initial phenylephrine contraction (PE). N=3-5; * = $p<0.05$ *versus* vehicle.

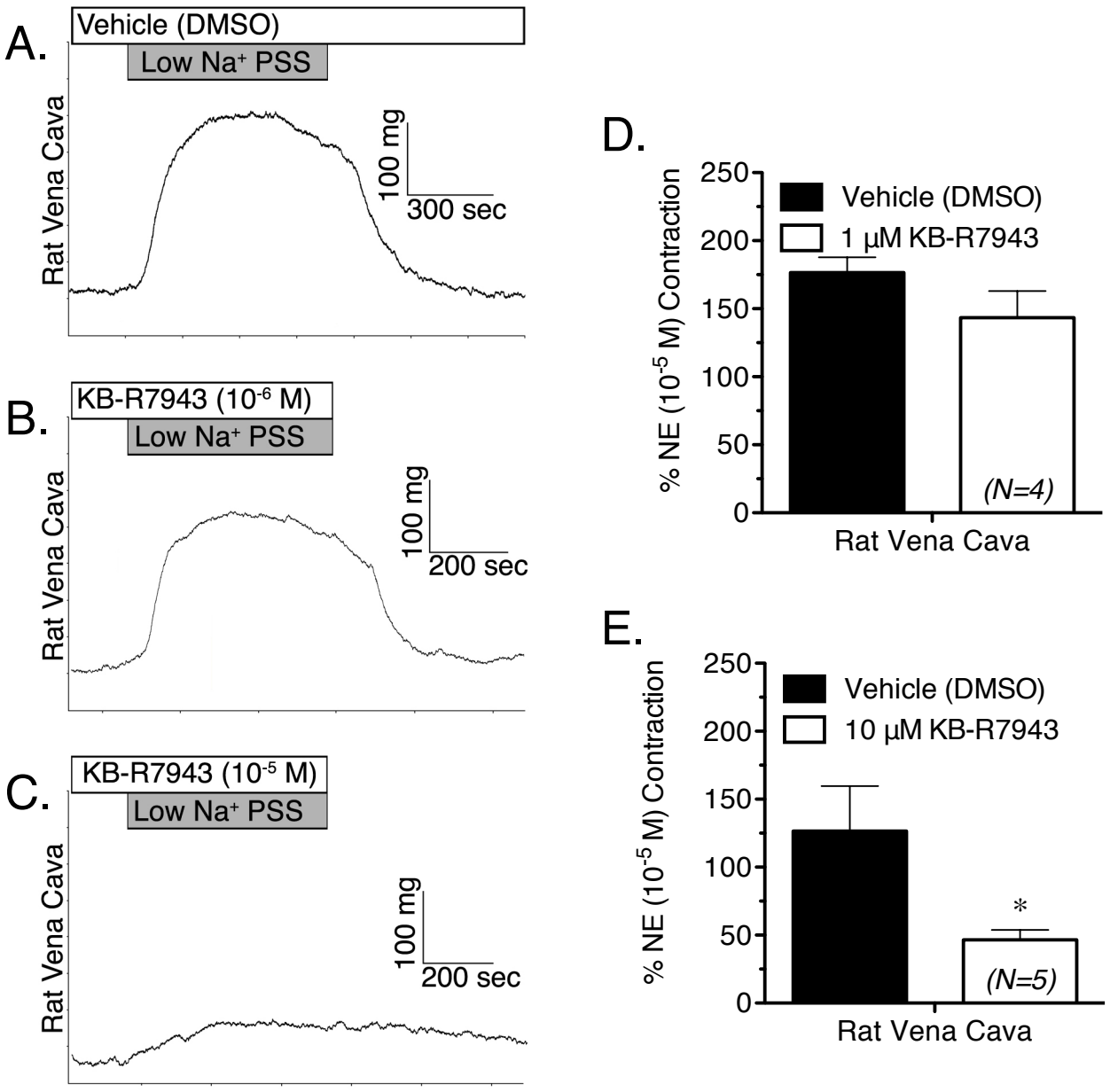

Figure 11. Representative tracings of rat vena cava contraction, in response to rapid exposure to low-Na$^+$ (~15 mM) physiological salt solution. Shown are responses from tissues incubated with vehicle (A), 1 µM KB-R7943 (B) and 10 µM KB-R7943 (C). Arrows indicate the baseline and maximal contraction used to measure the responses. (D,E) Summary graphs of low-Na$^+$-induced contraction in vena cava, in the

presence or absence of KB-R7943 (1 μM and 10 μM). All bars represent mean ± SEM for the number of animals indicated. Black bars represent vehicle-exposed tissues (differences between vehicle contractions were not significant). White bars represent tissues exposed to 1 μM KB-R7943 (D) or 10 μM KB-R7943 (E). Results are shown as percentages of initial noradrenaline contraction (NA). N=4-5; * = $p<0.05$ *versus* vehicle.

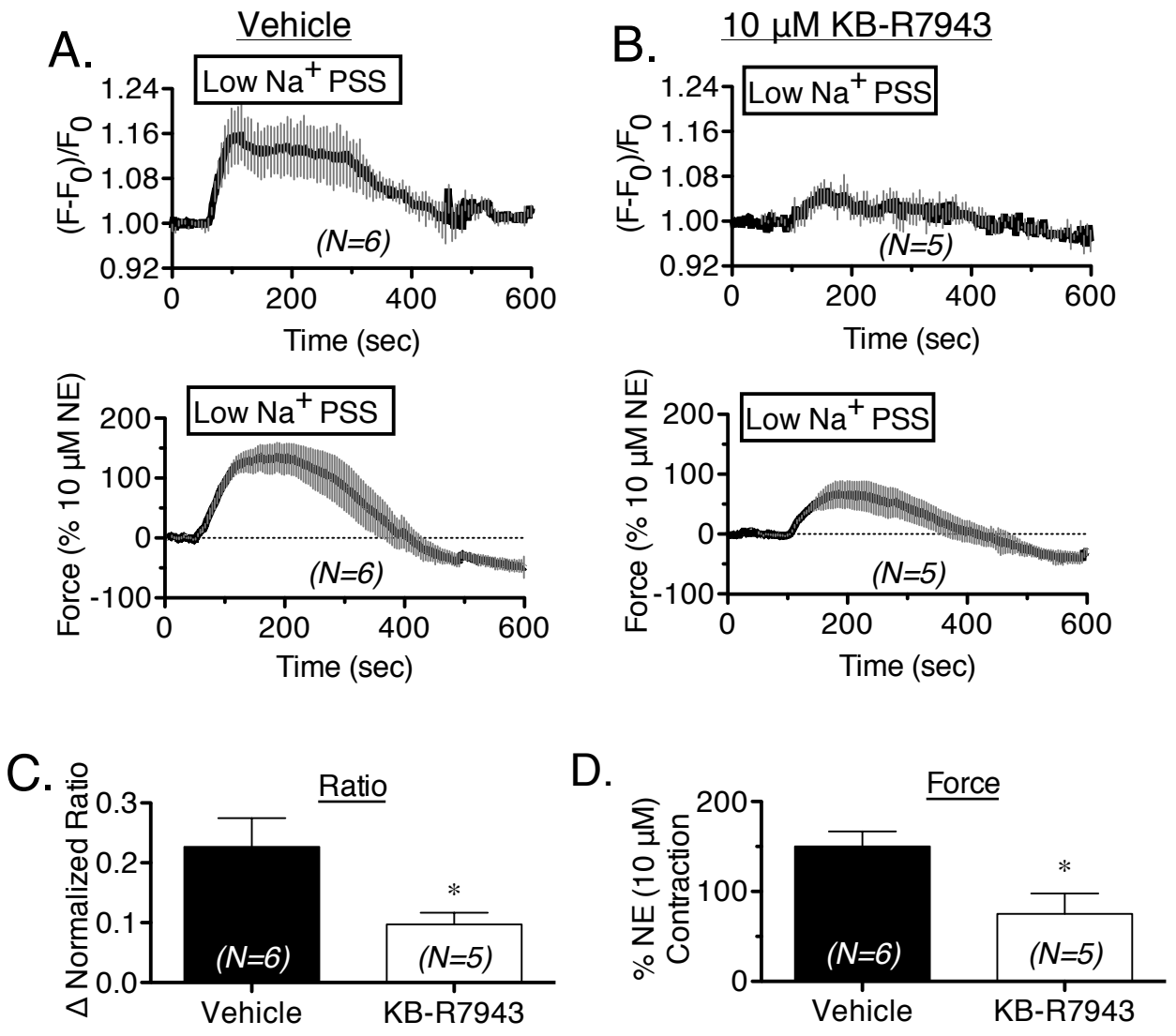

Figure 12. Simultaneous measurement of Fura2-AM fluorescence ratio and contraction in vena cava exposed to low Na^+ PSS. Responses were measured in the presence of vehicle (A) or 10 µM KB-R7943 (B). Lines represent mean ± SEM for the number of experiments indicated. (C,D) Summary bar graphs indicating the maximum change in fluorescence ratio (C) and contraction (D) from these same experiments. Black bars represent vehicle-exposed tissues. White bars represent tissues exposed to 10 µM KB-R7943. N=5-6; * = $p<0.05$ *versus* vehicle.

2.3. The effects of KB-R7943 on agonist-induced contraction

To investigate the contribution of Ca^{2+} influx through reverse-mode NCX during vascular contraction, isometric contraction to ET-1 was measured in an isolated tissue bath in the presence or absence of KB-R7943. KB-R7943 (1 μM) had no effect on ET-1-induced contraction in either RA or RVC (**Figure 13a,b**). However, KB-R7943 (10 μM) significantly attenuated maximal contraction to ET-1 in vena cava (52.93 ± 9.22% of control), but not aorta (90.06 ± 1.04% of control) (**Figure 14a,b**). The effects of KB-R7943 on KCl-induced contraction were also tested. KB-R7943 (10 μM) attenuated maximal contraction to KCl in aorta (47.81±4.77%) and nearly abolished the response to KCl in vena cava (8.77±2.20%) (**Figure 15a,b**).

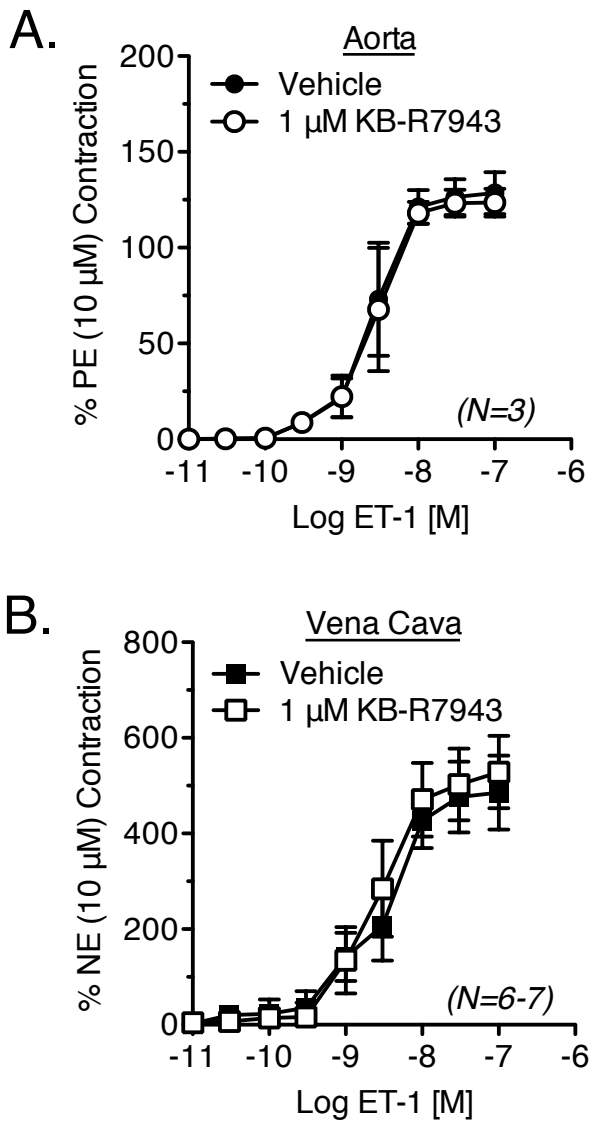

Figure 13. Measurement of endothelin-1-induced responses in aorta and vena cava, exposed to vehicle or KB-R7943 (1 μM). Vehicle or antagonists were incubated with aorta (A) and vena cava (B) for 1h prior to ET-1 exposure. Points represent mean ± SEM for the number of animals indicated in parentheses. * = $p<0.05$ *versus* vehicle.

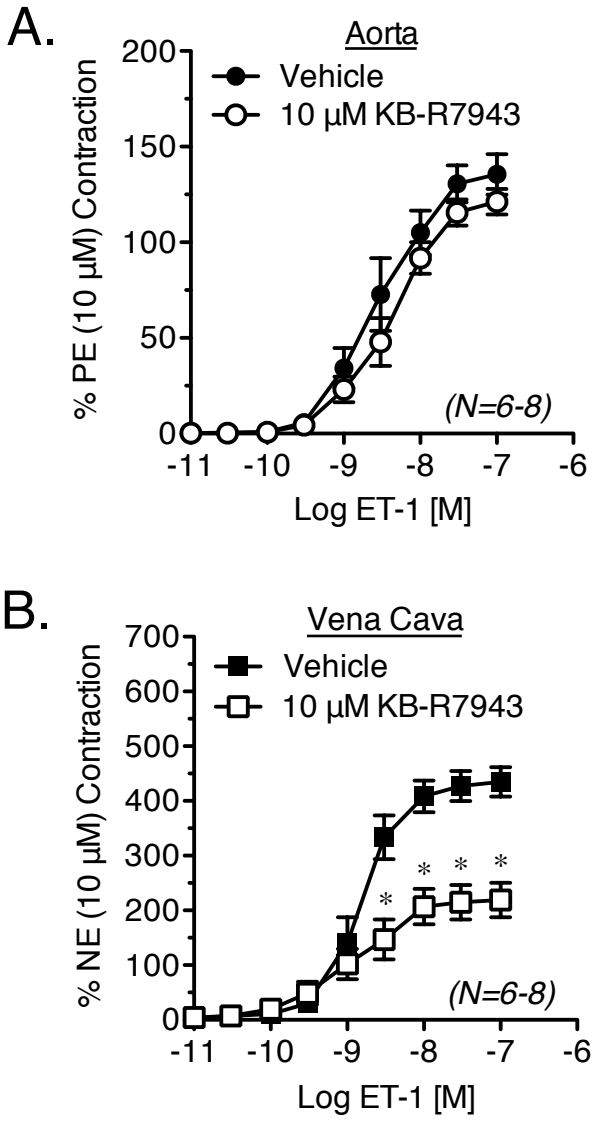

Figure 14. Measurement of endothelin-1-induced responses in aorta and vena cava, exposed to vehicle or KB-R7943 (10 µM). Vehicle or antagonists were incubated with aorta (A) and vena cava (B) for 1h prior to ET-1 exposure. Points represent mean ± SEM for the number of animals indicated in parentheses. * = $p<0.05$ *versus* vehicle.

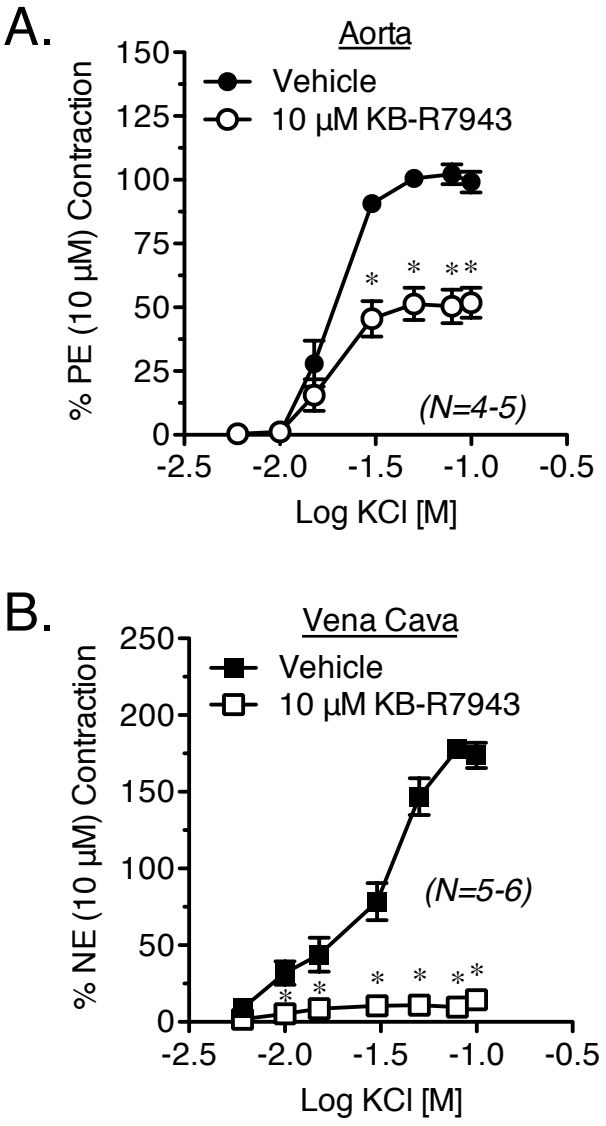

Figure 15. Measurement of KCl-induced contraction in aorta and vena cava, exposed to vehicle or KB-R7943 (10 µM). Vehicle or antagonists were incubated with aorta (A) and vena cava (B) for 1h prior to agonist exposure. Points represent mean ± SEM for the number of animals indicated in parentheses. * = $p<0.05$ *versus* vehicle.

2.4. Inhibition of Ca^{2+} influx by KB-R7943 during ET-1-induced contraction

To test if KB-R7943 inhibited extracellular Ca^{2+} influx during contraction to ET-1, contraction to increasing concentrations of $CaCl_2$ was measured in the presence of ET-1 (100 nM) as described above (*see* Methods). As compared to vehicle, KB-R7943 (10 μM) caused a 7.1-fold rightward-shift in the contractile response to $CaCl_2$ in aorta (EC_{50}=37.33 μM *vs.* 264.50 μM) but had no effect on maximal contraction to $CaCl_2$ (**Figure 16a**). In vena cava, KB-R7943 (10 μM) reduced the maximal contraction to $CaCl_2$ in addition to causing a 10.4-fold rightward shift in the contractile response (EC_{50}=55.90 μM *vs.* 580.00 μM) (**Figure 16b**). At a $CaCl_2$ concentration equivalent to that of our physiological salt solution used in the previous experiments (1.6 mM), KB-R7943 (10 μM) had no effect on maximal contraction to $CaCl_2$ in the presence of ET-1 in aorta, but significantly reduced the maximal contraction in vena cava (**boxes, Figure 16a-b**).

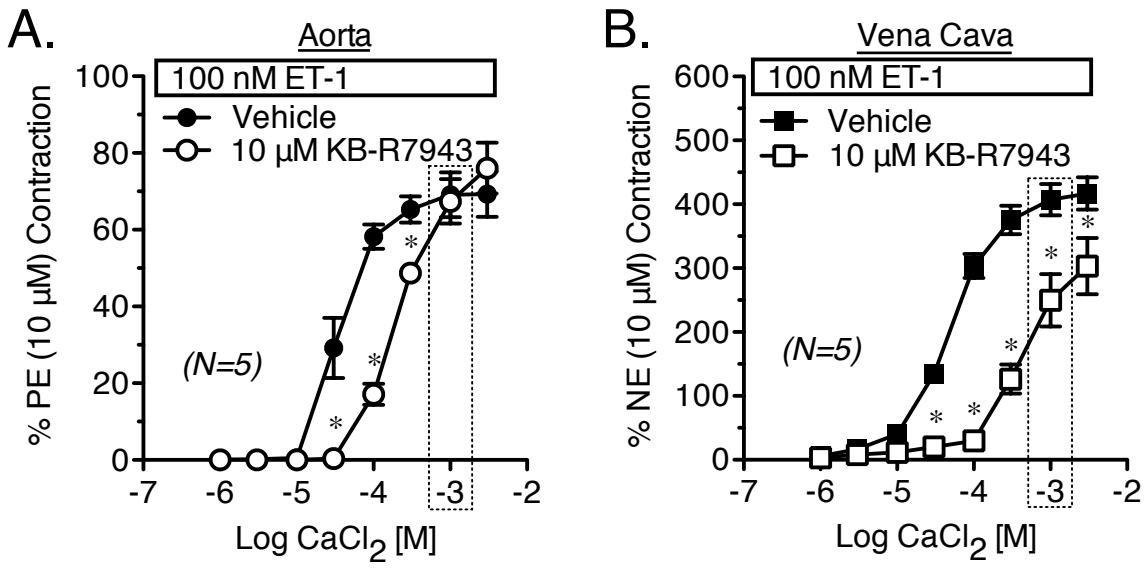

Figure 16. Measurement of $CaCl_2$ concentration response curves in the presence of ET-1 (100 nM), in aorta and vena cava. Aorta (A) and vena cava (B) were first incubated for 30 minutes in Ca^{2+}-free buffer with 1 mM EGTA, then in Ca^{2+}-free buffer (no EGTA) for 10 minutes before addition of 100nM ET-1. After plateau of any contraction to ET-1, tissues were incubated with vehicle (solid shapes) or 10 µM KB-R7943 (open shapes). Points represent mean ± SEM for the number of animals indicated in parentheses. Boxes represent the $CaCl_2$ concentration that is equivalent to that of physiological salt solution used in all other experiments. * = $p<0.05$ *versus* vehicle.

2.5. Potential Secondary Actions of KB-R7943

Our finding that KB-R7943 attenuated KCl-induced contraction suggested that the effects of KB-R7943 on ET-1-induced contraction could be due to voltage-gated Ca^{2+} influx inhibition and not inhibition of the reverse-mode NCX. To test this, we measured KCl- and ET-1-induced contraction in the presence or absence of the L-type Ca^{2+} channel antagonist nifedipine (1 μM), and compared these results to our previous experiments with KB-R7943. As with KB-R7943, nifedipine (1 μM) markedly attenuated the maximal contraction to KCl in both aorta (16.65±2.17%) and vena cava (69.55±15.88%) (**Figure 17a,b**). However, nifedipine had no effect on ET-1-induced contraction in either aorta or vena cava (**Figure 17c,d**). Thus, it was unlikely that the effects of KB-R7943 on ET-1-induced contraction were from off-target inhibition of voltage-gated Ca^{2+} channels.

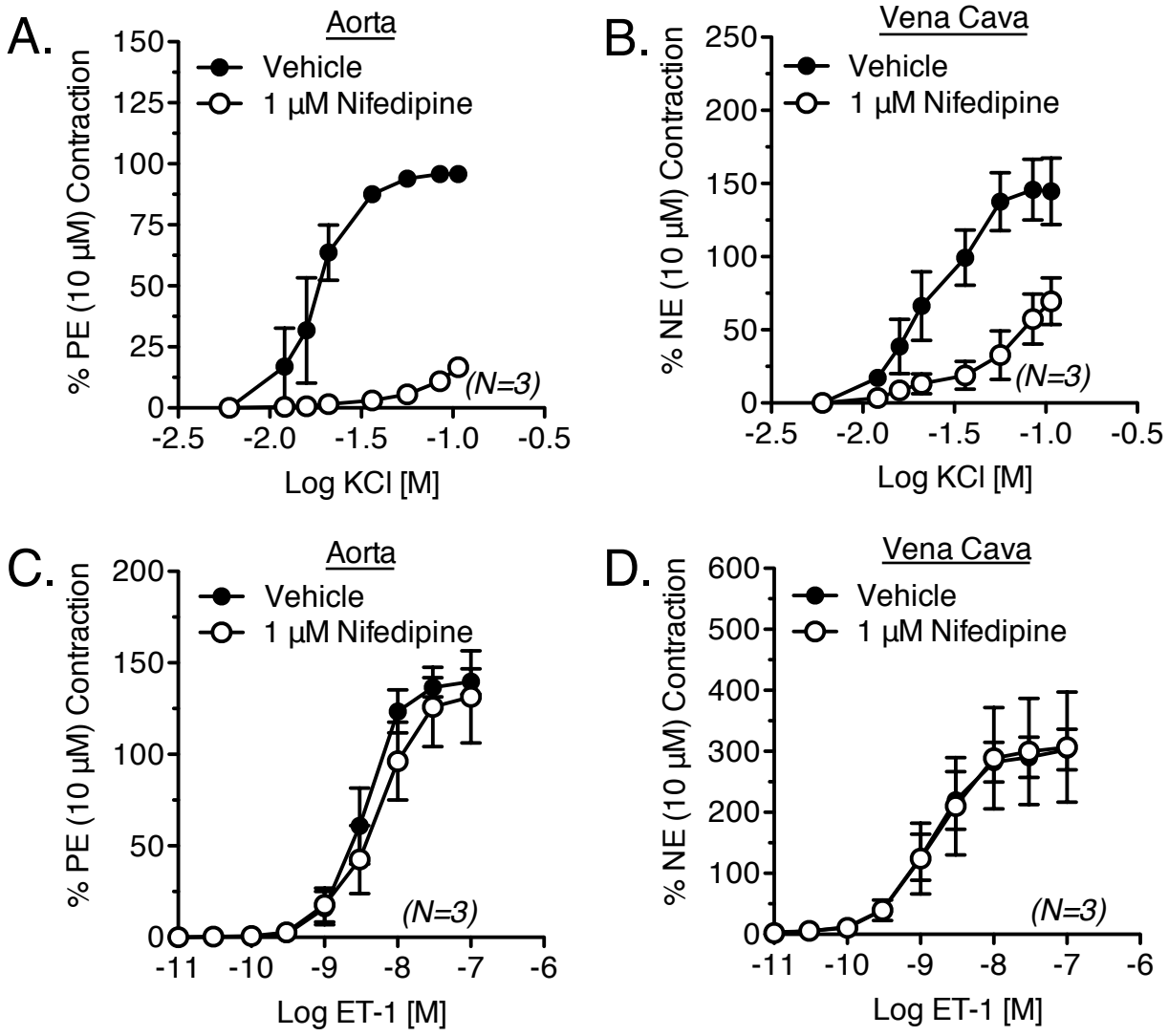

Figure 17. KCl- and ET-1-induced contraction in aorta and vena cava, in the presence or absence of nifedipine. *Top:* Measurement of KCl-induced contraction in aorta (a) and vena cava (b), exposed to vehicle or nifedipine (1 μM). *Bottom*: Measurement of ET-1-induced contraction in aorta (c) and vena cava (d), exposed to vehicle or nifedipine (1 μM). In (a-d), vehicle or antagonists were incubated with tissue for 1h prior to agonist exposure. Points represent mean ± SEM for the number of animals indicated in parentheses. * = $p<0.05$ *versus* vehicle.

3. Discussion

The principal and novel findings of this study are: (1) activation of the reverse-mode NCX by reducing extracellular Na^+ causes contraction and increases intracellular Ca^{2+} in vena cava but not aorta; (2) the reverse-mode NCX inhibitor KB-R7943 selectively attenuates contraction to ET-1 in vena cava but not aorta; and (3) 10 μM KB-R7943 also inhibits KCl-induced contraction to a greater degree in vena cava than in aorta. These latter results suggest that KB-R7943 may also inhibit contraction by inhibition of voltage-gated Ca^{2+} channels. However, we do not believe this accounts for the effects of KB-R7943 on ET-1-induced contraction, because the response to ET-1 appears to be independent of voltage-gated Ca^{2+} channels in both aorta and vena cava. The findings that KB-R7943 inhibits contraction and decreases intracellular Ca^{2+} during low Na^+ exposure in vena cava suggest that the effects of KB-R7943 on venous contraction are due, at least in part, to Na^+-dependent Ca^{2+} influx, possibly through reverse-mode NCX.

3.1. Reverse-mode NCX and Na^+-dependent contraction

We found that removal of Na^+ caused only a small, transient response in aorta that was not affected by KB-R7943. These data suggest that stimulation of reverse-mode NCX does not, in and of itself, cause contraction of aorta. The lack of a response was also not due to lack of protein, since aorta expressed NCX-1 protein robustly. Similar published results show that low Na^+ only caused arterial contraction when intracellular Ca^{2+} stores were depleted, suggesting that Ca^{2+} sequestration by the sarcoplasmic

reticulum attenuated any contraction that could be caused by low Na^+-dependent Ca^{2+} influx [165].

Unlike aorta, vena cava exhibited a prolonged and significant contraction and an increase in intracellular Ca^{2+} when exposed to low Na^+ PSS. The contraction and rise in intracellular Ca^{2+} were attenuated by KB-R7943, suggesting that both depended upon Ca^{2+} influx through the reverse-mode NCX. As with rat aorta, previous studies using rabbit inferior vena cava suggest that the reverse-mode NCX is active after sarcoplasmic stores depletion [163]. Our findings that low Na^+ PSS causes contraction and increases intracellular Ca^{2+} suggest that reverse-mode NCX contributes significantly to contraction in rat vena cava.

3.2. Reverse-mode NCX and agonist-induced contraction

We found that KB-R7943 (10 μM) attenuated ET-1-induced contraction only in vena cava, but attenuated KCl-induced contraction in both aorta and vena cava. However, the inhibitory effect of KB-R7943 on KCl-induced contraction was greater in vena cava than in aorta. KCl-induced contraction is primarily caused by membrane depolarization and subsequent influx of Ca^{2+} through voltage-gated Ca^{2+} channels . This may explain why contraction to KCl in both aorta and vena cava is inhibited by KB-R7943, since membrane potential is an important regulator of NCX function. Membrane depolarization causes the NCX to favor the reverse-mode, while membrane hyperpolarization causes the NCX to favor the forward-mode [158]. The different effects of KB-R7943 on contraction in these tissues may also be because the agonists we

tested increase Na^+ influx in vena cava but not aorta, or that venous smooth muscle contraction relies more heavily on Na^+ influx than aortic smooth muscle. Since the concentration gradient for Na^+ is also an important regulator of NCX function, agonists that increase smooth muscle Na^+ influx may be more likely to activate reverse-mode NCX. Also, KCl can increase Na^+ influx in aorta, since the voltage-gated Na^+ channel blocker TTX inhibited KCl-induced contraction in rat aortic rings [166]. Together, these data suggest that reverse-mode NCX is a significant source of Ca^{2+} influx in vena cava, but is minimally active – or activated only by certain agonists or depolarizing conditions – in aorta.

KB-R7943 caused a rightward shift in the $CaCl_2$ concentration-response curve in the presence of ET-1 (100 nM) in both aorta and vena cava. However, at a $CaCl_2$ concentration equivalent to that of our 'normal' PSS (1.6 mM), there was a ~25% reduction in contraction to calcium in vena cava but no reduction in aorta. These data support a greater role for NCX-mediated calcium influx during venous contraction as opposed to aortic contraction.

The differences between aorta and vena cava could also be due to receptor-mediated activation of protein kinase C (PKC), which enhances NCX function by phosphorylating the central cytosolic domain of the NCX [159]. ET-1 could cause NCX phosphorylation, since ET-1 activates PKC and up-regulates expression of several different PKC isoforms [167]. ET-1 can enhance NCX function in renal epithelial cells by activating PKC, but it is unknown if the same is true in smooth muscle [168]. Further study can

determine if the differences in NCX function between aorta and vena cava are due to differences in Na^+ handling or due to PKC-dependent modification of the NCX.

3.3. Secondary effects of KB-R7943

An increasing number of off-target effects of KB-R7943 have been discovered, leading to doubts about the selectivity of KB-R7943 for the NCX. At concentrations similar to those shown to block reverse-mode NCX, KB-R7943 has been described to inhibit L-type Ca^{2+} channels, TRPC channels, and ryanodine receptors [169-172]. Nevertheless, KB-R7943 continues to be used extensively to study the contribution of NCX to a variety of cellular functions, due in part to the lack of other potent, commercially available NCX inhibitors. Our intention was to validate our findings using other NCX inhibitors, but this proved extremely difficult. We attempted to obtain SEA-0400, another NCX inhibitor reported to have increased potency and selectivity as compared to KB-R7943, but it is not available for researchers at this time. The only other available NCX inhibitor, SN-6, was found to be insoluble in PSS for the duration of incubation required for our experimental paradigm, and thus useless as another NCX inhibitor for comparison to the experiments using KB-R7943. While we recognize the power of confirming our findings with the use of another NCX inhibitor, the insolubility and lack of availability of such compounds made us unable to do so. Instead, we conducted several experiments to differentiate the specific and non-specific effects of KB-R7943 in aorta and vena cava because of the potential for off-target effects.

3.4. Limitations

This study is not without limitations. While we did not assess the depletion of intracellular Ca^{2+} stores in our Ca^{2+} influx experiments, it is likely that sarcoplasmic reticular stores were depleted by incubation in Ca^{2+}-free PSS. Since Ca^{2+} influx *via* the reverse-mode NCX is activated after depletion of calcium stores, the rightward shift caused by KB-R7943 in aorta may be because NCX-mediated Ca^{2+} influx is important for replenishment of sarcoplasmic Ca^{2+} stores. Further experiments will be required to investigate KB-R7943-dependent inhibition of store-operated Ca^{2+} influx directly.

Since we did not investigate differences in NCX isoform expression between aorta and vena cava, it is unknown if our findings are due to differential expression of NCX-1, -2 and -3 in aorta and vena cava. While NCX-1 is expressed ubiquitously, there is disagreement about the predominant form expressed in smooth muscle [120,173]. Also, we did not determine if different splice variants of NCX-1 are expressed in aorta and vena cava. Although NCX1.3 is described as "smooth-muscle specific" [174], pulmonary arterial smooth muscle cells express a variety of variants within the same cell [175]. Nonetheless, KB-R7943 is believed to be non-specific in its ability to inhibit the different NCX isoforms [176], even though some selectivity has been reported at concentrations lower than those used here [177]. The sensitivity of NCX splice variants to KB-R7943 has not been established, and thus cannot be ruled out as another possible explanation for the differences seen between aorta and vena cava.

We did not directly examine the effects of KB-R7943 on TRP channel function. There is an increasing amount of evidence that NCX and TRP channels are either functionally or physically linked [178]. Na^{+} entry through TRP channels is a driving force for Ca^{2+}

entry caused by the reverse-mode NCX [179]. This association makes distinguishing between inhibition of TRP channels by KB-R7943 and inhibition of the NCX extremely difficult. Thus, we cannot be certain that our results are due solely to the actions of KB-R7943 on NCX and not at TRP channels, since the function of the NCX and the opening of TRP channels may be closely intertwined.

Since these experiments were performed in endothelium-intact tissues, we cannot be certain that inhibition of endothelial NCX did alter contraction in aorta and vena cava. Vena cava contain only a single layer of smooth muscle cells, making reliable denudation of the endothelium extremely difficult to accomplish without destroying vessel function. Thus, we elected to use endothelium-intact tissues in these experiments. Even though the endothelium was present in these tissues, it is unlikely that inhibition of endothelial NCX would attenuate contraction in aorta and vena cava. It is unlikely that endothelial NCX are responsible for our findings because activation of reverse-mode NCX in endothelial cells increases nitric oxide production and causes vasorelaxation [124,180,181]. Thus, inhibition of endothelial NCX would likely potentiate, and not inhibit, contraction. However, Inhibition of nitric oxide synthase and cyclooxygenase potentiated the inhibitory effects of KB-R7943 on ET-1-induced contraction in aorta and vena cava (data not shown), suggesting that a portion of the effects of KB-R7943 on ET-1-induced contraction is endothelium-dependent. Further investigation is required to determine is required to properly determine the roles of endothelial NCX *versus* smooth muscle NCX.

3.5. Conclusions

These data suggest that the NCX, while often considered only as a means of Ca^{2+} extrusion, has a prominent role in Ca^{2+} influx and contraction in the vena cava. While activation of reverse-mode NCX alone is incapable of contracting aorta, NCX activation increases intracellular Ca^{2+} and contracts vena cava. Reverse-mode NCX function in vena cava is also suspected during KCl- and ET-1-induced contraction, since the reverse-mode NCX inhibitor KB-R7943 markedly attenuated contraction to these agonists in vena cava. We propose that the effects of KB-R7943 on vena cava and aorta contraction are due to reverse-mode NCX inhibition and not because of one possible secondary action of KB-R7943, inhibition of voltage-gated Ca^{2+} channels. These studies suggest that there is an important difference between arteries and veins in terms of regulation of Ca^{2+} influx during contraction, and that this difference represents potential therapeutic targets for specifically targeting venous smooth muscle to treat vascular diseases like hypertension.

CHAPTER 4: RYANODINE RECEPTORS ARE UNCOUPLED FROM CONTRACTION IN RAT VENA CAVA

1. Rationale

Ryanodine receptors (RyR) are homotetrameric ion channels that are present in the sarcoplasmic reticulum (SR) of vascular smooth muscle that allow for the release of calcium from SR stores [151]. While vascular smooth muscle expresses all 3 known RyR isoforms (RyR1-3), it is primarily the activation of RyR1 and RyR2 that regulates excitation-contraction coupling [47]. These receptors are activated by Ca^{2+}, and can act as amplifiers of smaller Ca^{2+} signals caused by Ca^{2+} influx or inositol 1,4,5-trisphosphate (IP_3)-mediated Ca^{2+} release [57]. This amplification, called "calcium induced calcium release" (CICR), mobilizes large amounts of SR calcium into the cytosol, and serves an important role in excitation-contraction coupling in smooth muscle [126]. CICR from RyR can also terminate voltage-dependent Ca^{2+} influx *via* small, localized releases of Ca^{2+} called Ca^{2+} sparks [182]. Ca^{2+} sparks activate Ca^{2+}-sensitive potassium channels which leads to membrane hyperpolarization and closing of voltage-gated Ca^{2+} channels [183]. Thus, RyR-mediated Ca^{2+} release from SR stores and is both a positive and negative regulator of agonist-induced excitation-contraction coupling in vascular smooth muscle.

Relatively little is known about the mechanisms that govern contraction in venous smooth muscle beyond the general finding that venous contraction is regulated by Ca^{2+} [184,185]. Study of venous smooth muscle is becoming increasingly more relevant

since researchers linked changes in venous capacitance to increased blood pressure [1]. Impaired venous distensibility and decreased venous capacitance are seen in hypertensive patients, which can increase arterial blood volume by decreasing the storage capacity of veins [136,137]. Understanding the mechanisms governing contraction of the large, central veins is particularly important given that venous return to the heart is largely determined by central venous tone [1,76]. Defects in RyR-mediated Ca^{2+} signals are also linked to multiple human cardiovascular pathologies, including congestive heart failure, hypertension and polymorphic ventricular tachycardia [47,186,187]. Thus understanding how RyR regulate venous contractility may help clarify the role of the veins in hypertension and other vascular diseases where venous dysfunction is evident.

Our present goal was to investigate if veins depend on RyR-mediated Ca^{2+} release, as is observed in arteries, to better understand the relationship between Ca^{2+} mobilization and changes in vascular tone. In this study, we first tested the hypothesis that RyR are present in rat aorta and vena cava, and are directly coupled to contraction. For comparison, we then examined the coupling of RyR activation and contraction in two other pairs of arteries and veins to see if our results in vena cava were recapitulated in veins from other vascular beds. While both aorta and vena cava expressed predominantly RyR2, the RyR agonist caffeine (20 mM) caused significant Ca^{2+} release and contraction only in rat aorta. These data suggest that ryanodine receptors, while present in both tissues, are inactive and uncoupled from Ca^{2+} release and contraction in vena cava.

2. Results

2.1. Presence of Ryanodine Receptor mRNA and Protein

Real-time PCR was performed to measure mRNA for all 3 RyR subtypes in rat aorta and vena cava. Both aorta and vena cava expressed significantly more RyR-2 mRNA as compared to RyR-1 and RyR-3, when normalized to β-2-microglobulin expression (**Figure 18a, b**). Using an antibody against RyR1/RyR2 protein, the presence of RyR-1 and RyR-2 protein was then investigated using immunofluorescence and confocal microscopy in freshly dissociated aorta and vena cava smooth muscle cells (**Figure 19**). Most of the freshly dissociated cells express RyR-1/2 protein, as shown by positive red immunofluorescence (**Figure 19a, b**). The fluorescence signal was significantly greater than with secondary antibody alone (**Figure 19g, h**). The cells were also labeled with a FITC-conjugated smooth muscle alpha-actin antibody to distinguish between smooth muscle cells and other non-muscle cells (**Figure 19c, d**). The cells with positive fluorescence for smooth muscle alpha-actin also had positive fluorescence for RyR-1/2, indicating that smooth muscle cells from both aorta and vena cava express RyR-1 and RyR-2 (**Figure 19e, f**).

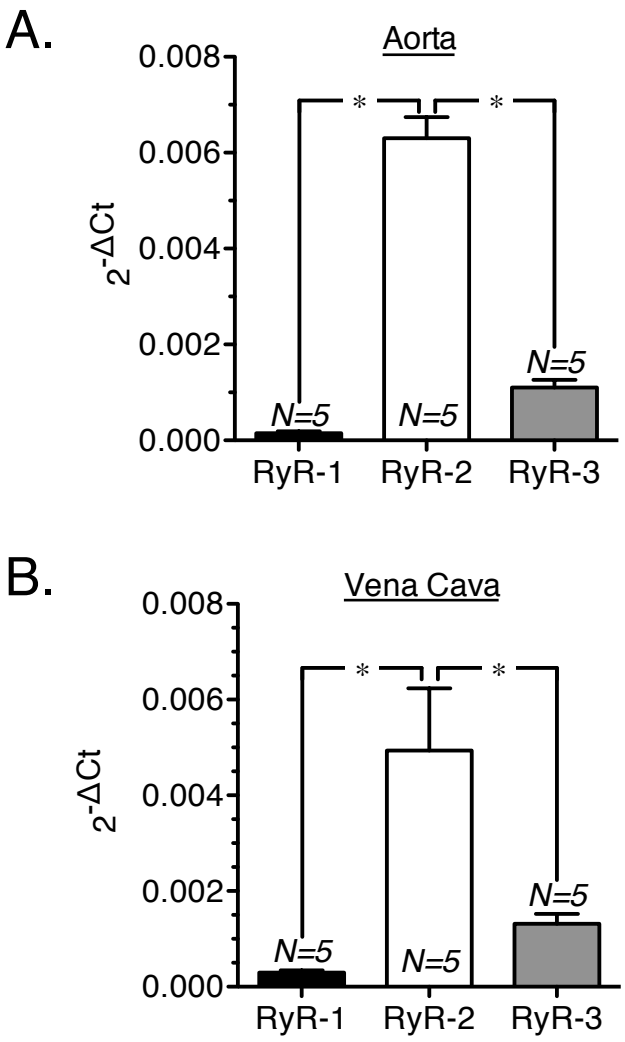

Figure 18. RyR mRNA expression measured by PCR. Summary graph of RyR-1, RyR-2 and RyR-3 mRNA expression in rat aorta (A) and vena cava (B), measured using real-time RT-PCR. White bars indicate RyR1 mRNA; gray bars indicate RyR2; and back bars indicate RyR3. All bars represent mean ± SEM for the number of animals indicated.

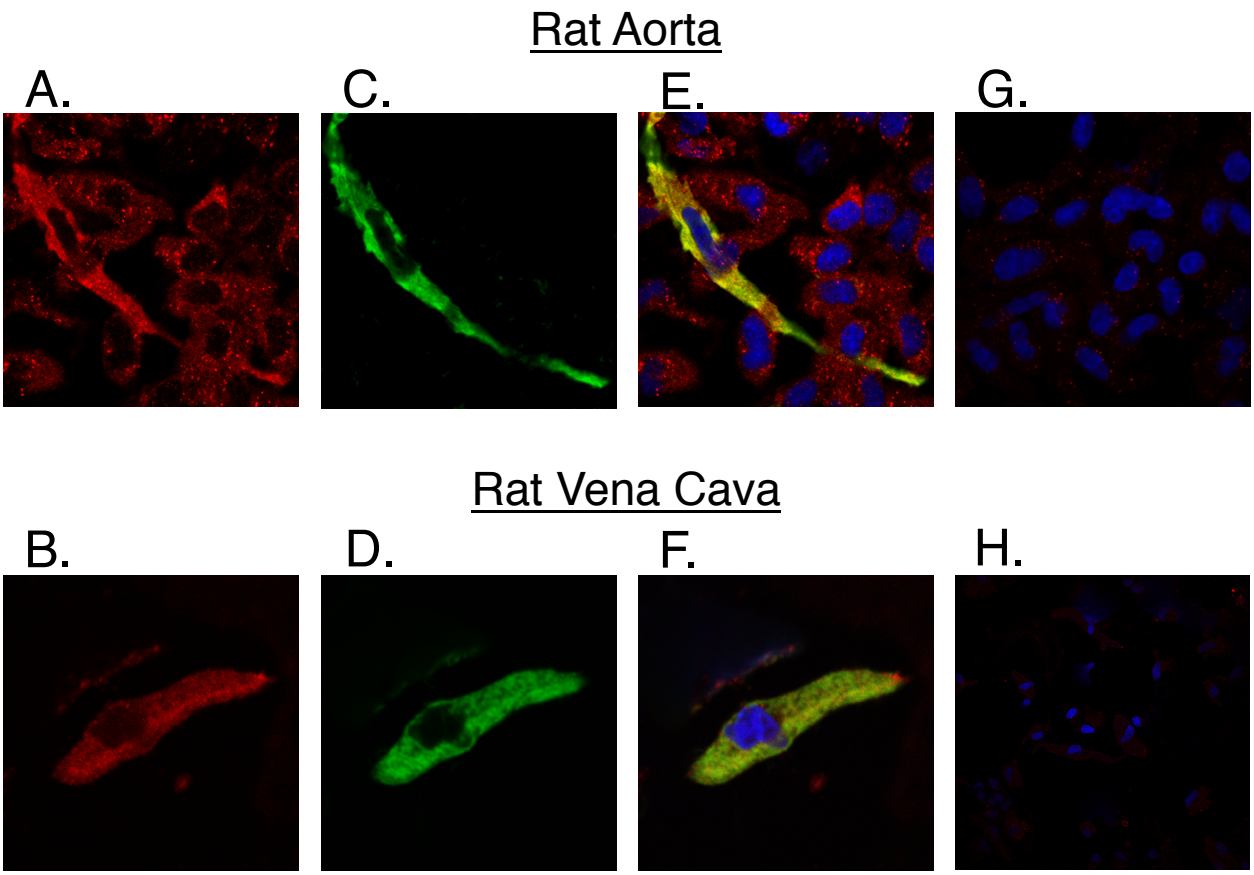

Figure 19. Representative immunohistochemical staining of RyR1/2 in freshly dissociated smooth muscle cells from aorta and vena cava. (A, B) Red fluorescence indicates the presence of RyR1/2 protein. (C, D) Green fluorescence indicates staining for smooth muscle α-actin. (E, F) Overlay of RyR1/2 (red), smooth muscle α-actin (green) and DAPI nuclear stain (blue). (G, H) Negative controls, where primary antibodies were absent. Representative of 3 experiments.

2.2. Aorta and Vena Cava have Sarcoplasmic Calcium Stores

As an indirect measurement of sarcoplasmic calcium stores in aorta and vena cava, store-operated calcium entry (SOCE) was measured in both tissues. SOCE is activated after intracellular Ca^{2+} stores depletion in smooth muscle, and thus the presence of SOCE is indicative of the presence of sarcoplasmic calcium stores [188]. To deplete intracellular Ca^{2+} stores, aorta and vena cava were placed in Ca^{2+}-free PSS and then exposed to vehicle or the irreversible sarcoplasmic reticulum calcium ATPase (SERCA) inhibitor thapsigargin (1 μM) for 1 hour. After one hour, Ca^{2+}-replete PSS was reintroduced to the tissues and the resulting contraction was measured (**Figure 20**). Upon reintroduction of extracellular Ca^{2+}, aorta and vena cava exposed to thapsigargin (1 μM) exhibited a sustained contraction that was absent in vehicle-exposed tissues (**Figure 20a-d**). This contraction was significantly greater in tissues exposed to thapsigargin (**Figure 20e**), and was thus indicative of store-operated calcium entry and the presence in intracellular Ca^{2+} stores in both tissues..

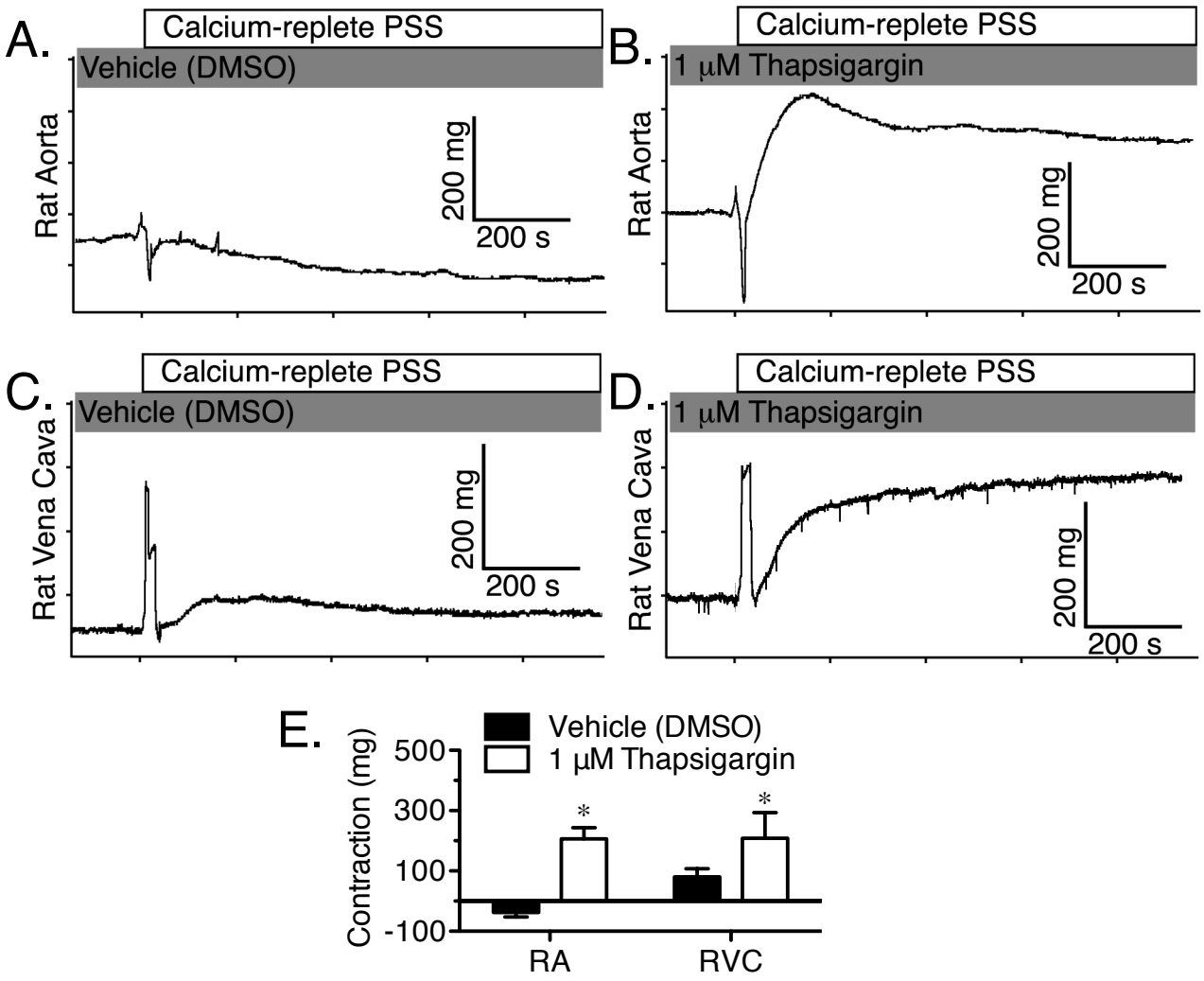

Figure 20. Rat aorta and vena cava contraction after sarcoplasmic calcium stores depletion and upon exposure to Ca^{2+}-replete PSS. Tissues were incubated in Ca^{2+}-free buffer for 15 minutes before addition of thapsigargin (1 μM). Tissues were incubated for 1 hour before reintroduction of Ca^{2+}. Shown are responses from tissues incubated with vehicle (A,C) and 1 μM thapsigargin (B,D). (E) Summary bar graph indicating the maximum contractile response in aorta (RA and vena cava (RVC). Black bars represent vehicle-exposed tissues. White bars represent tissues exposed to thapsigargin (1 μM). N=4; * = $p<0.05$ versus vehicle.

2.3. Ryanodine Receptor Activation by Caffeine

To test the relationship between RyR activation and smooth muscle function, isometric contraction to the RyR agonist caffeine was measured in aorta and vena cava (**Figure 21a,b**). Caffeine (20 mM) caused a significant and transient contraction in RA that was reproducible after a 45-minute washout period (**Figure 21c**). RVC exhibited no contraction; rather, caffeine caused a reproducible relaxation (**Figure 21c**). In RA, the RyR antagonists ryanodine (10 μM) or tetracaine (100 μM) inhibited contraction to caffeine by ~50% and ~75%, respectively (**Figure 22**).

To test if other veins were also unresponsive to 20 mM caffeine, caffeine-induced contraction was investigated in two other artery-vein pairs: (1) carotid artery and jugular vein; and (2) superior mesenteric artery and superior mesenteric vein. Unlike RVC, CA and JV contracted to 20 mM caffeine (**Figure 23a**). However, the caffeine-induced contraction in jugular vein was significantly less than in carotid artery. In superior mesenteric artery and vein, 20 mM caffeine elicited equivalent contractions in both tissues (**Figure 23b**). These data show that some veins do contract in the presence of caffeine, and thus the lack of response to caffeine in RVC is not representative of all veins.

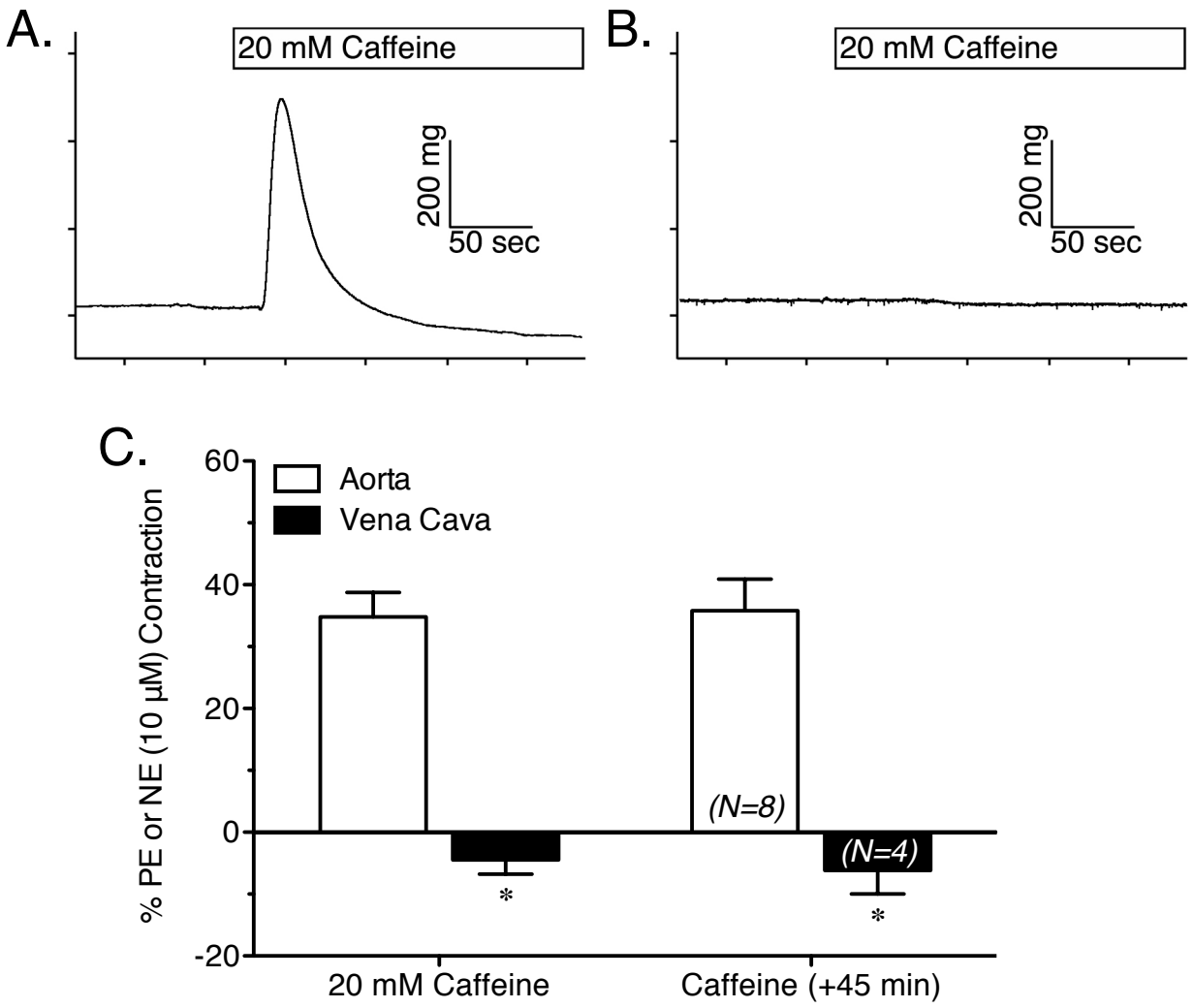

Figure 21. Representative tracings of contractile response to 20 mM caffeine. Tracings show response of rat aorta (a) and rat vena cava (b). (c) Summary bar graphs indicating the maximum response to initial caffeine exposure, and then to a second exposure after 45 minutes of washout. White bars represent aorta. Black bars represent vena cava. N=4-8; * = $p<0.05$ versus aorta.

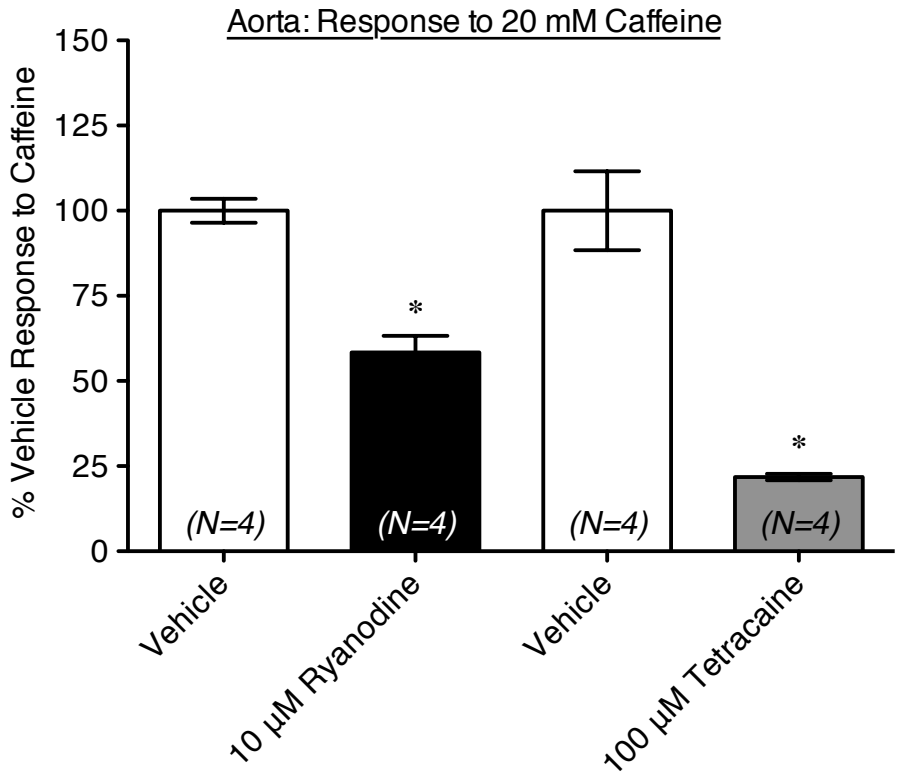

Figure 22. Measurement of 20 mM caffeine-induced contraction of rat aorta, in the presence of the ryanodine receptor antagonists ryanodine (10 µM) or tetracaine (100 µM). Vehicle or antagonists were incubated with tissue for 1h prior to caffeine exposure. White bars represent vehicle-exposed aorta. Black bars represent ryanodine-exposed aorta. Grey bars represent tetracaine-exposed aorta. Bars represent mean ± SEM for the number of animals indicated in parentheses. * = $p<0.05$ versus vehicle.

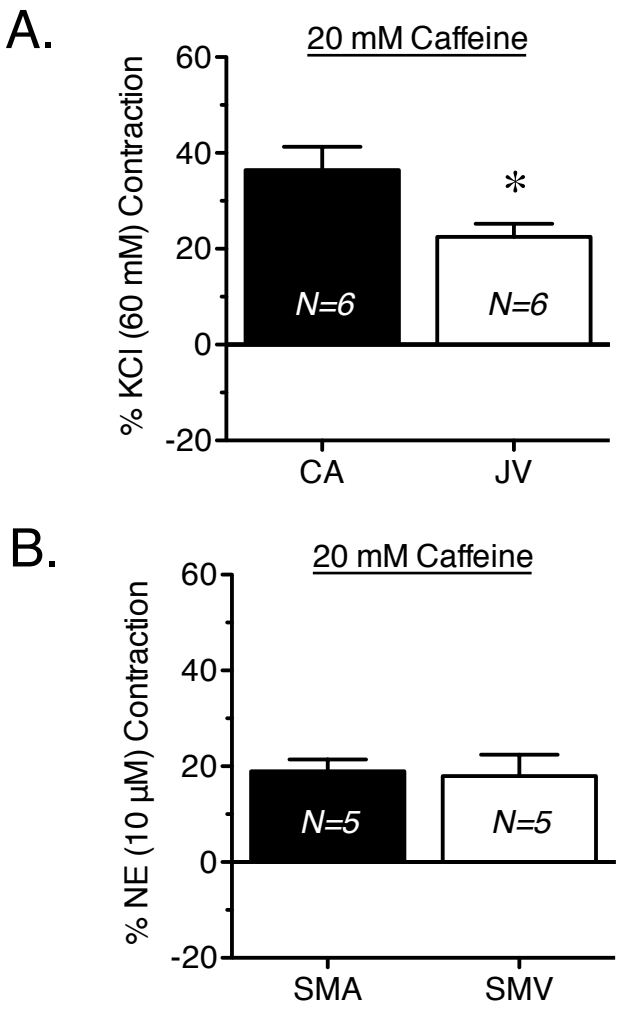

Figure 23. Responses to 20 mM caffeine in two other pairs of arteries and veins. Shown are responses to caffeine (20 mM) in: (A) carotid artery and jugular vein; and (B) superior mesenteric artery and vein. Summary bar graphs indicating the maximum response to caffeine exposure as a percent of initial contractile stimuli. Black bars represent carotid artery (CA) and superior mesenteric artery (SMA). White bars represent jugular vein (JV) and superior mesenteric vein (SMV). N=5-6; * = $p<0.05$ *versus* artery.

2.4. Ryanodine Receptor Activation and Intracellular Calcium Mobilization

RA contraction by caffeine (20 mM) also correlated to an increase in global intracellular calcium, as measured using the ratiometric calcium indicator Fura-2 (**Figure 24a**). However, no comparable increase in global calcium was seen in response to caffeine (20 mM) in RVC. Instead, a small transient increase in Ca^{2+} was superimposed upon a fall in global Ca^{2+} (**Figure 24b**). Consistent with the data presented in **Figure 21**, caffeine again caused relaxation in RVC, rather than contraction. These data indicate that RyR activation by caffeine was not able to cause contraction or a sustained increase in global cytosolic Ca^{2+} in RVC.

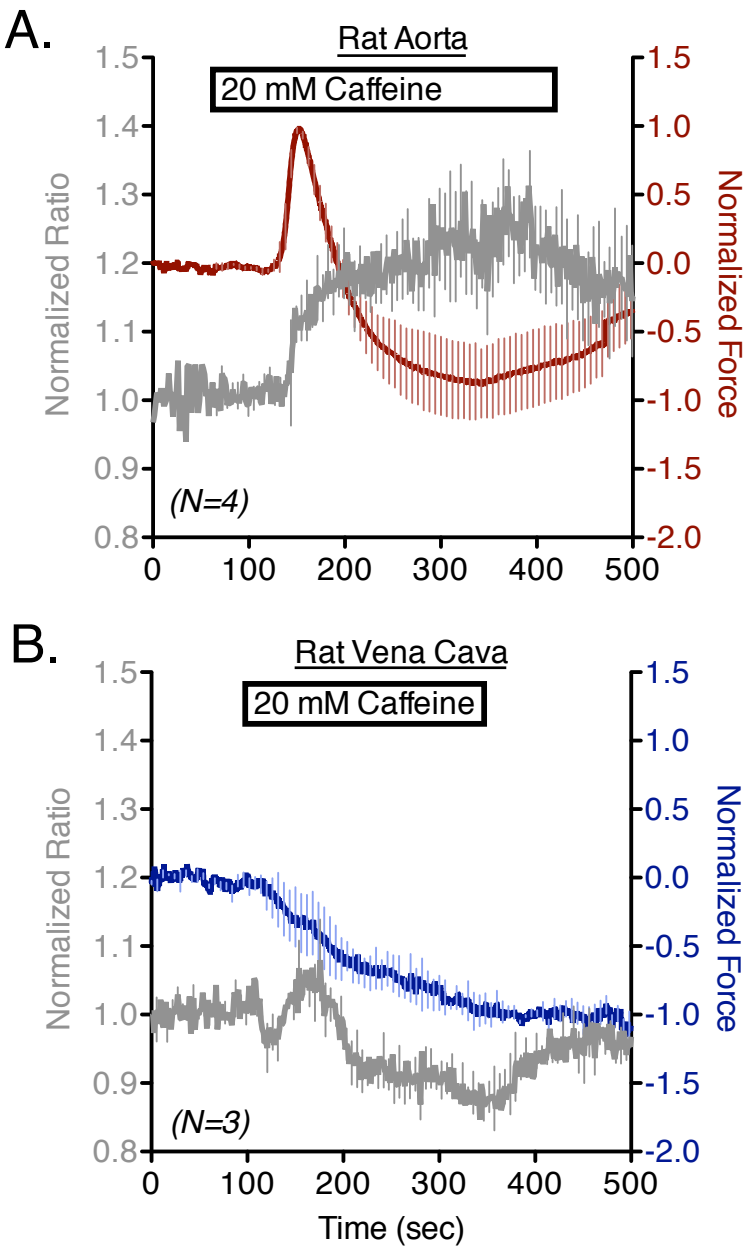

Figure 24. Intracellular Ca^{2+} and contraction in response to caffeine. Simultaneous measurement of Fura2-AM fluorescence ratio (grey, left axis) and caffeine response (red/blue, right axis) in vena cava (A) and aorta (B). Lines represent mean ± SEM for the number of experiments indicated. N=3-4.

3. Discussion

The principal and novel findings of this study are: (1) aorta and vena cava smooth muscle cells express ryanodine receptors; (2) RyR activation by caffeine neither contracts nor increases intracellular Ca^{2+} in vena cava; and (3) the lack of contraction to caffeine is unique to vena cava, since jugular vein and superior mesenteric vein contracted when exposed to caffeine. These findings were not because vena cava lacked intracellular Ca^{2+} stores, since both aorta and vena cava exhibited robust contraction after stores depletion and SERCA inhibition that is consistent with SOCE and the presence of readily releasable intracellular Ca^{2+} stores. These findings imply that the absence of RyR-mediated contraction is specific to vena cava, is not indicative of the responses to caffeine in other veins or arteries, and is not because vena cava lacks intracellular stores of Ca^{2+}.

3.1. Ryanodine Receptor Expression

While expression of RyR mRNA was similar in aorta and vena cava, RyR protein expression in these tissues could not be quantified reliably. Due to the large size of the RyR proteins (~550 kDa) [189], high molecular weight Western blotting techniques were required to reliably differentiate RyR protein from other proteins greater than ~300 kDa [190]. While we were able to consistently show RyR-1 and RyR-2 expression in positive controls (diaphragm and heart, respectively; data not shown), we were unable to show expression of any RyR protein in aorta or vena cava whole tissue homogenates. We were also unable to show RyR-3 expression with any specificity in our controls due to

the lack of an adequately selective RyR-3 antibody. Also, many of the published results showing RyR protein by Western blot utilized enriched, purified RyR protein [152,191-193]. This technique was inappropriate for testing our hypotheses since reasonable comparisons between venous and arterial RyR expression would be impossible after enrichment and purification. Instead, immunofluorescence was used to provide evidence, albeit qualitative, that RyR mRNA in aorta and vena cava smooth muscle cells is translated into RyR protein. RyR fluorescence intensity (**Figure 19a, b**) appears higher in aorta smooth muscle cells as compared to vena cava, but these experiments were analyzed under different conditions and on different days. Thus, it is impossible to know if the apparent differences in intensity were due to differences in protein expression or due to differences in detection parameters. Nonetheless, both tissues expressed positive immunofluorescence for RyR protein that was significantly greater than control. This positive immunofluorescence for RyR protein in both tissues suggests that the lack of physiological response in vena cava was because RyR were incapable of adequate Ca^{2+} release for contraction in response to caffeine. Further immunofluorescent experimentation will be required to quantify the amount of RyR protein expressed in both tissues, to determine if the lack of contraction to caffeine in vena cava is due to decreased RyR expression and not RyR dysfunction.

3.2. RyR-mediated Ca^{2+} release and contraction

The RyR activator caffeine (20 mM) caused a transient but significant contraction in aorta that was absent in vena cava, but present in mesenteric and jugular vein. While

these initial experiments implied that RyR activation is uncoupled from contraction in vena cava, these data did not measure changes in intracellular Ca^{2+} elicited by caffeine. Even though no contraction was evident, it was possible that caffeine was activating RyR-dependent Ca^{2+} release from the SR in a quantity that was insufficient to activate the contractile machinery of vena cava smooth muscle. When we investigated the global Ca^{2+} changes caused by caffeine in vena cava, caffeine did appear to cause a small, transient increase in global Ca^{2+} that was not associated with contraction. Instead, this increase occurred superimposed on a prolonged decrease in global intracellular Ca^{2+} that was associated with venorelaxation. Taken together, these data are consistent with the idea that vena cava contain functional RyR, but these receptors are uncoupled from contraction due to insufficient Ca^{2+} release.

One possible explanation for the inactivity of RyR in vena cava is that the receptor is locked in an inactive state by any one of a number of RyR regulating proteins, such as FKBP12 and sorcin [47,194]. Caffeine is an *activator* – not an *agonist* – of RyR, and it elicits Ca^{2+} release by changing the Ca^{2+} sensitivity of RyR from micromolar to nanomolar (or even picomolar) concentrations [195,196]. Since several RyR regulatory proteins are identified that act as allosteric inhibitors of RyR function, the receptors may be unresponsive to changes in calcium sensitivity and thus remain closed [189]. Further investigation will be required to determine which of the known allosteric modulators of RyR function are expressed in vena cava smooth muscle and if these proteins are responsible for the lack of caffeine-induced calcium release and contraction in vena cava.

Another explanation for the absence of contraction to caffeine in vena cava is that RyR are sparsely expressed on the SR membrane. For caffeine to cause contraction, RyR on the SR membrane need to be expressed in sufficient density and proximity to one another to cause CICR and subsequent contraction. If the spatial arrangement is such that CICR cannot occur, RyR activation would cause a small, transient release of SR Ca^{2+} that cannot propagate and thus contraction would be absent [45].

In arterial smooth muscle, localized Ca^{2+} release events from RyR, called Ca^{2+} sparks, activate large-conductance Ca^{2+}-activated K^+ (BK) channels to cause membrane repolarization and relaxation without increasing global cytosolic Ca^{2+} [182,183]. Ca^{2+} sparks have also been identified in mesenteric vein, and inhibition of these sparks causes contraction [138]. This suggests that functional RyR are present and coupled to contraction in other tissues from the venous circulation. While sparks have not yet been identified in vena cava, functional BK channels are expressed in vena cava smooth muscle [4,105,197]. Our experiments show that activation of RyR cannot significantly increase global cytosolic Ca^{2+} or cause contraction in vena cava, but we did not test for the presence of localized Ca^{2+} spark events. Further investigation will be required to determine if RyR-mediated Ca^{2+} sparks occur in vena cava smooth muscle, and to determine their effect on venous tone.

Finally, it is possible that RyR in vena cava are incapable of forming functional channels in the SR membrane. In the rat myometrium, for example, RyR are expressed but the tissue is completely insensitive to caffeine [4,198,199]. This insensitivity is linked to the expression of an RyR variant that is incapable of associating into a functional tetrameric

receptor [29,106,200]. Although we did not investigate the expression of RyR splice variants in vena cava, this is a possible explanation for the presence of RyR protein but the absence of a RyR-mediated response.

3.3. Conclusions

Our data suggest that ryanodine receptors, while present in vena cava, are uncoupled from contraction and incapable of causing a sustained increase in intracellular Ca^{2+}. In rat aorta, however, activation of RyR by caffeine causes intracellular Ca^{2+} release and contraction. The lack of RyR-mediated contraction also appears to be specific to vena cava, because both the jugular vein and superior mesenteric vein contract to caffeine. This suggests that regional heterogeneity of RyR function exists within the venous circulation. Consistent with this hypothesis, regional heterogeneity in the function and expression of RyR has previously been reported in other vascular tissue [30,201,202].

These data show that the vena cava is one of few – if not the only – blood vessel that is completely insensitive to caffeine, both in terms of contractile response and Ca^{2+} release. Furthermore, this insensitivity represents a fundamental difference between vena cava and aorta smooth muscle in terms of excitation-contraction coupling and Ca^{2+} mobilization during contraction. These studies also identify a new and important difference in SR Ca^{2+} release mechanisms present in vena cava, as compared to several other arteries and veins. Given the role of the vena cava in regulating venous return to the heart, this difference represents a novel area of research for potential

therapeutic targets that can specifically alter vena cava smooth muscle tone to treat vascular diseases like hypertension.

CHAPTER 5: VENOUS CONTRACTION TO ENDOTHELIN-1 IS DEPENDENT ON PHOSPHOLIPASE C, BUT INDEPENDENT OF IP_3 RECEPTOR ACTIVATION

1. Rationale

Cytosolic calcium is tightly regulated by a multitude of ion channels and exchangers that control Ca^{2+} influx, efflux and sequestration, as well as the release of calcium stores [32-34,107-109]. The majority of released Ca^{2+} is vascular smooth muscle comes from the sarcoplasmic reticulum (SR), mainly through the activation and opening of two Ca^{2+} channels: inositol 1,4,5-trisphosphate (IP_3) receptors and ryanodine receptors [46,47,110]. IP_3 is produced when phospholipase C (PLC) hydrolyzes phosphatidylinositol 4,5-bisphosphate (PIP_2), generating both IP_3 and diacylglycerol (DAG) [51,111]. IP_3 activates IP_3 receptors on the SER membrane, which then open and allow Ca^{2+} to leave the SR and enter the cytoplasm [52,112]. DAG activates protein kinase-C (PKC), which then can inhibit IP_3 production by PLC, and thus reduce IP_3-dependent Ca^{2+} release [54,113]. PKC also phosphorylates voltage-gated calcium channels, which alters their function to either inhibit or sustain Ca^{2+} influx [30,114,115]. This process can repeat rhythmically, causing "Ca^{2+} waves" of increasing and decreasing $[Ca^{2+}]_i$ to propagate throughout the entire cell [116,117,203].

Endothelin-1 (ET-1) is a 21-amino acid peptide, originally characterized as an endothelium-derived constricting factor in the vasculature [6,44]. The physiological responses elicited by ET-1 are attributed to the two G protein-coupled receptors (GPCR's) to which ET-1 binds: the ET_A and ET_B receptor [25,67,118]. Generally, the

effects of ET_A and ET_B receptors are in opposition to one another [119,204]. This is true in most vascular smooth muscle, where ET_A receptor stimulation causes contraction and ET_B stimulation causes relaxation [120,205]. However, veins also have functional ET_B receptors on smooth muscle that mediate contraction [121,148].

ET-1-induced contraction of arterial smooth muscle is a Ca^{2+}-dependent process, requiring both activation of extracellular Ca^{2+} influx and release of intracellular Ca^{2+} stores [122,206]. ET_A receptors on arterial smooth muscle are coupled to $G\alpha_Q$ and thus ET-1-mediated release of SR Ca^{2+} is regulated primarily by the production of IP_3 by phospholipase-C [123,207]. While Very little is known about ET-1-mediated Ca^{2+} signals in veins, ET-1 does cause wave-like Ca^{2+} oscillations in rabbit inferior vena cava, suggesting an important role for SR-mediated Ca^{2+} release during venous contraction to ET-1 [124,125,184].

More attention has been given to the physiology of veins since researchers linked changes in venous capacitance to increases in blood pressure [1,126]. The role of veins in regulating blood pressure is still largely overlooked, even though it was noted over 25 years ago that human hypertensive patients demonstrated impaired venous distensibility and decreased venous capacitance [127,136,137]. This change in distensibility could ultimately increase blood pressure by increasing arterial blood volume as the storage capacity of veins decreases. ET-1 may play an important role in regulating venous capacitance during both physiological and pathophysiological conditions, since veins are more sensitive to ET-1 than arteries and maintain sensitivity to ET-1 in hypertension [2,128,149].

Our present goal was to investigate if ET-1-induced contraction in veins depends on IP_3-mediated Ca^{2+} release, to better understand the relationship between ET-1-induced Ca^{2+} mobilization and venoconstriction. In this study, we first tested the hypothesis that IP_3 receptors are present in rat aorta and vena cava, and are directly coupled to contraction. We then tested the hypothesis that ET-1-induced contraction of aorta and vena cava depends on IP_3-mediated Ca^{2+} release from SR stores.

2. Results

2.1. Presence of IP_3 Receptor Protein

Whole-tissue homogenates of rat aorta and vena cava were used to investigate IP_3R protein expression by Western blot (**Figure 25**). A ~260 kDa band was present in all tissues, when probed with antibodies against each of the three IP_3R subtypes (**Figure 25a-c**, dashed boxes). Densitometry of the Western blot results found no significant differences in IP_3R subtype expression in aorta (**Figure 25d**). However, vena cava expressed significantly more IP_3R-3 protein as compared to IP_3R-1 (**Figure 25e**). The presence IP_3R protein in smooth muscle was then investigated using immunofluorescence and confocal microscopy in freshly dissociated smooth muscle cells from aorta (**Figure 26**) and vena cava (**Figure 26**). Aortic smooth muscle cells showed positive red immunofluorescence for IP_3R-1 (**Figure 26a**), IP_3R-2 (**Figure 26b**) and IP_3R-3 (**Figure 26c**). The IP_3R-positive cells also positively expressed smooth muscle alpha-actin (**Figure 26d-f**), indicating that these cells were smooth muscle cells and not another cell type. The fluorescence for both IP_3R and alpha-actin was significantly greater than in samples using secondary antibody alone (**Figure 26g-i**). Vena cava smooth muscle cells also showed positive red immunofluorescence for all three IP_3R subtypes (**Figure 27a-c**) in smooth muscle cells expressing alpha-actin (**Figure 27d-f**). As in aorta, fluorescence for both IP_3R and alpha-actin in vena cava smooth muscle cells was significantly greater than in samples using secondary antibody alone (**Figure 27g-i**).

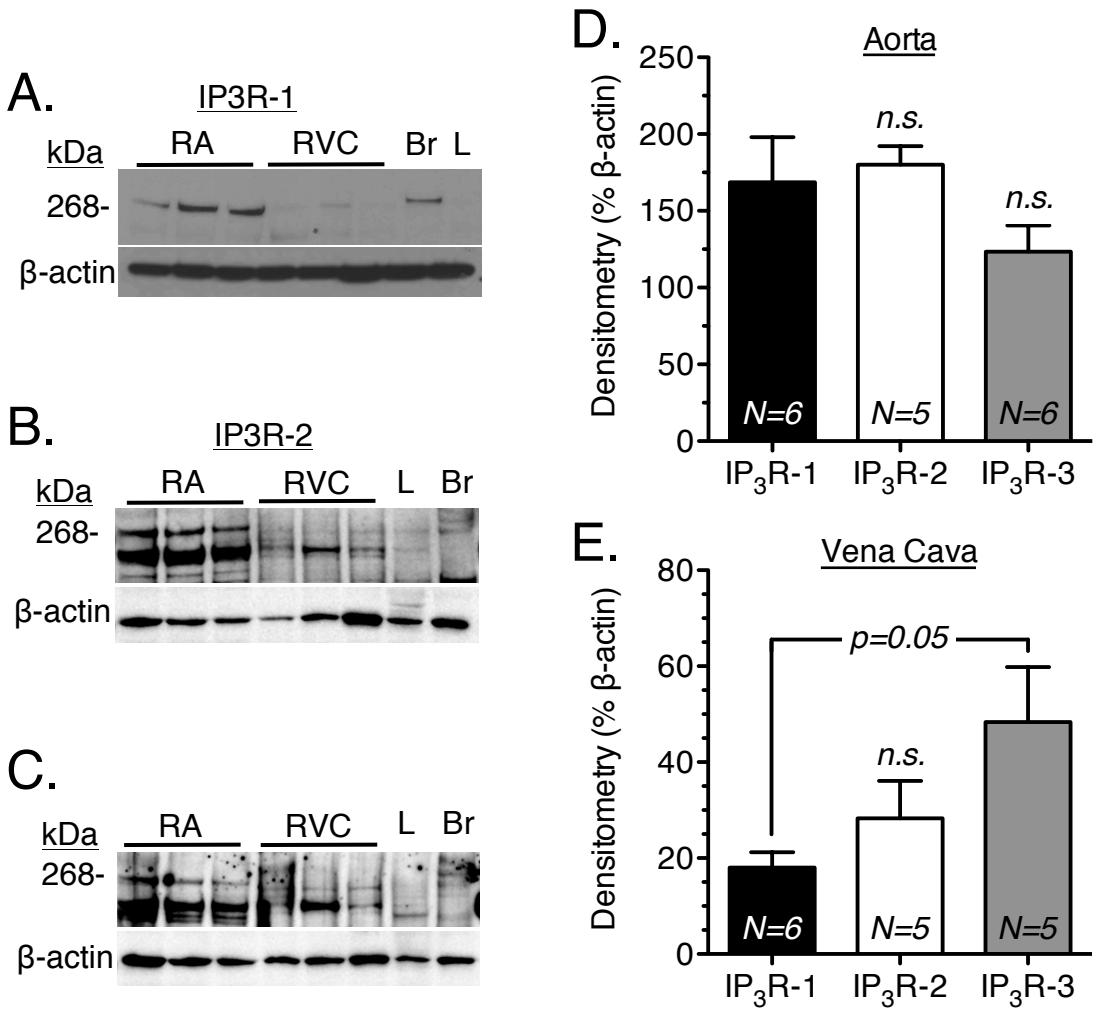

Figure 25. Representative Western blot analysis of IP_3R protein expression. 50 µg of whole-tissue homogenate from rat aorta (RA) and vena cava (RVC) were used, and homogenate from rat brain (Br) and liver (L) were also included as controls. Blots were probed using antibodies against IP_3R-1 (A), IP_3R-2 (B) and IP_3R-3 (C), as well as β-actin (loading control). (D) In rat aorta, densitometry of IP_3R western blot analysis shows no significant difference in IP_3R-1 (black bars), IP_3R-2 (white bars) and IP_3R-3 (grey bars). (E) In rat vena cava, densitometry shows significantly more IP_3R-3 protein as compared to IP_3R-1. n.s. = $p>0.05$; N=5-6.

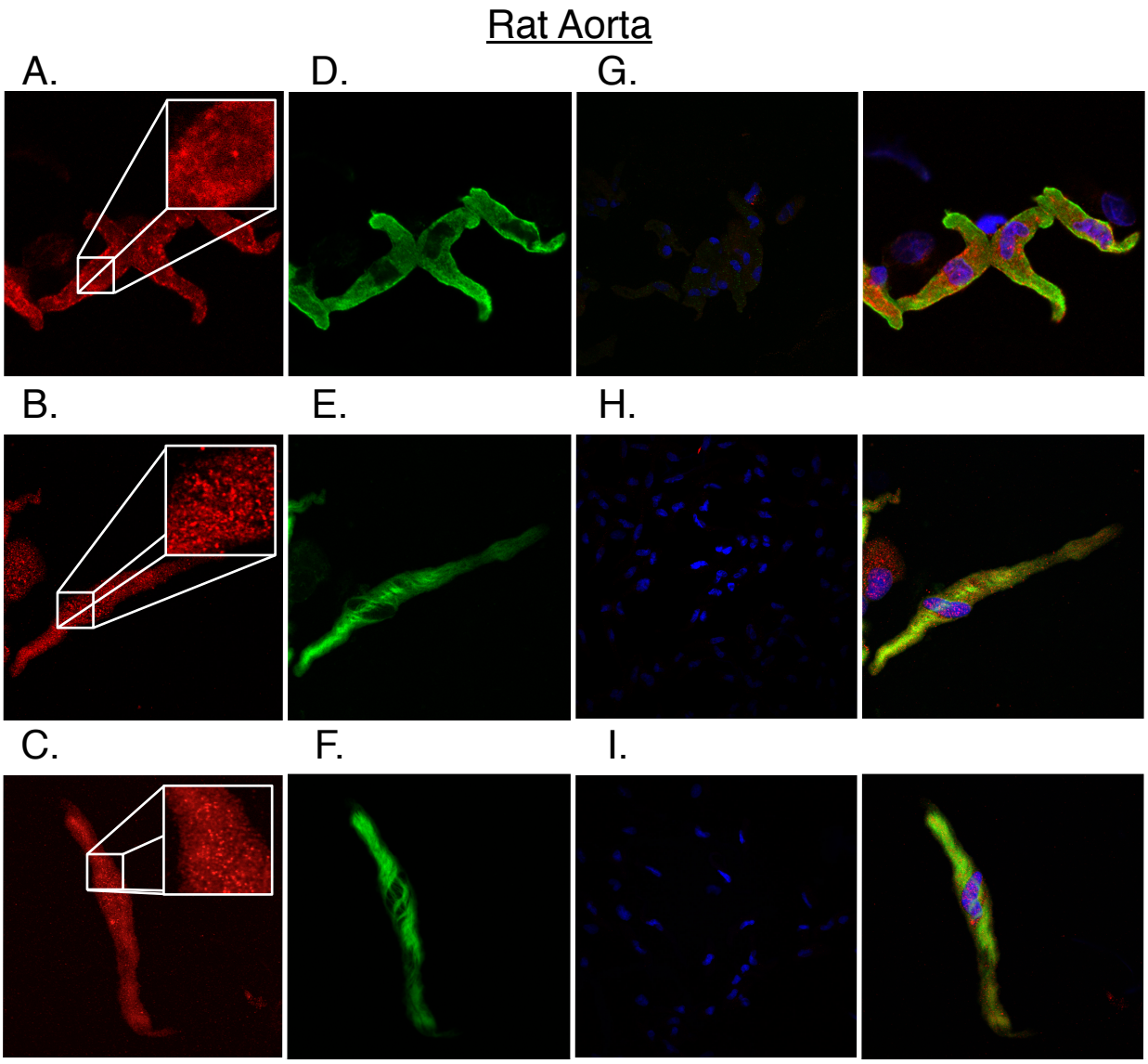

Figure 26. Representative immunohistochemical staining for all IP_3R subtypes in freshly dissociated smooth muscle cells from rat aorta. (A-C) Red fluorescence: punctate staining (*inset*) for IP_3R-1 (A), IP_3R-2 (B) and IP_3R-3 (C) protein. (D-F) Green fluorescence: smooth muscle α-actin. (G-I) Negative controls: primary antibodies were absent. Also shown is an overlay (right) of IP_3R (red), smooth muscle α-actin (green) and DAPI nuclear stain (blue). Representative of 4 experiments.

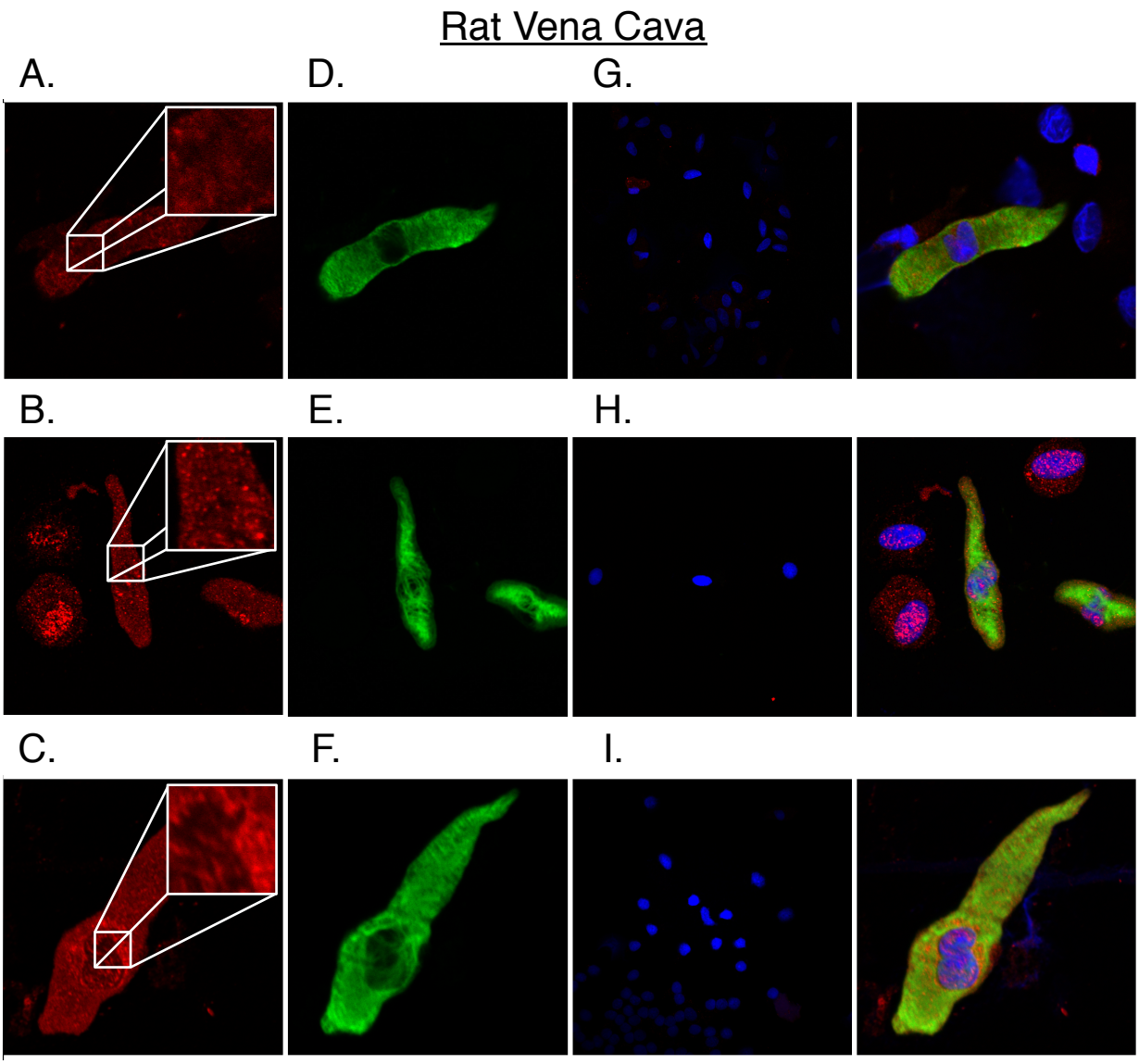

Figure 27. Representative immunohistochemical staining for al IP_3R subtypes in freshly dissociated smooth muscle cells from rat vena cava. (A-C): Red fluorescence: punctate staining (*inset*) for IP_3R-1 (A), IP_3R-2 (B) and IP_3R-3 (C) protein. (D-F) Green fluorescence: smooth muscle α-actin. (G-I): Negative controls: primary antibodies were absent. Also shown is an overlay (right) of IP_3R (red), smooth muscle α-actin (green) and DAPI nuclear stain (blue). Representative of 4 experiments.

2.2. IP_3 Receptor Activation and Contraction

To test the relationship between IP_3R activation and smooth muscle function, isometric contraction of aorta and vena cava was measured in the presence of the membrane permeable IP_3 analog Bt- IP_3. Bt- IP_3 (10 μM) caused a prolonged contraction in aorta (**Figure 28a**) and vena cava (**Figure 28b**), suggesting that IP_3R activation was coupled to contraction in both aorta and vena cava.

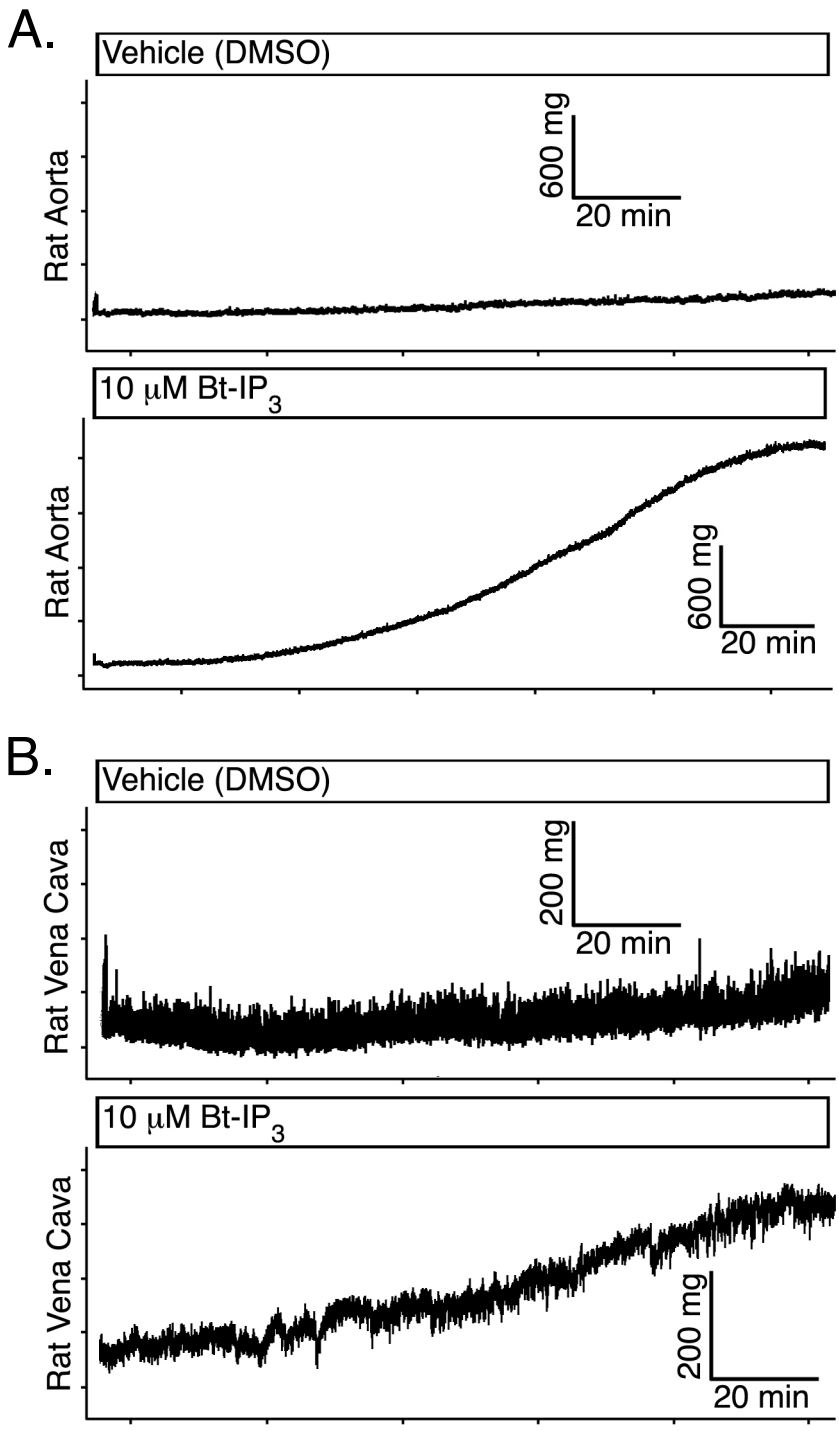

Figure 28. Rat aorta and vena cava contract to the membrane permeable IP_3 analogue, Bt-IP_3. Representative tracings of rat aorta (A) and vena cava (B)

contraction during exposure to Bt-IP_3, a membrane permeable analogue of IP_3. Shown are responses from tissues incubated with vehicle (*top*) and 10 μM Bt-IP_3 (*bottom*). Representative of 4 experiments.

2.3. IP_3-Mediated Calcium Release

Ca^{2+} waves are localized increases in Ca^{2+} that propagate globally across a cell [129,208]. In vascular smooth muscle, Ca^{2+} waves are mediated primarily by IP_3-dependent Ca^{2+} release from the SR [53,130]. Using confocal microscopy and the intensiometric Ca^{2+} indicator Fluo-4, Ca^{2+} waves were measured in aorta and vena cava smooth muscle exposed to no agonist, an adrenergic agonist (NE or PE, 10 μM) and ET-1 (100 nM). Aorta and vena cava exhibited spontaneous wave-like Ca^{2+} oscillations (**Figure 29**). In aorta, calcium waves were synchronous in virtually all cells in the absence of agonist (**Figure 30a**), and in the presence of 10 μM PE (**Figure 30b**) or 100 nM ET-1 (**Figure 30c**). Ca^{2+} waves in vena cava were asynchronous in the absence of agonist (**Figure 31a**) and in the presence of 10 μM NE (**Figure 31b**). In the presence of ET-1 (100 nM), vena cava smooth muscle began to exhibit synchronous Ca^{2+} waves (**Figure 31c**). We next examined the amplitude, occurrence, frequency and velocity of Ca^{2+} waves in venous smooth muscle. While wave amplitude was similar under all conditions (**Figure 32a**), both NE and ET-1 increased the occurrence of Ca^{2+} waves in vena cava (**Figure 32b**). Only ET-1 significantly increased the frequency and velocity of Ca^{2+} waves (**Figure 32c,d**).

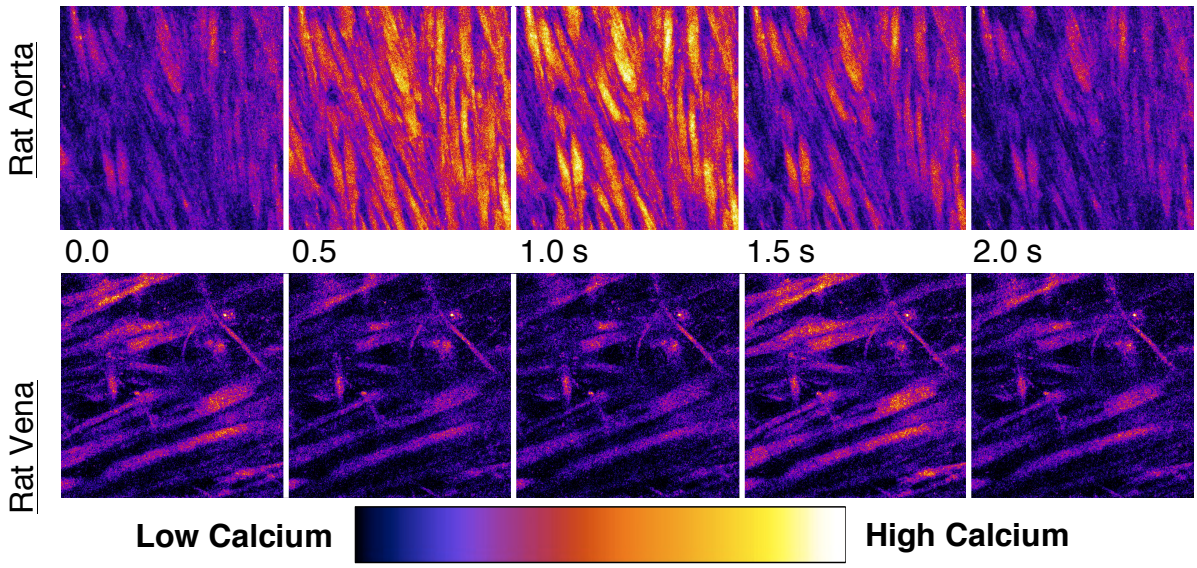

Figure 29. Aorta and vena cava exhibit calcium waves. Sequential images, taken every 0.5 seconds, of aorta (top) and vena cava (bottom) loaded with Fluo 4-AM Ca^{2+} indicator in the absence of agonist. Images are pseudo-colored to show increases in Ca^{2+} fluorescence as increases in fluorescence intensity, from low (*black*) to high (*white*).

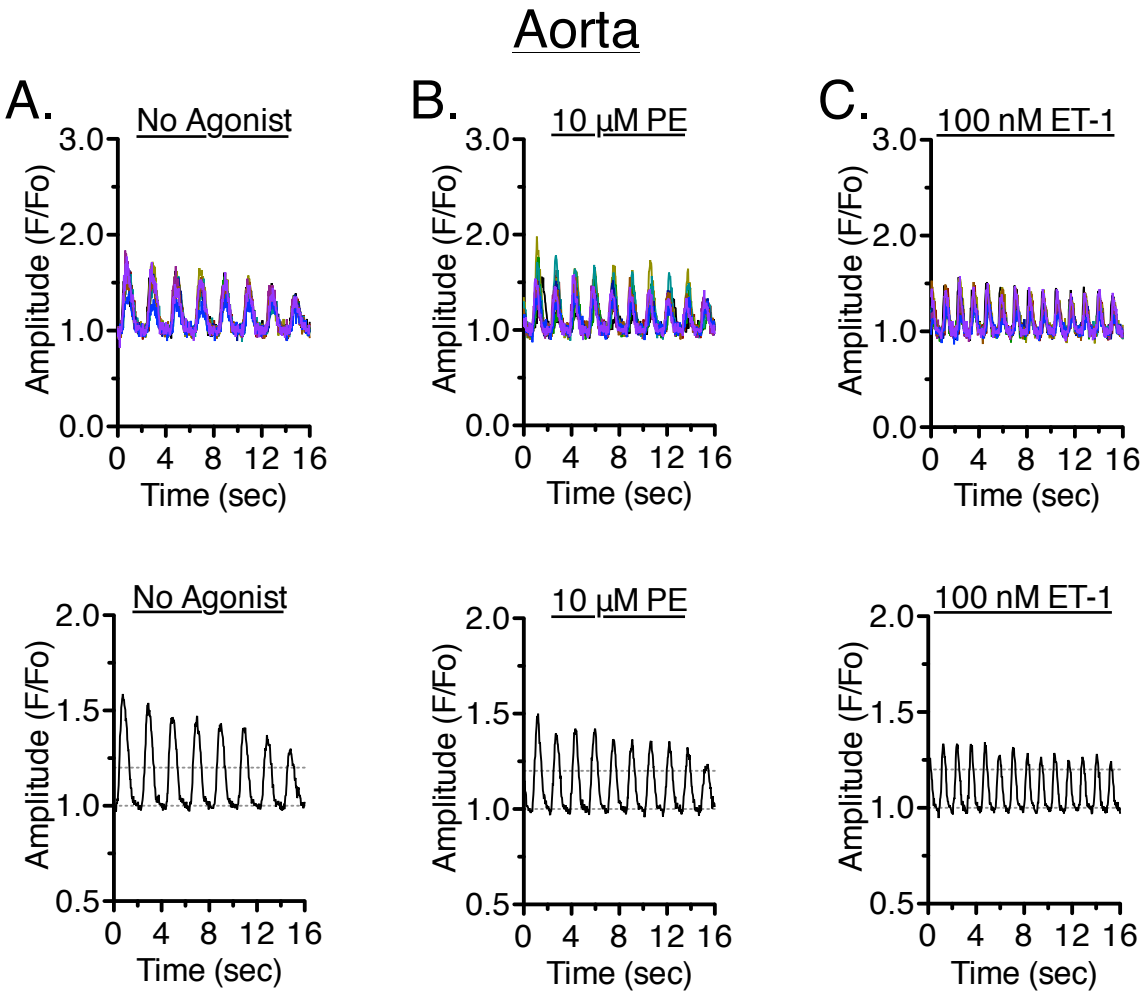

Figure 30. Synchrony of calcium waves in rat aorta. (*top*) Representative graphs of Ca^{2+} waves in rat aorta loaded with Fluo 4-AM Ca^{2+} indicator. Lines represent changes in fluorescence intensity in each of 10 randomly selected regions of interest over time, in the presence of no agonist (A), 10 µM phenylephrine (B) and 100 nM ET-1 (C). (*bottom*) Mean amplitude of all 10 of the regions of interest. Dashed lines represent baseline and the minimum threshold used to identify Ca^{2+} waves (F/Fo>1.2). PE = phenylephrine. Representative of more than 11 experiments.

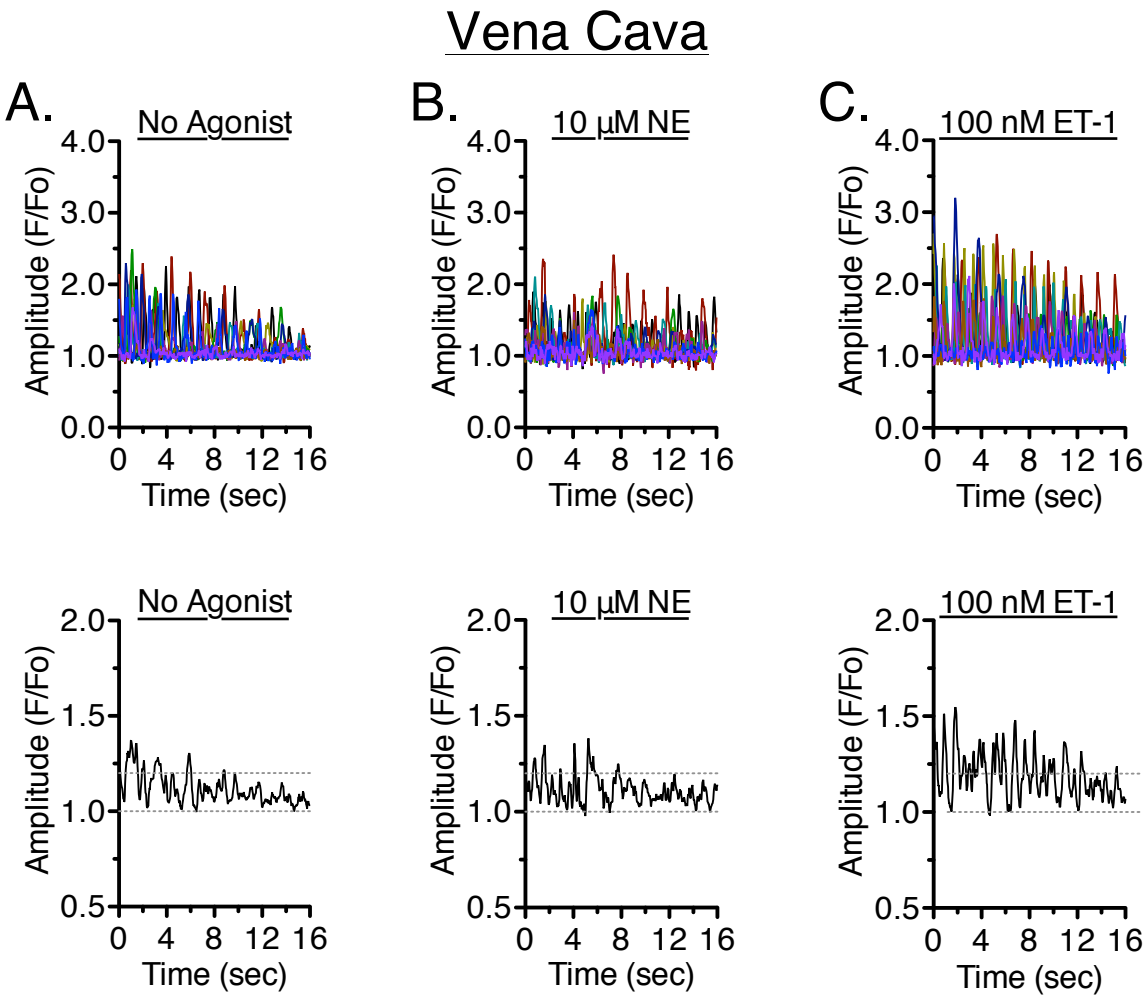

Figure 31. Synchrony of calcium waves in vena cava. (*top*) Representative graphs of Ca^{2+} waves in rat vena cava loaded with Fluo 4-AM Ca^{2+} indicator. Lines represent changes in fluorescence intensity in each of 10 randomly selected regions of interest over time, in the presence of no agonist (A), 10 μM norepinephrine (B) and 100 nM ET-1 (C). (*bottom*) Mean amplitude of all 10 of the regions of interest. Dashed lines represent baseline and the minimum threshold used to identify Ca^{2+} waves (F/Fo > 1.2). NE = norepinephrine. Representative of more than 11 experiments.

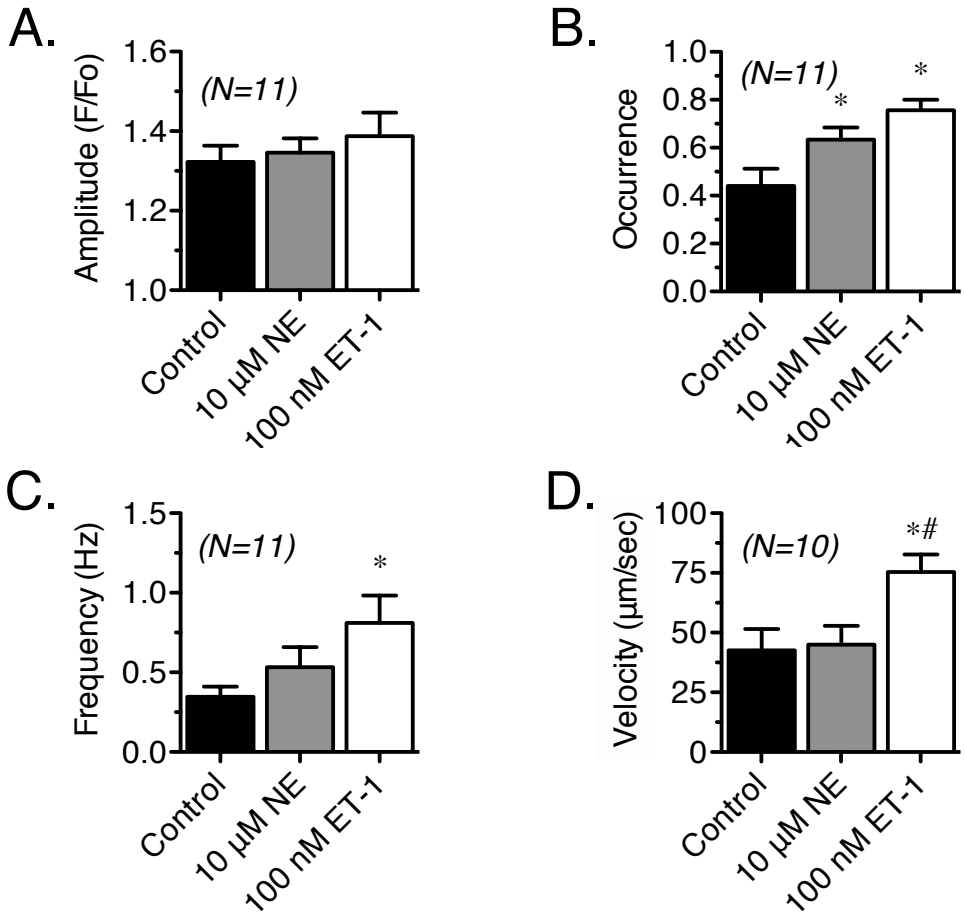

Figure 32. Characteristics of calcium waves in vena cava. Bar graphs representing calcium wave amplitude (a), occurrence (b), frequency (c) and velocity (d) in vena cava. All parameters were recorded in the presence of no agonist (control, black bars), adrenergic agonist (norepinephrine, grey bars) and 100 nM ET-1 (white bars). Bars represent mean +/-SEM. NE = norepinephrine. * = $p<0.05$ *versus* control. # = $p<0.05$ *versus* norepinephrine. N = 10-11.

2.4. IP_3 Receptor Inhibition during ET-1-induced Contraction

The role of IP_3R-dependent calcium release during ET-1-induced contraction in aorta and vena cava was also investigated. Isometric contraction to increasing concentrations of ET-1 was measured in aorta and vena cava, in the presence and absence of the IP_3R antagonist 2-APB (100 μM) (**Figure 33**). 2-APB (100 μM) significantly attenuated ET-1-induced contraction in aorta (**Figure 33a**) but not vena cava (**Figure 33b**).

Because 2-APB had no effect on contraction in vena cava, we next examined the effects of phospholipase-C (PLC) inhibition on ET-1-induced contraction using the PLC inhibitor U-73122 (1-10 μM) and its inactive analogue U-73343 (1-10 μM). In aorta, U-73122 (1 μM), but not U-73343, had a small but significant inhibitory effect on ET-1-induced contraction (**Figure 34a,c**). Increasing the concentration of U-73122 from 1 to 10 μM caused a more robust inhibition of ET-1-induced contraction, but also caused significant inhibition of ET-1-induced contraction by the inactive analogue U-73343 (**Figure 34b,d**). In vena cava, 1 μM U-73122 markedly attenuated ET-1-induced contraction, while 1 μM U-73343 had no effect (**Figure 35a,c**). However, 10 μM U-73122 as well as U-73343 nearly abolished ET-1-induced contraction in vena cava (**Figure 35b,d**).

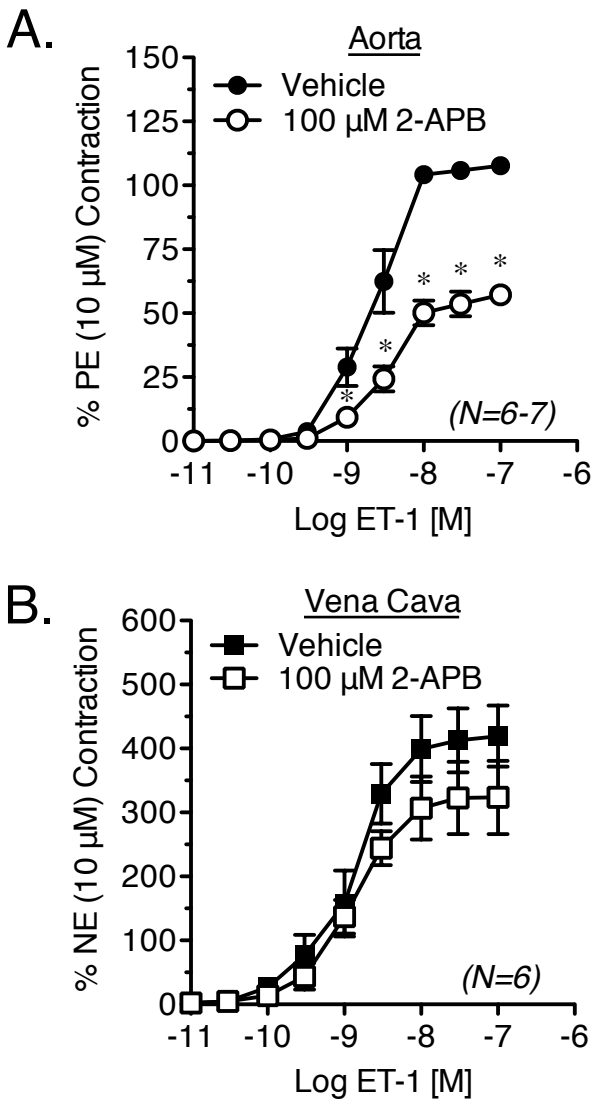

Figure 33. Contractile response to increasing concentrations of ET-1 in rat aorta and vena cava, in the presence or absence of the IP_3R antagonist 2-APB (100 µM). (A) rat aorta; (B) rat vena cava. Vehicle or antagonists were incubated with tissue for 1h prior to ET-1 exposure. Points represent mean ± SEM for the number of animals indicated in parentheses. NE = norepinephrine; PE = phenylephrine. * = $p<0.05$ *versus* vehicle.

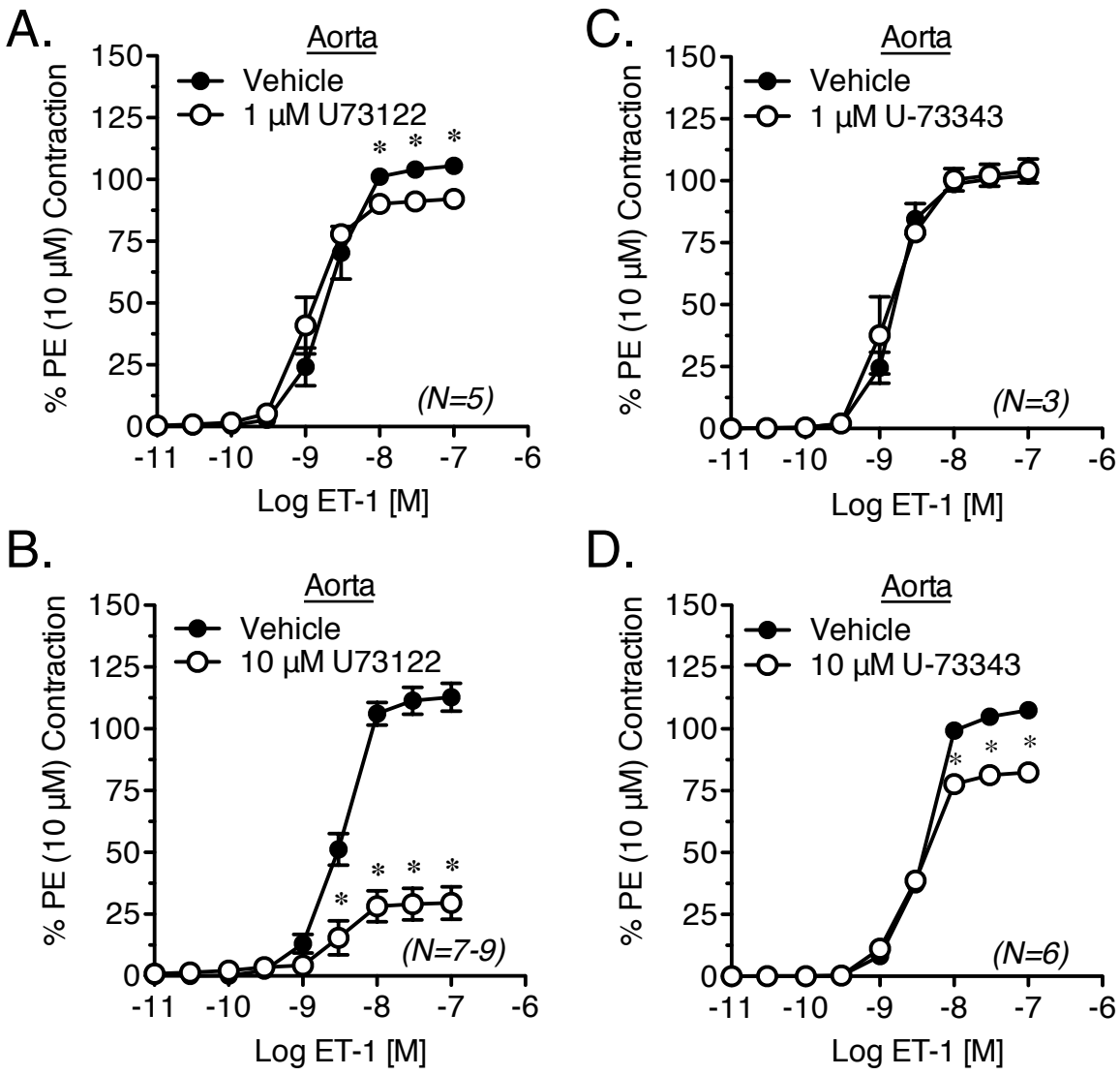

Figure 34. Effects of phospholipase-C inhibition on ET-1-induced contraction in aorta. Measurement of ET-1-induced contraction in rat aorta exposed to vehicle, multiple concentrations of U-73122 (A,B) or its inactive analogue U-73343 (C,D). Vehicle or antagonists were incubated with tissue for 1h prior to agonist exposure. Points represent mean ± SEM for the *N* indicated in parentheses. ET-1=endothelin-1; PE=phenylephrine. * = $p<0.05$ *versus* vehicle.

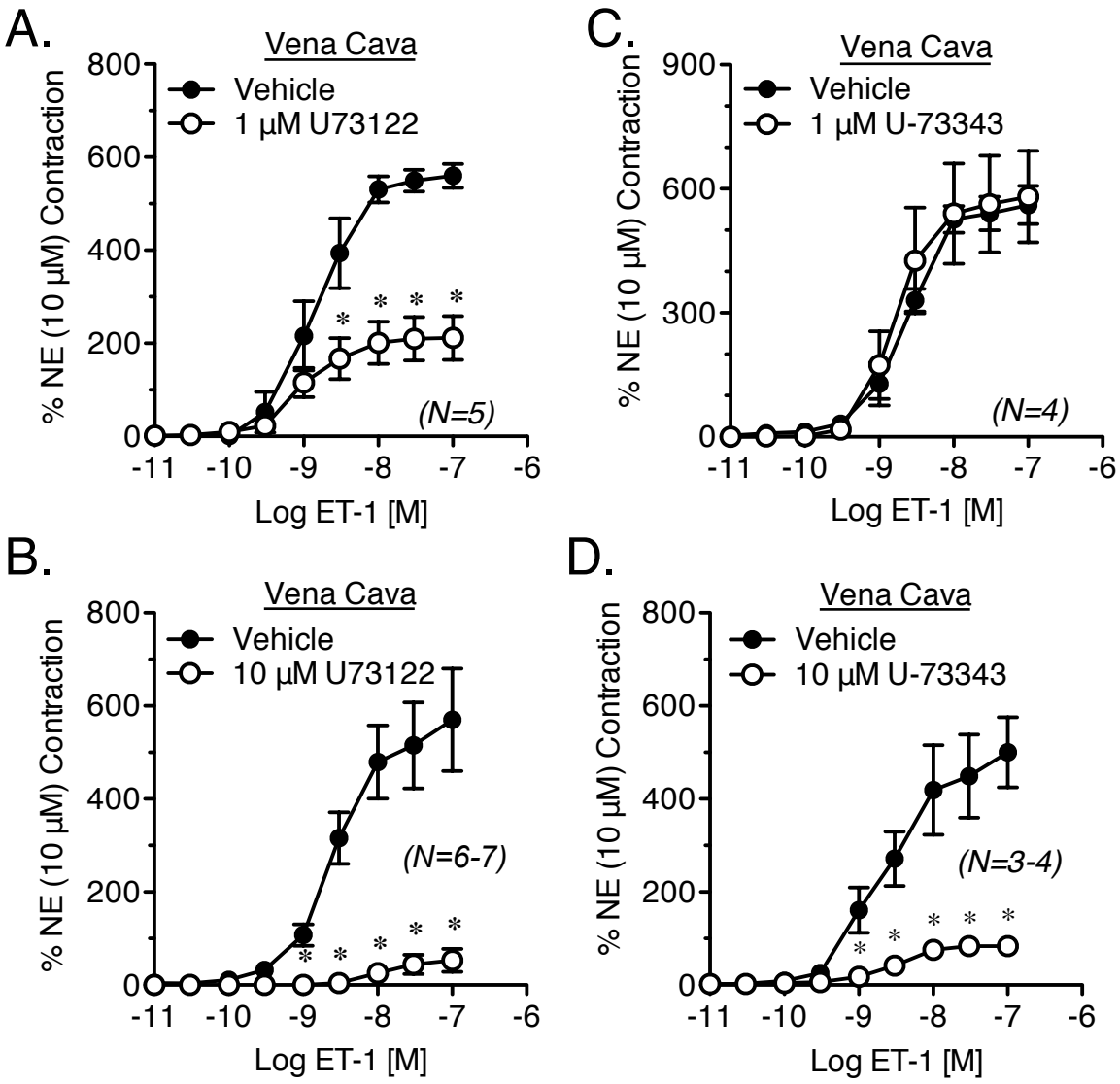

Figure 35. Effects of phospholipase-C inhibition on ET-1-induced contraction in vena cava. Measurement of ET-1-induced contraction in rat vena cava exposed to vehicle, multiple concentrations of U-73122 (A,B) or its inactive analogue U-73343 (C,D). Vehicle or antagonists were incubated with tissue for 1h prior to agonist exposure. Points represent mean ± SEM for the *N* indicated in parentheses. ET-1=endothelin-1; NE=norepinephrine. * = $p<0.05$ *versus* vehicle.

2.5. DAG-Mediated Contraction

To test the relationship between DAG and smooth muscle function, isometric contraction of aorta and vena cava was measured in the presence of increasing concentrations of the membrane permeable DAG analogue 1-oleoyl-2-acetyl-*sn*-glycerol (OAG). OAG caused a significant and concentration-dependent contraction in vena cava (**Figure 36a**) that was absent in aorta (**Figure 36b**). This contraction was completely reversed by the PKC antagonist chelerythrine (10 μM), indicating that OAG-mediated contraction is due to PKC activation (**Figure 36c**). These data suggest that DAG, by activation of PKC, can cause contraction in vena cava but not aorta.

2.6. PKC Inhibition during ET-1-Induced Contraction

To test the effects of PKC inhibition on ET-1-induced contraction, isometric contraction of aorta and vena cava to ET-1 was measured in the presence or absence of the PKC inhibitor chelerythrine (10 μM). While chelerythrine significantly attenuated ET-1-induced contraction in aorta (**Figure 37a**), ET-1-induced contraction in vena cava was abolished by chelerythrine (**Figure 37b**). These data suggest that ET-1-induced contraction in vena cava is PKC-dependent, and reinforces our finding that DAG is an important regulator of contraction in vena cava.

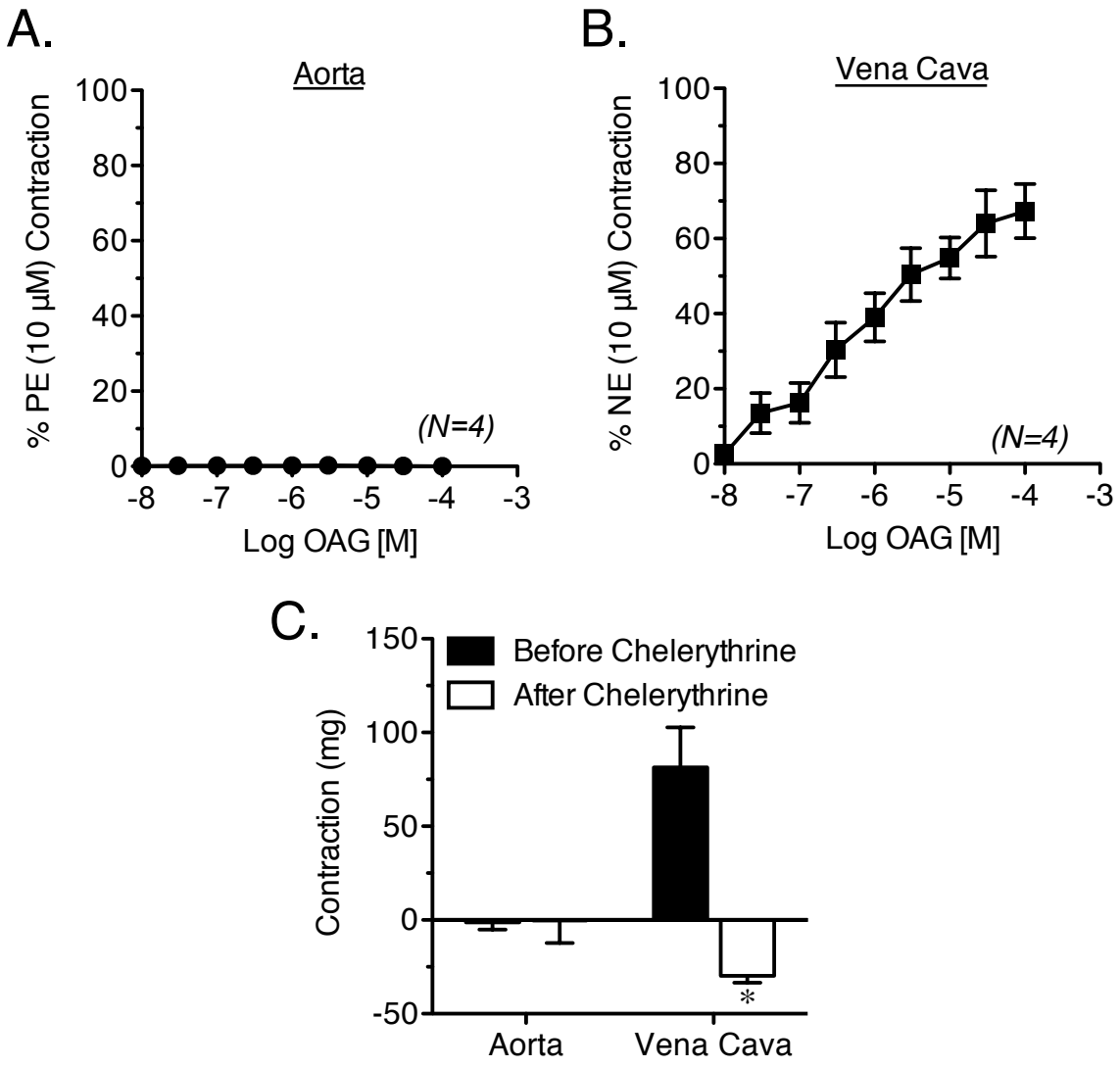

Figure 36. OAG-induced contraction in aorta and vena cava. (A,B): Measurement of OAG-induced contraction in aorta (A) and vena cava (B). (C): Bar graph representing relaxation of OAG-induced contraction in aorta and vena cava. Black bars represent maximal contraction to OAG (100 µM). White bars represent maximum contraction to OAG after addition of chelerythrine (10 µM). PE=phenylephrine; NE=norepinephrine; * = $p<0.05$ *versus* control. N=4.

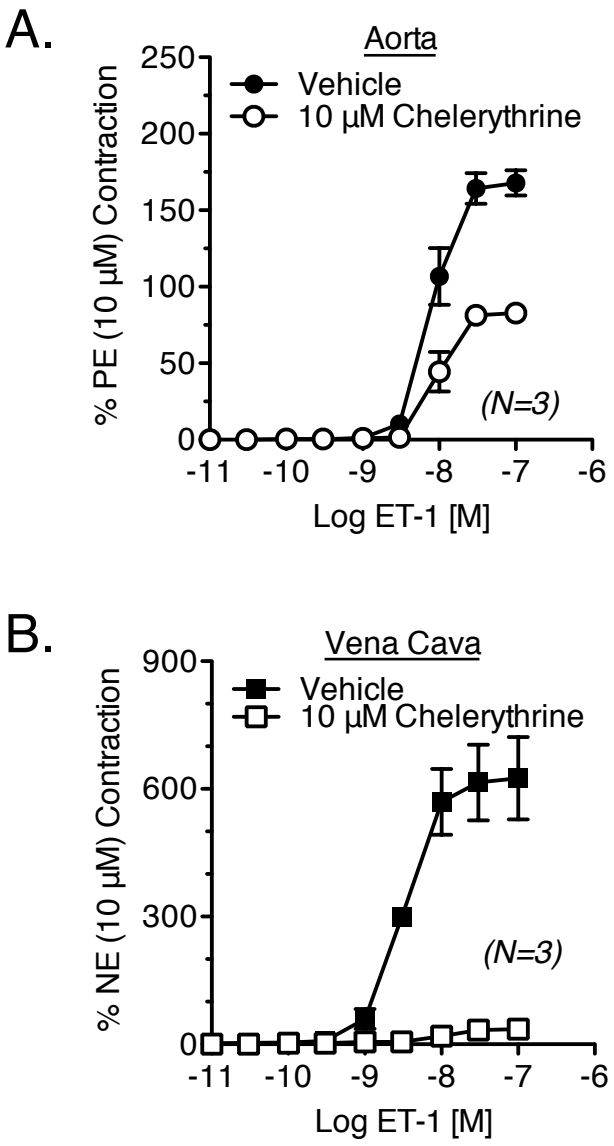

Figure 37. Effects of protein kinase C (PKC) inhibition on ET-1-induced contraction in aorta and vena cava. Measurement of ET-1-induced contraction in rat aorta and vena cava exposed to vehicle or the PKC inhibitor chelerythrine (10 µM). Vehicle or antagonists were incubated with tissue for 1h prior to agonist exposure. Points represent mean ± SEM for the *N* indicated in parentheses. ET-1=endothelin-1; NE=norepinephrine. * = $p<0.05$ *versus* vehicle.

3. Discussion

The principal and novel finding of this study is that ET-1 activates PLC in rat vena cava, but contraction to ET-1 is not mediated by IP_3. Even though vena cava express all three IP_3R subtypes and exhibit Ca^{2+} wave events normally associated with IP_3-mediated Ca^{2+} release, inhibition of IP_3R had no effect on ET-1-induced contraction in vena cava. These findings imply that ET-1-induced contraction in vena cava does not require IP_3, and that Ca^{2+} waves caused by ET-1 are either IP_3-independent or do not regulate ET-1-induced contraction. Furthermore, it may be the production of DAG, and not IP_3, that regulates contraction to ET-1 in vena cava since inhibition of PLC nearly abolishes ET-1-induced contraction.

3.1. IP_3 receptor expression and IP_3-mediated contraction.

We found that smooth muscle from both aorta and vena cava expresses all three IP_3R subtypes. While no specific subtype predominated in aorta, IP_3R-3 receptor expression was the significantly greater in vena cava as compared to IP_3R-1. Unfortunately, no comparisons could be drawn between the quantities of IP_3R protein expression in aorta *versus* vena cava, since aorta have substantially more smooth muscle than vena cava [2,144]. Instead, we used immunofluorescent labeling of IP_3R in freshly dissociated smooth muscle cells to compare IP_3R expression in aorta *versus* vena cava. Both aorta and vena cava smooth muscle contain all 3 IP_3R subtypes, showing that the differences in total IP_3R expression we saw in Western blotting experiments were not indicative of differences in smooth muscle IP_3R expression between aorta and vena cava. More

importantly, IP_3R receptors were functionally coupled to contraction in both tissues, as shown by the prolonged contraction caused by Bt-IP_3 (10 μM). Taken together, these data are consistent with the idea that IP_3R expressed in venous and arterial smooth muscle, that the receptors are functional, and that activation of IP_3R is coupled to contraction in vena cava as well as aorta.

3.2. Calcium waves as a measure of IP_3 receptor activity.

In addition to contraction by Bt-IP_3, we investigated the occurrence, frequency, amplitude and velocity of Ca^{2+} waves in venous smooth muscle as a measure of IP_3R activity. Several mathematical and experimental models have associated Ca^{2+} waves with propagation of Ca^{2+}-induced Ca^{2+} release (CICR) and contraction of smooth muscle cells [1,48,58,209]. The frequency, amplitude and occurrence of Ca^{2+} waves also positively correlates with smooth muscle contraction [131-134,210,211]. As such, we sought to determine if Ca^{2+} waves were present in vena cava smooth muscle, and if the properties of these waves were altered by ET-1.

Vena cava exhibited asynchronous Ca^{2+} waves in the absence of agonist, showing that spontaneous Ca^{2+} events occur in a small population of venous smooth muscle cells even under resting conditions. The number of cells exhibiting Ca^{2+} waves increased with the addition of NE, but the amplitude, frequency and velocity of the waves remained unchanged. This indicates that NE recruits more smooth muscle cells to exhibit Ca^{2+} waves, but the properties of the waves remain unchanged as compared to waves in the absence of agonist. This agrees with data from other published results,

where non-propagating, Ca^{2+} wave-like oscillations were described in rabbit inferior vena cava in the presence of another adrenergic stimulus, phenylephrine [76,135].

The occurrence, frequency, synchrony and velocity of Ca^{2+} waves was increased in the presence of ET-1, suggesting that ET-1-mediated contraction is associated with global, wave-like oscillations in venous smooth muscle presumed to be regulated by CICR and initiated by IP_3. Taken together, these data suggest that contraction in rat vena cava depends upon Ca^{2+} release, but the mechanisms regulating changes in cytosolic Ca^{2+} differ between aorta and vena cava.

3.3. Role of IP_3R during ET-1-induced contraction.

While our measures of Ca^{2+} wave parameters suggested the involvement of IP_3R in ET-1-induced venous contraction, the IP_3R antagonist 2-APB (100 μM) had no effect on vena cava contraction to ET-1. 2-APB did, however, significantly attenuate ET-1-induced contraction in aorta, which supports the idea that $G\alpha_q$-mediated IP_3 production and subsequent Ca^{2+} release are important regulators of arterial contraction to ET-1 [11,136,137]. While the results of our contractile experiments in vena cava appear to be in stark contrast with our Ca^{2+} wave measurements, they do suggest that the Ca^{2+} waves induced by ET-1 in venous smooth muscle are either not associated with smooth muscle contraction or regulated by a mechanism other than IP_3-mediated Ca^{2+} release. One such mechanism suggested to regulate Ca^{2+} oscillations in venous smooth muscle is the influx and efflux of Ca^{2+} through the Na^+/Ca^{2+} exchanger, which can rapidly reverse the direction of Ca^{2+} flux in response to changes in local Ca^{2+} concentration

and membrane potential [144,163]. Even though our results also suggest that Ca^{2+} waves are not regulated by IP_3, the role of other mechanisms like the NCX remains to be investigated.

3.4. Regulation of ET-1-induced Contraction by Phospholipase-C.

We next investigated the role of PLC in ET-1-induced contraction. Both aorta and vena cava contraction to ET-1 was markedly attenuated by the PLC inhibitor U-73122, suggesting that contractile ET receptors in veins signal through a similar $G\alpha_q$-mediated pathway as is seen in arteries [150,212]. These data, combined with the lack of inhibition of ET-1-induced contraction by IP_3R inhibition, suggest that DAG, and not IP_3, may regulate venous contraction to ET-1. Whereas IP_3 then activates SR Ca^{2+} release, DAG can both negatively and positively affect cytosolic Ca^{2+} by its actions as an activator of PKC or several different TRP channels in the plasma membrane [1,135,213-215]. These experiments did not examine the mechanisms by which DAG regulates venous contraction to ET-1, but they did investigate the ability of DAG to cause contraction. The DAG analogue OAG did cause significant contraction in vena cava but not aorta, and this contraction was reversed by the PKC inhibitor chelerythrine (10 μM) (**Figure 36**). Also, ET-1-induced contraction was nearly abolished by the PKC inhibitor chelerythrine (10 μM) in vena cava (**Figure 37**). These findings imply that DAG can cause contraction of vena cava by activation of PKC, and that PKC is also an important mediator of ET-1-induced contraction in veins. Also, these data represent another stark difference between contractile mechanisms in aorta and vena cava. Thus, the role of

DAG as a positive regulator of agonist-induced contraction in veins is a viable and interesting mechanism in need of further investigation,

3.5. Conclusions

These data suggest that ET-1 activates PLC in aorta and vena cava, but contraction to ET-1 is not regulated by IP_3 in vena cava as it is in the aorta. Rather, our findings suggest that DAG may regulate ET-1-induced contraction in vena cava, perhaps through activation of PKC or by activation of Ca^{2+} influx pathways. Ca^{2+} waves elicited by ET-1, traditionally thought to mediate contraction in an IP_3-dependent manner, may be uncoupled from contraction in vena cava or regulated by an IP_3-independent mechanism. These studies outline a new and fundamental difference between venous and arterial smooth muscle, in terms of excitation-contraction coupling and Ca^{2+} mobilization during ET-1-induced contraction, and further reinforce the heterogeneity of vascular smooth muscle.

CHAPTER 6: SUMMARY AND PERSPECTIVES

Over 40 years ago, the observation was made that vascular smooth muscle contraction was due to "the penetration of Ca^{2+} ions into the smooth muscle fibers" [48,151,152,216]. When these observations were first made in the 1960's, it was recognized that two mechanisms regulated these changes in intracellular Ca^{2+} concentration: influx of Ca^{2+} from the extracellular space and the release of intracellular Ca^{2+} from intracellular stores [217]. Since that time, countless researchers have examined Ca^{2+} signaling in smooth muscle, showing that the mechanisms of Ca^{2+} influx and Ca^{2+} release that regulate smooth muscle contraction are indeed extremely complex and variable between the tissues and agonists being investigated. Nonetheless, Ca^{2+} signaling in venous smooth muscle had been largely ignored, leading to a gap in our knowledge regarding how Ca^{2+} could regulate vascular tone in the venous circulation. Thus, the overall goal of this project was to explore how increases in intracellular Ca^{2+} affect venous contractility, determine the mechanisms by which ET-1 increases intracellular Ca^{2+} in veins, and elucidate the differences between ET-1-mediated calcium signaling in veins and arteries.

While prior research in our laboratory discovered numerous differences between arteries and veins in terms of their contractile responses to agonists, particularly in the case of ET-1 (**Table 3**) [2,148,154,218,219], my preliminary experiments showed many similarities between arteries and veins in terms of ET-1-induced Ca^{2+} handling. ET-1-induced contraction in aorta and vena cava is Ca^{2+}-dependent, since removal of

extracellular Ca^{2+} nearly abolished ET-1-induced contraction, and the changes in intracellular Ca^{2+} caused by ET-1 suggested both extracellular Ca^{2+} influx an intracellular Ca^{2+} release (**Figure 7** and **Figure 8**). However, three important differences between arteries and veins were discovered in the course of this project:

(1) reverse-mode NCX is an important regulator of ET-1-induced contraction in vena cava but not aorta; (2) ryanodine receptors are uncoupled from contraction in vena cava but not aorta; and (3) ET-1-induced contraction strongly depends on PKC in vena cava moreso than aorta.

I also discovered stark differences in the pharmacology of ET-1-induced contraction in arteries and veins, specifically:

(1) veins are more sensitive than arteries to the PLC inhibitor U-73122 and its ”inactive” analogue U-73343; (2) the DAG analogue OAG contracts veins but not arteries; and (3) ET-1-induced contraction of veins is abolished by the PKC inhibitor chelerythrine. Taken together, these findings represent several new and important differences between arteries and veins in terms of ET-1-induced Ca^{2+} signaling.

1. ET-1-Mediated Calcium Influx

Mechanisms of ET-1-induced Ca^{2+} influx have been described in rat aorta, and suggest NSCC’s and VGCC’s are the primary means of Ca^{2+} entry during contraction to ET-1 [155,206,220]. I began to investigate the mechanisms of ET-1-induced Ca^{2+} influx in vena cava by testing the hypothesis that different Ca^{2+} channels were responsible for

ET-1-mediated Ca^{2+} influx in vena cava than in aorta. Contraction to ET-1 in aorta and vena cava was not significantly inhibited by any single NSCC antagonist or L-type VGCC antagonist (*see* **Table 4**). This led me to two different conclusions about ET-1-mediated Ca^{2+} influx: (1) multiple types of Ca^{2+} channels were responsible for Ca^{2+} influx during ET-1-induced contraction in aorta and vena cava; and (2) another mechanism, other than Ca^{2+} influx through Ca^{2+} channels, was activated by ET-1 in aorta and vena cava.

As described in Chapter 3, the NCX has the unique property of being both a means of Ca^{2+} efflux and Ca^{2+} influx, depending on the electrochemical gradients for Na^{+} and Ca^{2+} [156,165]. Of particular interest to me was that knockout of NCX1 protein from smooth muscle not only attenuated arterial vasoconstriction, but it also reduced blood pressure in mice [154,157]. Thus, I hypothesized that Ca^{2+} influx through the reverse-mode NCX was a significant means of Ca^{2+} entry during ET-1-induced contraction in aorta and vena cava. To test this hypothesis, I used the compound KB-R7943 (10 μM), which is reported to be an NCX inhibitor that selectively inhibits the reverse mode of the NCX (Ca^{2+} influx) as opposed to forward mode (Ca^{2+} efflux) [120,221]. KB-R7943 significantly inhibited ET-1-induced contraction in vena cava but not aorta (**Figure 14**). This was, to my knowledge, the first example of a drug that selectively inhibited contraction in vena cava and not aorta. I also performed an extensive series of experiments to verify that the effects of KB-R7943 were due to inhibition of the reverse-mode NCX. An accepted means of activating reverse-mode NCX is to rapidly reduce extracellular Na^{+}, to reverse the concentration gradient for Na^{+} and activate NCX-

dependent Ca^{2+} influx. Reduction of extracellular Na^+ caused a prolonged contraction in vena cava that was inhibited by KB-R7943, but had no significant effect in aorta (**Figure 11**). These data suggested that: (1) the effects of KB-R7943 on ET-1-induced contraction were, at least in part, due to inhibition of reverse-mode NCX; and (2) an important difference between aorta and vena cava was the role of Na^+ as a mediator of agonist-induced contraction.

The role of Na^+ as a mediator of smooth muscle contraction has largely been overlooked, even though several mechanisms for Na^+ influx exist in vascular smooth muscle. First, vascular smooth muscle may express voltage-gated Na^+ channels ($Na_V1.2$) [158,166]. Second, many of the TRP channels expressed in vascular smooth muscle (TRPC-3, -5, -6, and -7) have roughly equal preference for Na^+ and Ca^{2+} [55,159,222,223]. Lastly, TRPC-3 in cardiac muscle and TRPC-6 in vascular smooth muscle are in close proximity to, and interact with, the NCX and Na^+/K^+ ATPase (NKA) [160,179,224]. Fameli *et al* have modeled these microdomains, and concluded that TRPC-6 and NCX are in such close proximity that localized Na^+ concentrations would become high enough to cause the NCX to extrude Na^+ in exchange for Ca^{2+}. If this arrangement actually exists in smooth muscle, I propose that it is also energetically favorable. **Figure 38** describes two scenarios, where TRP channels allow Ca^{2+} influx and where TRP channels allow Na^+ influx. In **Figure 38A**, the increase in local Ca^{2+} concentration would cause the NCX to function in “forward mode”, moving Ca^{2+} out of the cell in exchange for Na^+. As the concentration of intracellular Na^+ increases, the NKA would transport Na^+ ions out of the cell at the expense of ATP. In scenario 2, the

increase in local Na^+ would cause the NCX to function in “reverse mode”, moving Na^+ out of the cell in exchange for Ca^{2+}. The NCX has a very high capacity for transport as compared the Na^+/K^+ ATPase, and can move a large amount of Na^+ out of the cell very rapidly and without the use of ATP [124,161]. So, TRP-mediated Na^+ influx may actually increase intracellular Ca^{2+} more efficiently, more rapidly and at a lower energetic cost than TRP-mediated Ca^{2+} influx.

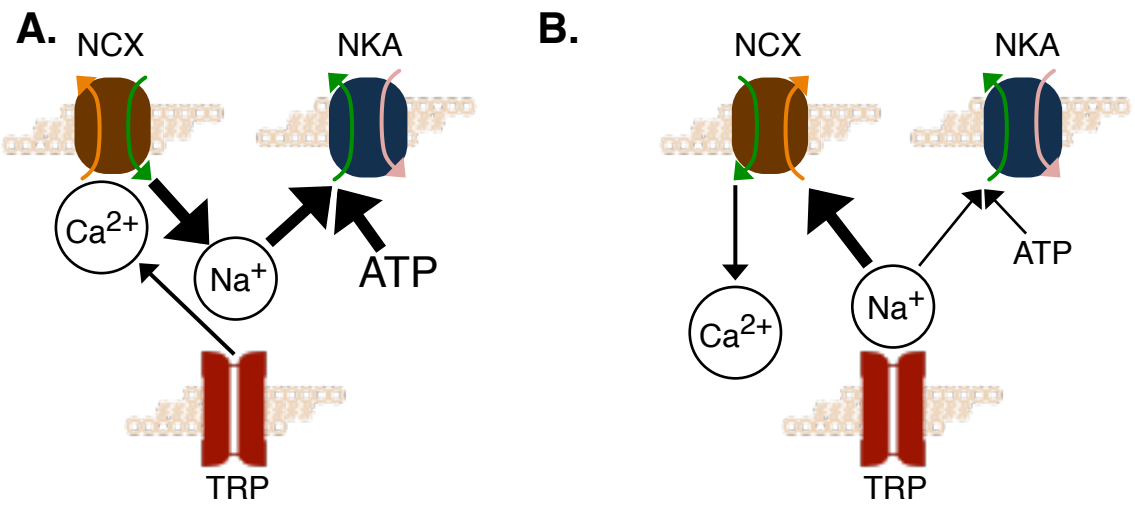

Figure 38. Proposed effects of Ca^{2+} influx and Na^{+} influx in the TRP/NCX/NKA microdomain. (A) Ca^{2+} influx through TRP channels increases local Ca^{2+} concentrations, which causes the NCX to move Ca^{2+} out of the cell and Na^{+} into the cell. This increase in local Na^{+} would be countered by the actions of the NKA, which would efflux Na^{+} at the expense of ATP. (B) Na^{+} influx causes the NCX to remove the majority of Na^{+} in exchange for Ca^{2+}. This minimizes Na^{+} efflux and ATP consumption by the NKA.

2. ET-1-Mediated Calcium Release

Both aorta and vena cava contain sarcoplasmic Ca^{2+} stores, since both tissues exhibited store-operated Ca^{2+} entry upon depletion of intracellular Ca^{2+} by thapsigargin (**Figure 20**). ET-1 can cause both RyR-mediated and IP_3-mediated release of sarcoplasmic Ca^{2+} stores. Thus, I first tested the hypothesis that ET-1 caused RyR-mediated Ca^{2+} release in aorta and vena cava. In several vascular tissues, ET-1 activates ADP ribosyl cyclase, which produces cyclic ADP ribose (cADPR) [154,225]. CADPR can then activate RyR directly, and causes release of sarcoplasmic Ca^{2+} stores [107,162].. I began by measuring the response to the RyR activator caffeine (20 mM) in aorta and vena cava, to determine if both tissues expressed functional RyR. In aorta, caffeine caused a transient contraction that was inhibited by the RyR antagonists ryanodine and tetracaine (**Figure 22**). However, caffeine did not cause a contraction in vena cava (**Figure 21**), nor did it cause a prolonged increase in intracellular Ca^{2+} (**Figure 24**). Even though this suggested that RyR are uncoupled from contraction in vena cava, I wanted to confirm that RyR were not activated by ET-1. Neither ryanodine nor tetracaine inhibited ET-1-induced contraction in vena cava, which was consistent with my conclusion that RyR were uncoupled from contraction in vena cava. Additionally, ET-1-induced contraction in aorta was also unchanged by RyR antagonists (**Figure 39**). Thus, I concluded that ET-1 did not cause sarcoplasmic Ca^{2+} release by activating RyR in aorta and vena cava.

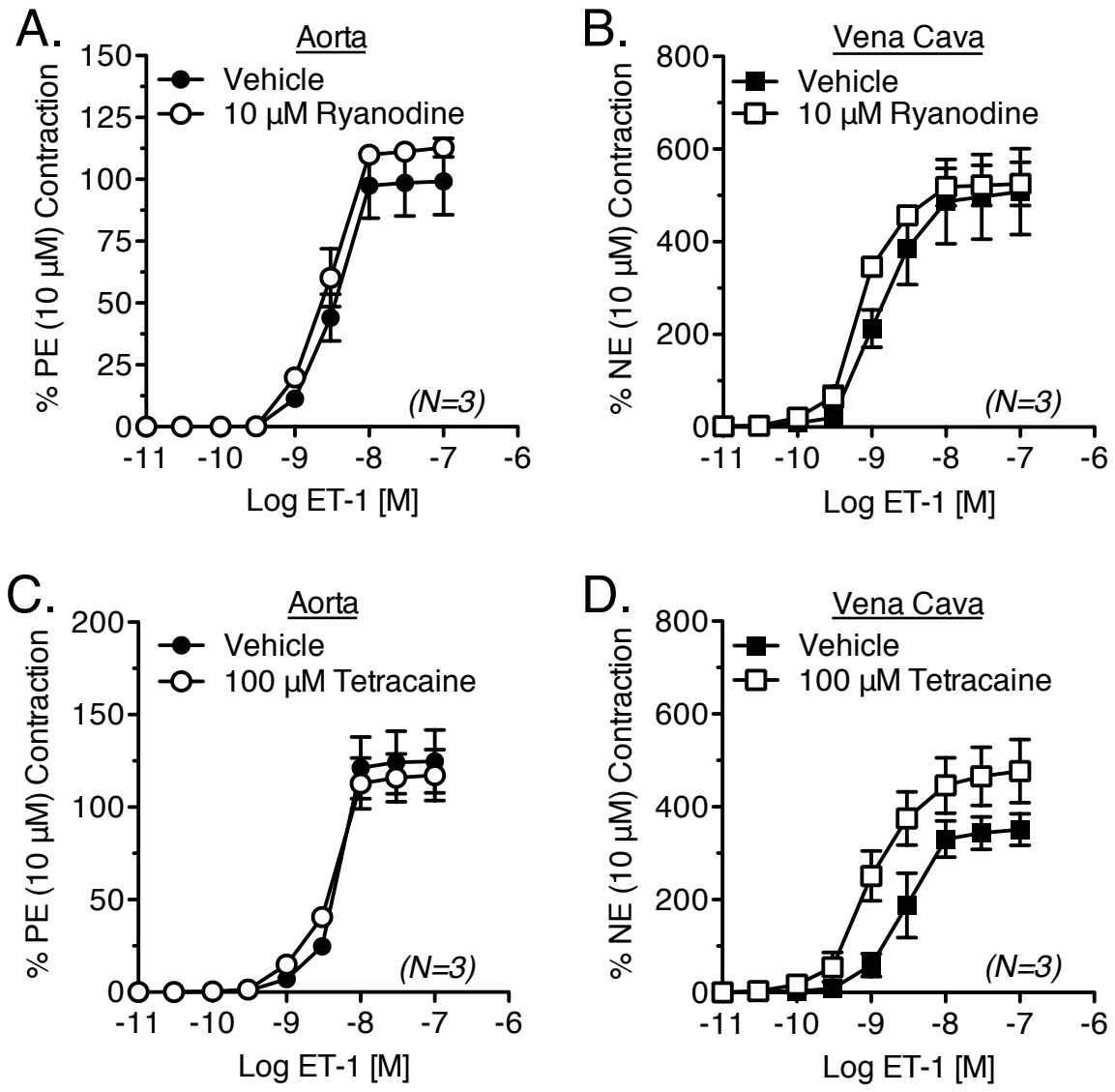

Figure 39. The effect of ryanodine receptor antagonists on ET-1-induced contraction in aorta and vena cava. Shown are responses to vehicle or ryanodine (10 µM) in aorta (a) and vena cava (b), and tetracaine (100 µM) in aorta (c) and vena cava (d). Vehicle or antagonists were incubated with tissue for 1h prior to ET-1 exposure. Points represent mean ± SEM for the number of animals indicated in parentheses. * = $p<0.05$ *versus* vehicle.

Since RyR were not involved in ET-1-mediated contraction, I hypothesized that ET-1-induced contraction of aorta and vena cava must depend on IP_3-mediated release of intracellular Ca^{2+} stores. ET_A receptors are coupled to $G\alpha_q$, which activates PLC and thus increases IP_3 production [1,226]. Little was known about ET-1-induced intracellular Ca^{2+} release in veins, except that ET-1 caused asynchronous Ca^{2+} oscillations in rabbit inferior vena cava [76,163,164]. Rat vena cava exhibited asynchronous Ca^{2+} waves, similar to the waves described by Dai *et al* in the rabbit inferior vena cava. In the presence of ET-1, the wave frequency, occurrence and velocity significantly increased, indicating that these waves were associated with responses to ET-1 in vena cava. While these data could be interpreted as evidence that IP_3-mediated Ca^{2+} release was mediating ET-1-induced contraction, they do not establish a causal relationship between Ca^{2+} waves and contraction. So, I next measured ET-1-induced contraction in the presence of the IP_3R inhibitor 2-APB (100 μM). Consistent with the literature, 2-APB significantly attenuated ET-1-induced contraction in the aorta, suggesting IP_3-mediated Ca^{2+} release was important for contraction to ET-1 (**Figure 33**). However, 2-APB had no effect on ET-1-induced contraction in vena cava. The lack of inhibition of ET-1-induced contraction in vena cava could not be attributed to differences in IP_3R subtype expression, since 2-APB has similar affinity for all 3 IP_3R subtypes [165,227]. Thus, I concluded that IP_3R were not activated during ET-1-induced contraction in veins. Taken together, these findings suggest that the role of intracellular Ca^{2+} stores release during ET-1-induced contraction is minimal in vena cava,

The possibility remained that ET receptors in vena cava were not coupled to $G\alpha_q$, and thus did not activate PLC and IP_3 production. When I inhibited PLC using U-73122, ET-1-induced contraction in both aorta and vena cava was markedly attenuated (**Figure 34** and **Figure 35**). Since PLC was activated by ET-1 but IP_3R were not, I concluded that it is DAG, and not IP_3, that plays an important role in regulating ET-1-induced contraction in vena cava. However, the sensitivity of ET-1-induced contraction to inhibition by U-73122 was higher in vena cava than aorta. Also supporting this conclusion was my finding that OAG, a DAG analogue, contracted vena cava but not aorta (**Figure 36**). DAG is most often associated with activation of PKC, which can phosphorylate a number of proteins that affect Ca^{2+} signaling including L-type VGCC's, NCX and RyR [228-230]. PKC can also phosphorylate CPI-17, an important inhibitor of myosin light-chain phosphatase, to enhance the Ca^{2+} sensitivity of smooth muscle [231]. If DAG activated PKC-dependent phosphorylation of RyR and VGCC's in vena cava, then inhibition of RyR or VGCC's should have attenuated ET-1-induced contraction. Since this did not occur, I find it very unlikely that activation of PKC-dependent phosphorylation of VGCC's and RyR's is a major determinant of ET-1-induced contraction in vena cava. However, the PKC inhibitor chelerythrine nearly abolished OAG-induced contraction in vena cava, which suggests that OAG is causing contraction in a PKC-dependent manner. So, instead of phosphorylating ion channels, PKC may be altering the Ca^{2+} sensitivity of the contractile machinery in venous smooth muscle.

DAG is also well-characterized as an activator of TRP channels, leading to influx of Ca^{2+} and Na^{+} [223]. DAG can also be broken down into other vasoactive molecules.

For instance, diacylglycerol lipase (DGL) converts DAG into arachidonic acid (AA) [213]. AA can directly activate several Ca^{2+} channels, including arachidonate-regulated Ca^{2+} (ARC) channels, TRP-C channels and TRP-V channels, to regulate extracellular Ca^{2+} influx [232]. Meves *et al* also provide evidence that AA can cause sarcoplasmic Ca^{2+} release, as well as alter the Ca^{2+} sensitivity of the smooth muscle contractile machinery. However, the PKC inhibitor chelerythrine nearly abolished ET-1-induced contraction in vena cava, which suggests that DAG is activating PKC to regulate contraction in venous smooth muscle.

Taken together, my results suggest that release of intracellular Ca^{2+} stores (through activation of RyR and IP_3R) is minimally important in ET-1-induced contraction in veins. Rather, the major determinants of ET-1-induced contraction in veins are PKC activation and extracellular Na^+ influx regulated by DAG.

3. A Proposed Pathway of ET-1-Mediated Calcium Signaling in Veins

Based on all of my findings, I propose that the following pathway regulates ET-1-induced contraction in the vena cava. First, ET-1 binds to a $G\alpha_q$-coupled ET receptor, activating PLC. PLC cleaves PIP_2 into IP_3 and DAG, and DAG then activates DAG-sensitive TRP-C channels and PKC. Opening of TRP-C channels allows for the influx of extracellular Na^+, which activates Ca^{2+} influx *via* reverse-mode NCX. PKC phosphorylates the NCX and CPI-17, enhancing Ca^{2+} influx through the NCX and making the contractile machinery in venous smooth muscle more sensitive to Ca^{2+}.

This increase in Ca^{2+} and sensitivity subsequently leads to smooth muscle contraction. Even though this proposed pathway is supported by much of my data, several major questions still exist that merit further investigation:

- *If IP_3R are not involved in ET-1-induced contraction, then what is producing and regulating Ca^{2+} waves?*

Several possible explanations exist. These waves may indeed by IP_3-mediated, but unrelated to Ca^{2+} increases that cause contraction. Instead, these fluxes in intracellular Ca^{2+} may regulate other ET-1- and Ca^{2+}-dependent cellular responses, such as expression of remodeling genes and smooth muscle cell proliferation [233,234]. Also, I did not measure the effects of IP_3R antagonists on Ca^{2+} waves in vena cava, so it is not yet clear that these waves are mediated by IP_3. While usually associated with IP_3R activation, RyR activation can also cause Ca^{2+} waves [53]. Fameli *et al* even suggest that the NCX is capable of sustaining Ca^{2+} oscillations in vascular smooth muscle [163]. If NCX inhibitors block these waves, it would support my conclusions about the importance of reverse-mode NCX during venous contraction and validate the model proposed by Fameli *et al* for NCX-mediated Ca^{2+} waves. If these waves are unaffected by NCX, RyR and IP_3R inhibitors, then they represent a new and unknown mechanism for regulation of intracellular Ca^{2+} oscillations that is worthy of further investigation.

- *In veins, ET_B receptors are also coupled to contraction. What is their role?*

Since ET-1 has equivalent affinities for both ET receptors, I was unable to distinguish between the effects of ET_A and ET_B receptor activation. In peritubular smooth muscle cells, ET_B receptors activate Ca^{2+} release that comes from a thapsigargin-dependent but IP_3-independent intracellular store [107]. This suggests that each ET receptor subtype is capable of activating different Ca^{2+} signaling mechanisms to cause contraction. Veins are relatively unique in that they express functional ET_B receptors on smooth muscle that are coupled to contraction [148]. Also, ET_B receptor activation causes hypertension in rats, presumably in a venous-specific manner [235]. This suggests that each individual ET receptor subtype is capable of regulating contraction, and may also do so through different mechanisms. Since transgenic rats are available that lack functional ET_B receptors in the vasculature, these animals could be utilized to distinguish between the Ca^{2+} signaling mechanisms activated by ET_A receptors and ET_B receptors. Given that the role of ET-1 in hypertension is not entirely clear, it would be worthwhile to investigate how each receptor subtype increases intracellular Ca^{2+}.

- *Do ET receptors interact with one another, and does this change Ca^{2+} signaling?*

GPCR's are capable of forming homodimers (e.g. 2 β_2 adrenergic receptors together) and heterodimers (e.g. M_2 muscarinic receptor with an M_3 muscarinic receptor) [236,237]. Research into GPCR dimerization is increasing as the physiological relevance of GPCR dimers becomes more apparent [238]. HEK-293 cells transfected with human ET_A receptors, human ET_B receptors, or both ET_A and ET_B receptors show that these receptors can form both homodimers (ET_A/ET_A; ET_B/ET_B) and heterodimers

(ET_A/ ET_B) [239]. The physiological and pharmacological evidence of ET receptor dimers continues to grow as well, as ET_A and ET_B receptors functionally interact in human bronchi, saphenous vein, and C6 glioma cells [146,240-243]. When the transfected HEK-293 cells were used to investigate the effects of ET receptor dimers on ET-1-induced Ca^{2+} signaling, ET_A and ET_B homodimers mediated transient increases in intracellular Ca^{2+} (approximately 1 minute), while $ET_{A/B}$ heterodimers caused a sustained increase in intracellular Ca^{2+} that lasted over 10 minutes [244,245]. Thus, the presence of different ET receptor homo- and heterodimers changes the profile of the Ca^{2+} response. Our lab previously showed pharmacological evidence of ET receptor dimerization in the vein, but not the artery. ET_A receptor antagonists did not shift venous contraction to ET-1 without first desensitizing ET_B receptors [146]. This type of response is characteristic of receptor dimers, and thus is functional evidence that venous ET receptors interact in ways arterial ET receptors do not. Unfortunately, showing functional ET receptor dimers from aorta and vena cava has proven unsuccessful. Also, **Figure 8** shows that both the rapid and prolonged increases in intracellular Ca^{2+} caused by ET-1 appear similar in aorta and vena cava, suggesting that differences in ET receptor homodimerization or heterodimerization may not be responsible for the differences in ET-1-mediated Ca^{2+} signaling in aorta and vena cava. Nonetheless, the mechanisms by which ET receptor homodimers and heterodimers control Ca^{2+} signaling are still unknown, and may represent an important source of regulation of in ET-1-mediated Ca^{2+} signaling in arteries and veins.

- *If calcium stores are not released by ET-1 during contraction, what is responsible for the contraction that remains in the absence of calcium?*

ET-1 also alters the sensitivity of the smooth muscle contractile machinery to Ca^{2+} by inhibiting myosin light chain phosphatase activity and increasing phosphorylation of myosin light chain kinase [246]. In my experiments where extracellular Ca^{2+} was removed, there was still a small amount of Ca^{2+} remaining in solution (~2.3 nM). It is possible that the remaining contraction was due an ET-1-dependent change in Ca^{2+} sensitivity in the presence of a minimal amount of free Ca^{2+}. Cho *et al* also suggest that there are Ca^{2+}-independent mechanisms of contraction, whereby myosin light-chain kinase activity is enhanced in the absence of Ca^{2+} [247]. While their research showed this to be true for contraction caused by calyculin-A, this mechanism is not yet associated with ET-1-induced contraction. Nonetheless, these data do show that the majority of ET-1-induced contraction in vena cava depends upon extracellular Ca^{2+} influx and minimally on intracellular Ca^{2+} stores release.

4. Clinical Relevance

While changes in venous capacitance are linked to increased blood pressure, relatively little is known about the mechanisms that govern contraction in venous smooth muscle. The venous circulation has been ignored clinically due to the lack of understanding of its function in maintaining cardiovascular homeostasis. However, recent research has shown that changes in venous capacitance are associated with a multitude of medical

conditions, including syncope, hemorrhage, shock, heat stroke and congestive heart failure [248-252]. Even with the breadth of research into Ca^{2+} signaling in smooth muscle, the mechanisms responsible for Ca^{2+} mobilization by ET-1 (particularly in terms of ET-1-induced venous contraction) remain unclear. Thus, my findings about the mechanisms of ET-1-induced Ca^{2+} signaling in venous smooth muscle may broaden our understanding of the pathophysiology of a number of important cardiovascular diseases, and help to better define the role of ET-1 in the pathogenesis of cardiovascular disease.

The endothelin system in veins is an interesting therapeutic target unto itself, since veins maintain contractility to ET-1 in hypertension [149]. Furthermore, the existence of contractile ET_B receptors in venous smooth muscle [148] suggested that ET_B receptor antagonists could be ideal candidates as venous-specific inhibitors of ET-1-induced contraction. However, inhibition of ET_B receptors would not only block the contractile ET_B receptors in veins but also inhibit the relaxant ET_B receptors in arteries, and thus provide no benefit to hypertensive patients that have normal endothelial function. Instead, dual ET_A/ET_B receptor antagonists may be more beneficial, since they would inhibit both the contractile ET_A receptors in arteries as well as the contractile ET_B receptors in veins. Dual ET receptor antagonists have shown better clinical efficacy than ET_A-selective antagonists, but have found limited clinical use beyond the treatment of pulmonary hypertension, due to the high incidence of side effects [253]. New pharmacological agents have been developed that have different affinities for the ET_A and ET_B receptor, which decrease the potential for inhibiting relaxant ET_B receptors

while still inhibiting the contractile ET_A receptors in vascular smooth muscle [254]. Because veins contain contractile ET_B receptors that are absent in arteries, the additional efficacy of these compounds may be due to inhibition of ET_B-mediated venous contraction to ET-1. Further research is required to determine if the antihypertensive properties of these drugs are due to inhibition of contractile ET_B receptors in veins.

The greatest therapeutic potential from this project arises from the finding that the NCX is integral in regulating Ca^{2+} influx in vena cava, and that KB-R7943 is a venous-specific inhibitor of ET-1-induced contraction. Thus, the finding that ET-1-induced contraction is selectively inhibited in veins by NCX inhibition represents the potential for a venous-specific therapy that could potentially avoid the side effects of ET receptor antagonism. The potential problem with using an NCX inhibitor to clinically treat hypertension is the effect of NCX inhibition on cardiac function. At concentrations that cause therapeutic inhibition of NCX and blood pressure reduction, KB-R7943 caused significant decline in cardiac function [255]. Thus, while KB-R7943 reduced blood pressure it also had deleterious effects on cardiac function that prevent it from being a viable clinical therapy. However, recent evidence suggests that NCX have multiple tissue-specific splice variants that have different functional and pharmacological properties. For instance, NCX1.3, which is expressed in smooth muscle and kidneys, presents a potential therapeutic target as it is not expressed in the heart [256]. Targeting this vascular-specific NCX spice variant would allow selective inhibition of vascular NCX without the potential for adverse cardiac events. Other NCX inhibitors,

such as SEA-0400 showed potent inhibition of NCX with minimal cardiac side effects, suggesting that this compound had potential as a therapeutic treatment. Further investigation and research could uncover other NCX-selective compounds with increased therapeutic potential.

APPENDICES

APPENDIX A

An imaging apparatus for simultaneous measurement of isometric contraction and Ca^{2+} fluorescence in large blood vessels of the rat

While simultaneous measurement of vessel contraction and Ca^{2+} transients can be measured in small vessels (< 3 mm diameter), few strain gauges are available small and sensitive enough for concurrent measurement of Ca^{2+} transients and contraction in larger vessels (> 3 mm diameter). We constructed a highly sensitive, low-noise strain gauge for the simultaneous measurement of vessel tension development and Ca^{2+} transients using fluorescent Ca^{2+} indicators. The force transducer was fabricated from aluminum and produced a sensitivity of 0.26 μV/mg over a broad range of applied load (0.05 to 5 g) and a rapid (102.8 Hz) frequency response. Blood vessels mount to the transducer with two stainless steel pins submerged above a coverslip in a 5 ml preparation bath.

1. Design and Fabrication

The design of the transducer (**Figure 40**) is based, in part, upon a similar device described in the literature [257]. The transducer was fabricated from a beam of 6063-grade aluminum, measuring 55 x 15 x 0.4064 mm. The cantilever beam was installed in a custom-fabricated aluminum clamp, making the final beam length 45 mm. To create the transducer, four, 350Ω strain gages (SGD-3/350-LY13, temperature compensated

for aluminum; Omega Engineering, Stamford, CT USA) were affixed to the top and bottom of the beam using a thin layer of cyanoacrylate adhesive. The strain gages were then connected to each other in a full Wheatstone bridge configuration *via* terminal pads and wire (0.127 mm diameter, PTFE-coated; Omega Engineering) (**Figure 41**). The transducer was connected to an amplifier using 5-wire shielded cable.

The myograph chamber was milled into a 15 cm x 25 cm sheet of 9 mm-thick Plexiglas. The chamber was built large enough and deep enough to allow for application of resting tension and imaging from above with upright microscope objectives. The bottom of the chamber consisted of a microscope coverslip mounted flush with the bottom of the chamber, allowing for imaging on inverted microscopes. Tubing was inserted for inflow and outflow of solutions. Blood vessel rings were attached to two stainless steel pins, one mounted on the transducer and the other on an aluminum rod. The rod and transducer were attached to XYZ micromanipulators (MT-XYZ; Newport Corporation, Irvine, CA USA) so precision adjustments to vessel position and resting tension could be made (**Figure 42**).

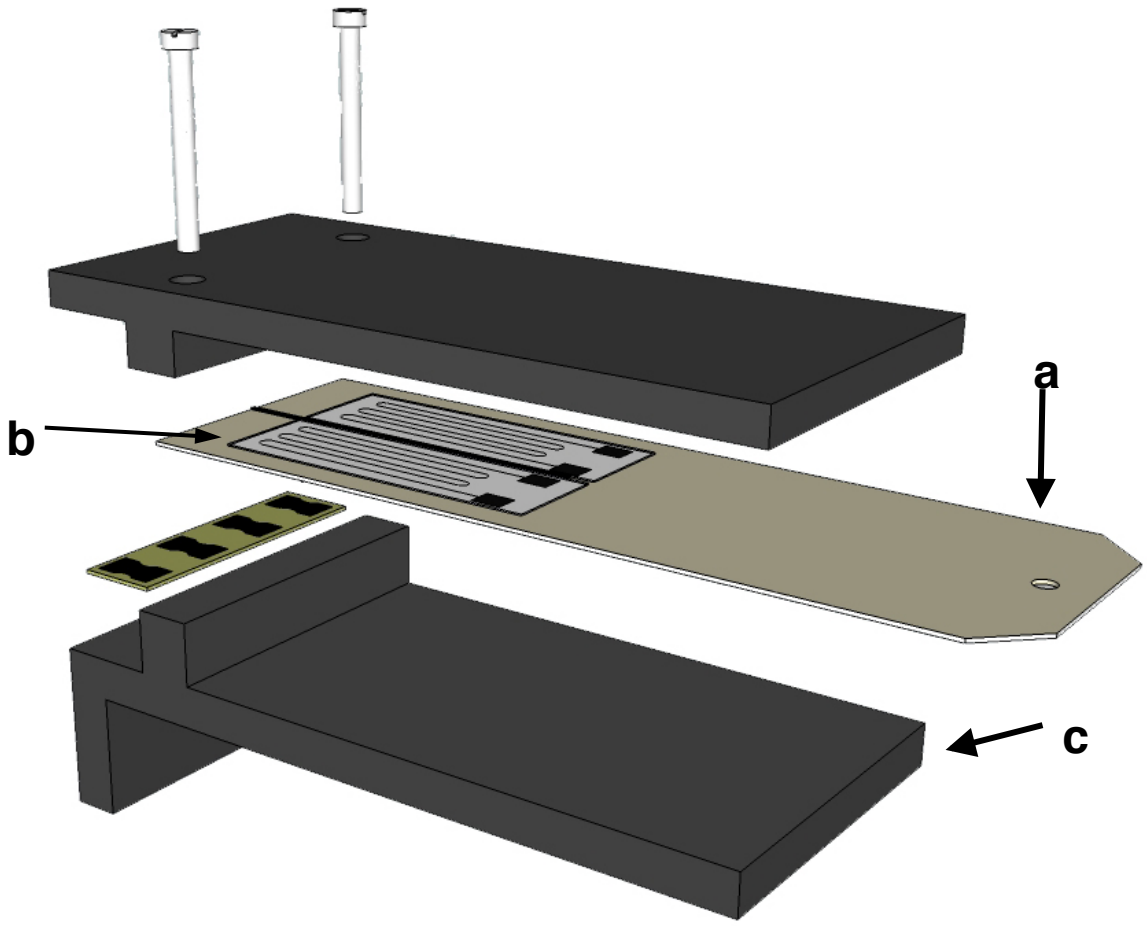

Figure 40. Construction of the transducer used in the myograph. Schematic drawing of the force transducer, showing the cantilevered aluminum beam (a), four strain gauges (b) and aluminum chassis (c).

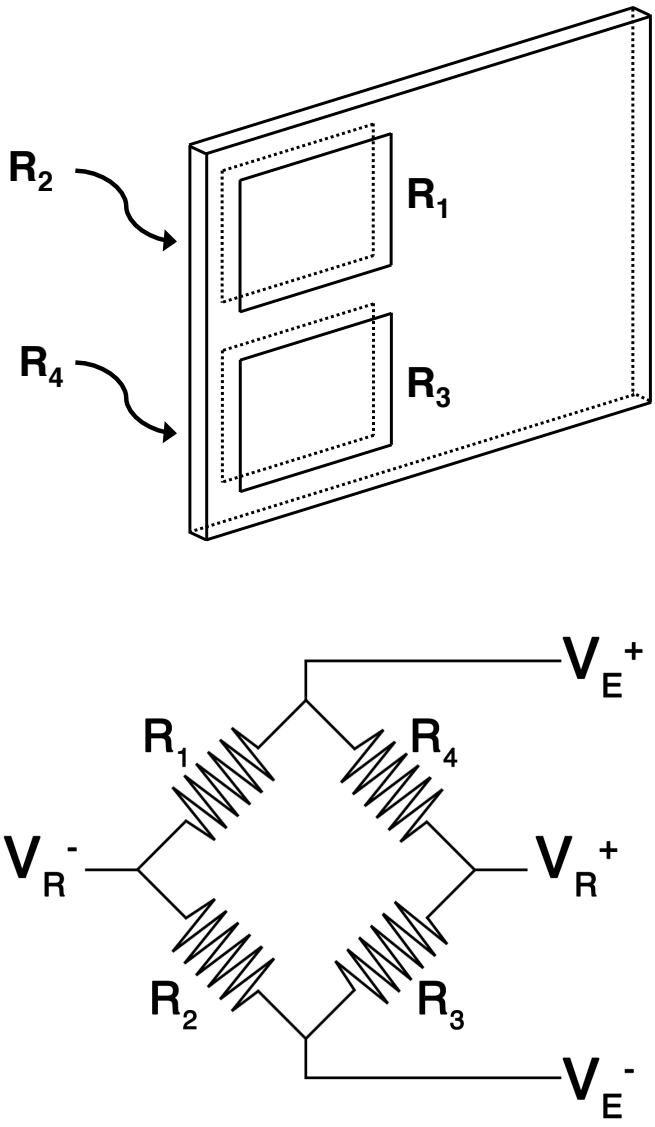

Figure 41. Diagram of the strain gauge arrangement and circuitry. The four strain gauges (R_1-R_4) are affixed to either side of the beam *(top)* and connected to form a full Wheatstone bridge *(bottom)*. V_E= excitation voltage; V_R= read voltage.

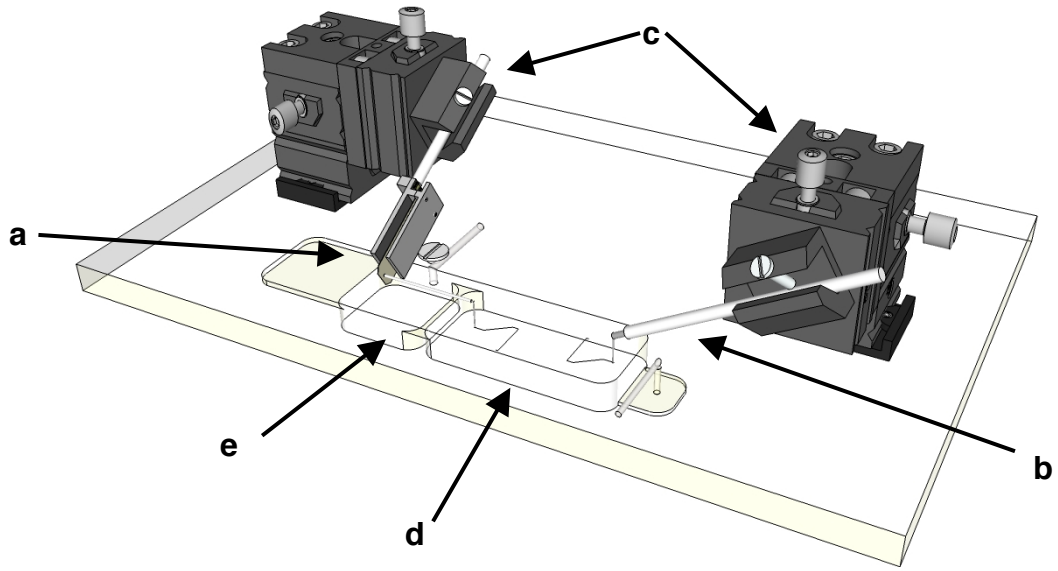

Figure 42. Schematic of the assembled imaging apparatus. Shown are the placements of the force transducer (a), aluminum rod (b) and XYZ micromanipulators (c). The volume of solution in the myograph chamber (d) is regulated by a second spillover chamber (e) from which solution is removed by vacuum suction or peristaltic pump.

2. Validation

For verification of transducer function, we compared the working range and frequency response of our custom transducer to that of a commercially available force transducer (Grass FT.03 force transducer; Grass Technologies, West Warwick, RI USA). The custom transducer was more sensitive than the commercial transducer, over a range of applied loads that simulate expected experimental conditions (**Figure 43a**). Both transducers had comparable frequency responses, although the decay of the response was more rapid in the commercial transducer (**Figure 43b**).

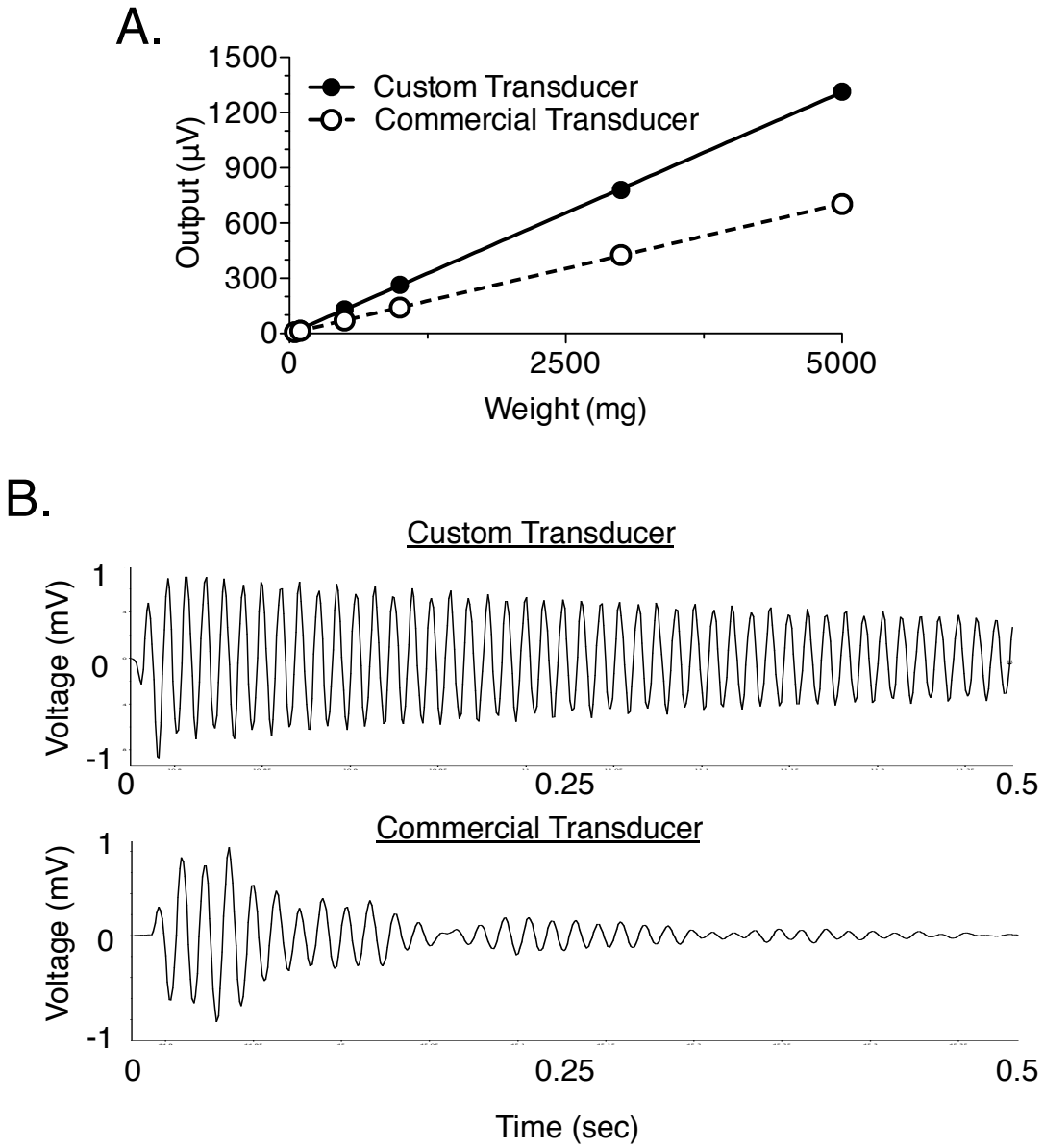

Figure 43. Working range and frequency response comparison of custom and commercial transducers. (A) Output voltage of the custom transducer as compared to a commercial transducer over a range of weights (0.5-5 g). (B) Frequency response of both transducers, elicited by a tap with a screwdriver.

APPENDIX B

ET_B receptors in arteries and veins – multiple actions in veins [148]

1. Rationale

Endothelin-1 (ET-1) is a 21-amino acid peptide that acts as a potent endogenous vasoconstrictor [258]. Although also made by other cell types, the dominant producers of ET-1 in the vasculature are endothelial cells. ET-1 has been implicated in the pathology of pulmonary arterial hypertension as well as systemic hypertension models, including deoxycorticosterone acetate-salt hypertension [259]. ET-1 binds to and activates two G-protein coupled receptor subtypes: the ET_A and ET_B receptor [11]. In both arteries and veins, ET_A receptor stimulation causes contraction [220]. In contrast, the role of ET_B receptors is much less clear and differs between vessel types.

Several reports characterize the ET_B receptor as a “clearance receptor”, the primary function of which is to sequester and remove circulating ET-1 from the blood [260]. In this capacity, ET_B receptors decrease the amount of ET-1 available to interact with ET_A receptors and thus decrease vascular contraction due to ET_A receptor stimulation. Researchers have since discovered that ET_B receptor stimulation can directly modulate vascular tone in arteries and veins, albeit with different functions. In arteries, functional ET_B receptors exist in endothelial cells, where receptor stimulation causes relaxation by increasing endothelial nitric oxide production [84]. In veins, ET_B receptors can mediate contraction [205] as well as relaxation [261]. There is evidence that both supports and

negates the involvement of the ET_B receptor in mediating contraction in arteries. For example, the ET_B receptor agonists sarafotoxin 6c (S6c) and IRL1620 do not cause arterial contraction directly in many arterial beds and isolated arteries [2,262,263]. However, as supported through antagonism studies, ET_B receptors mediate contraction in arteries from special circulations including the coronary artery [205,264], pulmonary artery [265,266] and skin [267]. Finally, there are arteries in which ET_A and ET_B receptors mediate contraction [268,269]. Thus, the literature is mixed in terms of the role played by the ET_B receptor in arterial contractility. In the pair of vessels we will use – the thoracic aorta and vena cava – S6c causes contraction in the vena cava but not the aorta.

It is unclear if different arterial and venous responses to ET_B receptor stimulation are because endothelial ET_B receptors are linked to different mechanisms in arteries and veins, or if veins have functional endothelial and smooth muscle ET_B receptors. Given the apparent differences in arterial *versus* venous contractile response to S6c, we hypothesize that relaxant ET_B receptor mechanisms in RVC would be different than those in RA. To test this hypothesis, we used pharmacological inhibition of ET receptors in normal rat tissues, as well as ET_B -deficient tissues from a novel strain of dopamine-beta-hydroxylase (DβH)-ET_B receptor transgenic rats (sl/sl). These rats carry the spotting-lethal ET_B receptor mutation, which abrogates functional ET_B receptor expression due to a deletion of the first and second putative transmembrane domains. The DβH-ET_B transgene rescues these rats from a perinatally lethal gastrointestinal congenital abnormality (Gariepy *et al*, 1996). The resulting adult rats do not express

ET_B receptors in vascular tissues, and provide confirmation of specific ET_B receptor functions.

2. Results

2.1. Localization of ET_A and ET_B Receptors

Both aorta and vena cava showed positive ET_B receptor staining in adventitial, medial, and intimal layers (**Figure 44a**). Sections of aorta and vena cava untreated with primary antibody (**Figure 44b**), or exposed to primary antibody and competing peptide (not shown), showed no DAB staining. This verifies that staining was specific for the primary ET_B antibody. To establish the presence of ET_B receptors in endothelial cells, freshly dissected vena cava were methanol-fixed and exposed to antibodies for both the ET_B receptor and platelet/endothelial cell adhesion molecule (PECAM-1). ET_B receptor and PECAM-1 localization was observed in vena cava (**Figure 45a,b**). DAPI was added to locate cell nuclei (**Figure 45c**). An overlay of all three images showed localization of ET_B receptors within the endothelial cell cytoplasm (**Figure 45d**). Parallel experiments using rat aorta were unsuccessful due to background auto-fluorescence, which made any specific staining indistinguishable from background staining.

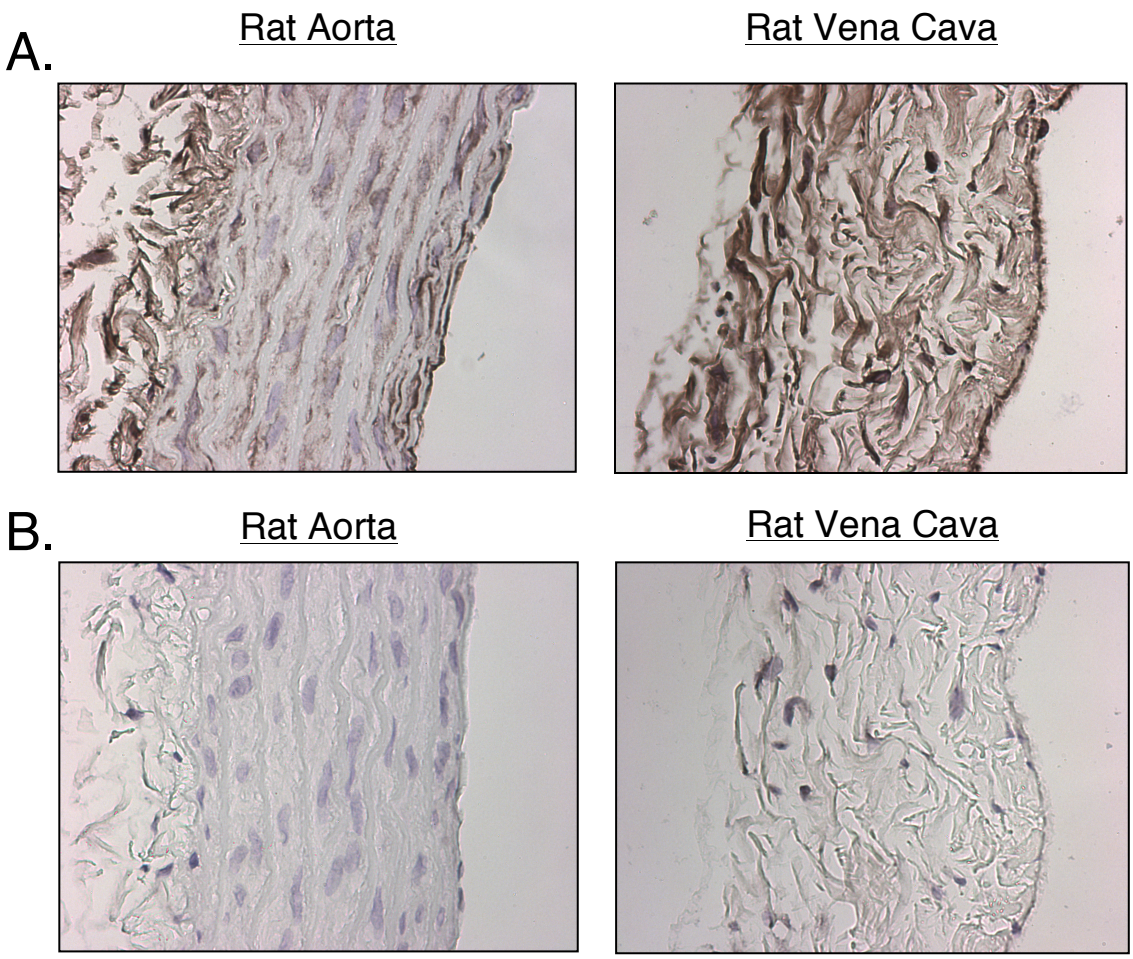

Figure 44. Representative immunohistochemical staining of ET_B receptor in paraffin-embedded, formalin-fixed rat aorta and vena cava. Positive staining for ET_B receptor antibody is shown in brown (A) as compared to non-specific staining in the absence of primary antibody (B). Blue Hematoxylin staining is used to locate cell nuclei in all pictures. Representative of 4 experiments.

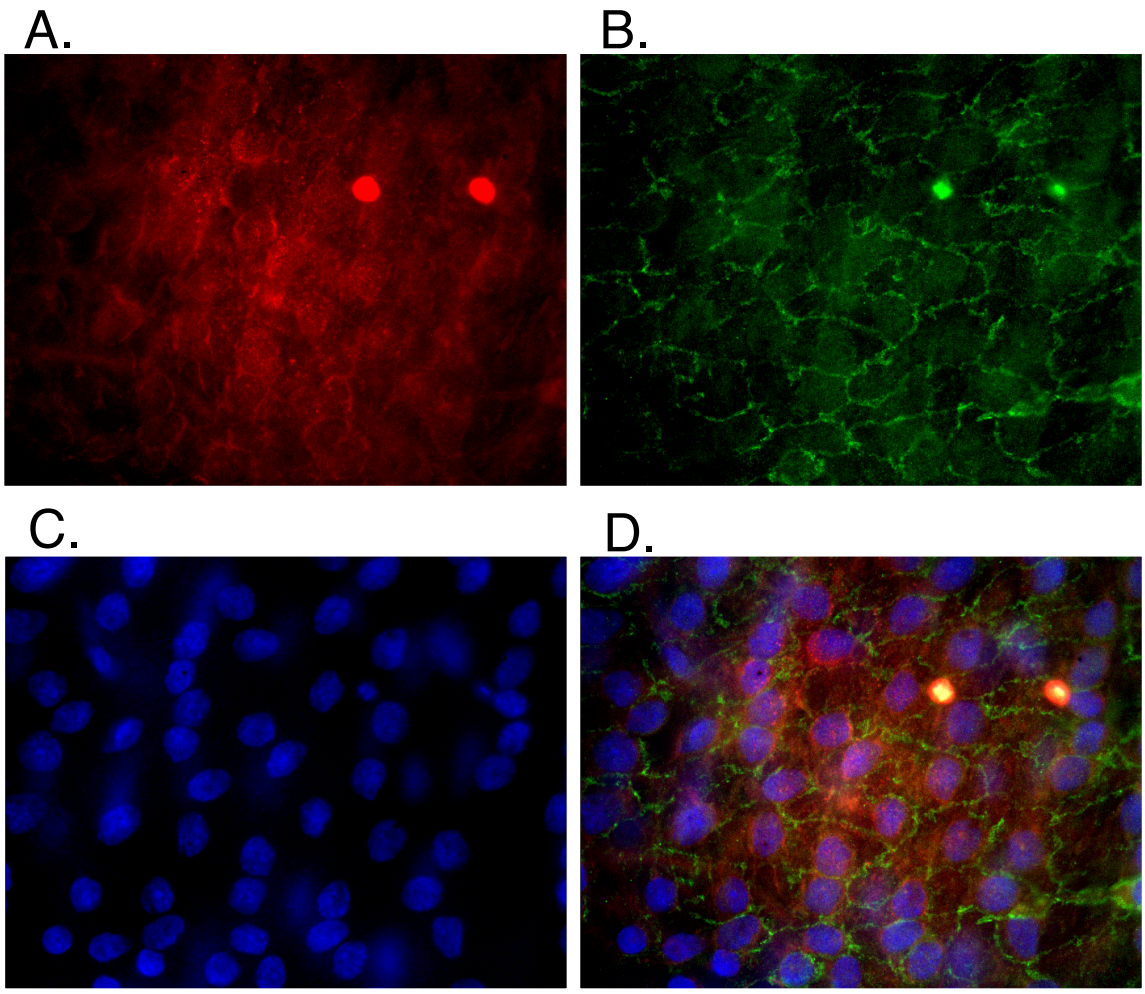

Figure 45. Representative immunohistochemical staining of methanol-fixed, *en face* mounted rat vena cava. (A) Rhodamine fluorescent staining of ET_B receptor antibody. (B) FITC fluorescent staining of platelet and endothelial cell adhesion molecule (PECAM-1) antibody. (C) DAPI nuclear staining. An overlay of all three pictures shows the location of ET_B receptors, PECAM-1, and nuclei of endothelial cells (D). Representative of 4 experiments.

2.2. Mechanism of ET_B receptor-mediated Relaxation in Aorta and Vena Cava

Thoracic aorta and vena cava from male Sprague-Dawley rats were used to establish the effects of ET_B receptor stimulation from basal tone. S6c (100 nM) did not cause contraction of aorta, but caused contraction of short duration (< 2 minutes) in vena cava (**Figure 46**). A maximal concentration of S6c, as opposed to a cumulative concentration response curve, was used because of the desensitization that occurs with this agonist [2]. Next, vessels were contracted with PGF-2α (20 μM) before being exposed to S6c (100 nM) (**Figure 47**). S6c caused relaxation in both aorta and vena cava.

Aorta and vena cava were next incubated with N-(ω)-nitro-L-arginine (LNNA) (100 μM) for 1h or denuded of endothelium, and contracted with PGF-2α (20 μM) before being exposed to S6c (100 nM). Endothelial denudation and LNNA (100 μM) abolished relaxation to Ach (1 μM) and S6c (100 nM) in aorta (**Figure 48a**). In vena cava, however, endothelial denudation and LNNA (100 μM) abolished relaxation to ACh (1 μM) but only attenuated relaxation to S6c (100 nM)(**Figure 48b**). Inhibition of COX 1 and 2 by indomethacin (5 μM) did not alter S6c- or ACh-induced relaxation in either the aorta or vena cava. PGF-2α contraction, established prior to addition of S6c, was not significantly different ($p > 0.05$) from vehicle (121.6±6.6% PE contraction) in the presence of indomethacin (134.9±19.1% PE contraction) or endothelial denudation (123.0±4.1% PE contraction), but was significantly increased by LNNA (163.0±10.5% PE contraction, $p<0.05$). Likewise, PGF-2α contraction in vena cava was not significantly changed by indomethacin (430.3±50.6% NE contraction) or denudation

(239.5±33.5% NE contraction), but was significantly increased by LNNA (564.8±45.3% NE contraction, $p<0.05$) as compared to vehicle (309.5±31.9% NE contraction).

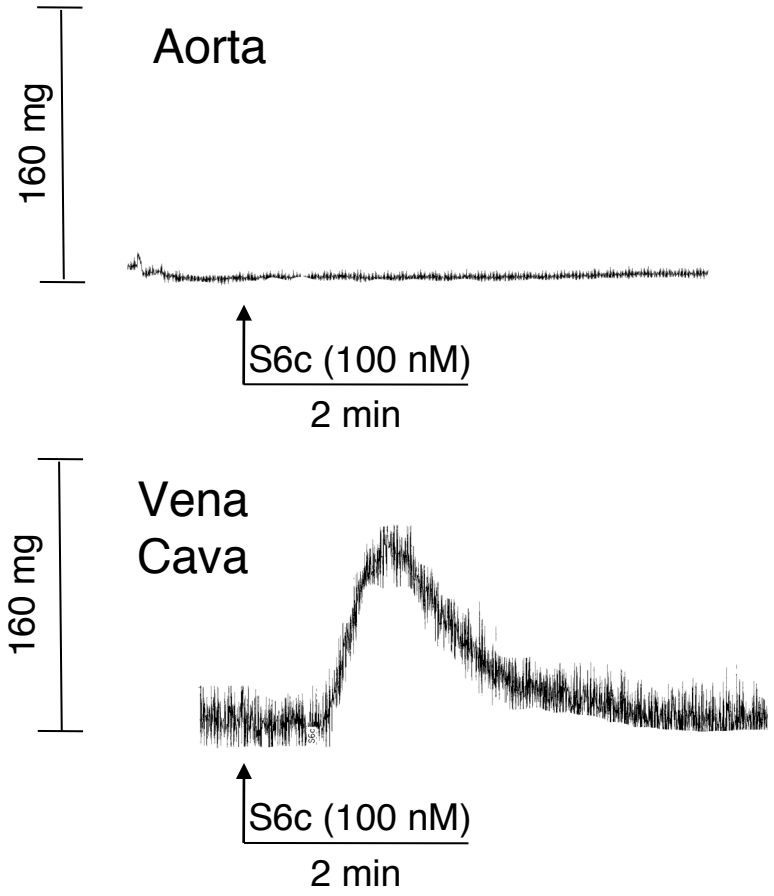

Figure 46. ET_B receptor-dependent contraction of aorta and vena cava by S6c. Representative tracings of aorta (top) and vena cava (bottom), showing contractions resulting from ET_B receptor stimulation with Sarafotoxin-6c (S6c) (100 nM). Horizontal black bar represents 2 minutes of elapsed time. Representative of greater than 50 experiments.

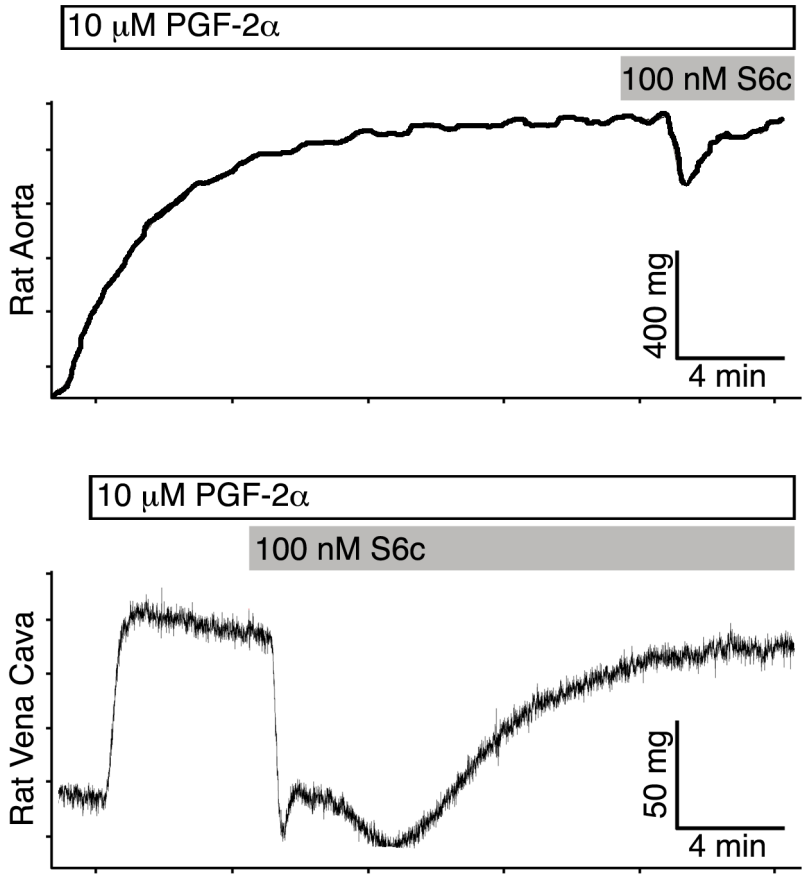

Figure 47. Representative tracing of endothelium-intact aorta (top) and vena cava (bottom). Tracings show relaxation by ET_B receptor stimulation with 100 nM sarafotoxin 6c (S6c) in vessels contracted with 20 μM PGF-2α. Representative of 6 experiments.

A.

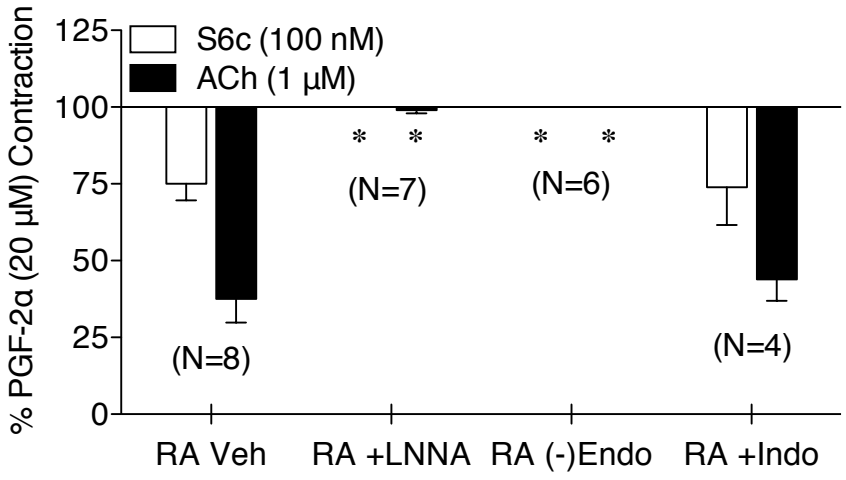

B.

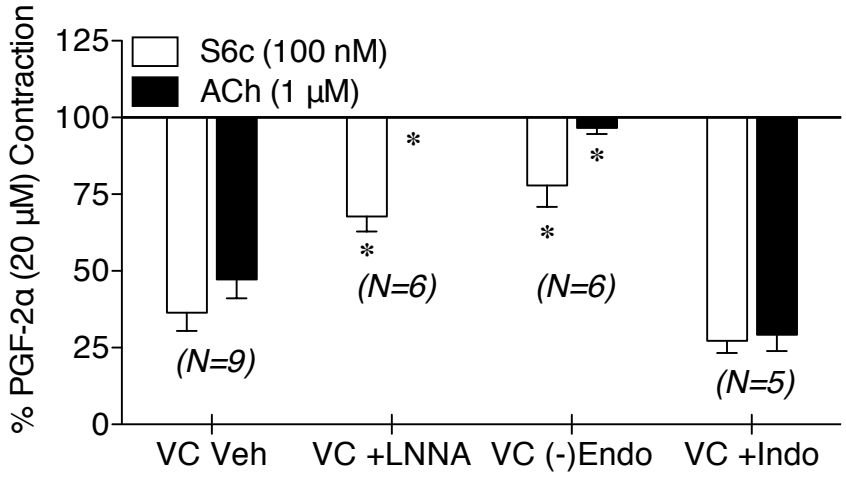

Figure 48. Relaxation to S6c and ACh in PGF-2α-contracted aorta and vena cava. Aorta (A) and vena cava (B) were exposed to different inhibitors for 1h or endothelium-denuded (-endo). All bars represent mean ± SEM for the number of animals indicated. White bars represent relaxation to S6c. Black bars represent relaxation to ACh. Results are shown as percentages of initial PGF-2α (20 μM) contraction. Veh=vehicle treatment; LNNA= N-(ω)-nitro-L-arginine (100 μM); Indo=indomethacin (5 μM); * = $p<0.05$ *versus* vehicle.

2.3. Endothelin-1-induced Relaxation in Aorta and Vena Cava

PGF-2α (10 μM)-contracted vessels were exposed to increasing concentrations of ET-1 (10 pM – 100 nM). Vessels were incubated with vehicle, the ET_A receptor antagonist atrasentan (30 nM), or atrasentan (30 nM) and the ET_B receptor antagonist BQ-788 (100 nM), to distinguish between the effects of ET_A and ET_B receptor stimulation. ET-1 caused a concentration-dependent contraction in aorta treated with vehicle (**Figure 49a**). Aorta incubated with atrasentan (30 nM) relaxed to ET-1, reaching a sustained minimum at a concentration of 10 nM. As the concentration of ET-1 was increased from 30 nM – 100 nM, aorta then contracted. Incubation with atrasentan (30 nM) and BQ-788 (100 nM) caused a rightward shift in the relaxant response of the aorta to ET-1, but contraction to ET-1 was not observed.

In contrast to the aorta, ET-1 caused concentration-dependent relaxation of vehicle-incubated vena cava with a maximal relaxation attained at 1 nM (**Figure 49b**). As concentrations of ET-1 increased, the vena cava contracted in a concentration-dependent manner. When exposed to atrasentan (30 nM), the vena cava relaxed in a concentration-dependent fashion up to 10 nM ET-1 before contracting as concentration increased. Incubation with both atrasentan (30 nM) and BQ-788 (100 nM) shifted the relaxation response curve to the right, and contraction was not observed.

To further investigate the contribution of ET_B receptors to ET-1-induced relaxation, tissues from male (DβH)-$ET_B^{(sl/sl)}$ transgenic rats (sl/sl) and their DβH-ET_B:$ET_B^{(+/+)}$ male littermates (+/+) were tested in the same protocol. Contractions to ET-1 in (sl/sl)

aorta contracted with PGF-2α (10 μM) were not statistically different from those of (+/+) aorta, nor did aorta relax to ET-1. (**Figure 50a**). ET-1 caused only concentration-dependent contraction in (sl/sl) vena cava contracted with PGF-2α (10 μM), whereas ET-1-stimulated relaxation was observed in (+/+) vena cava (**Figure 50b**).

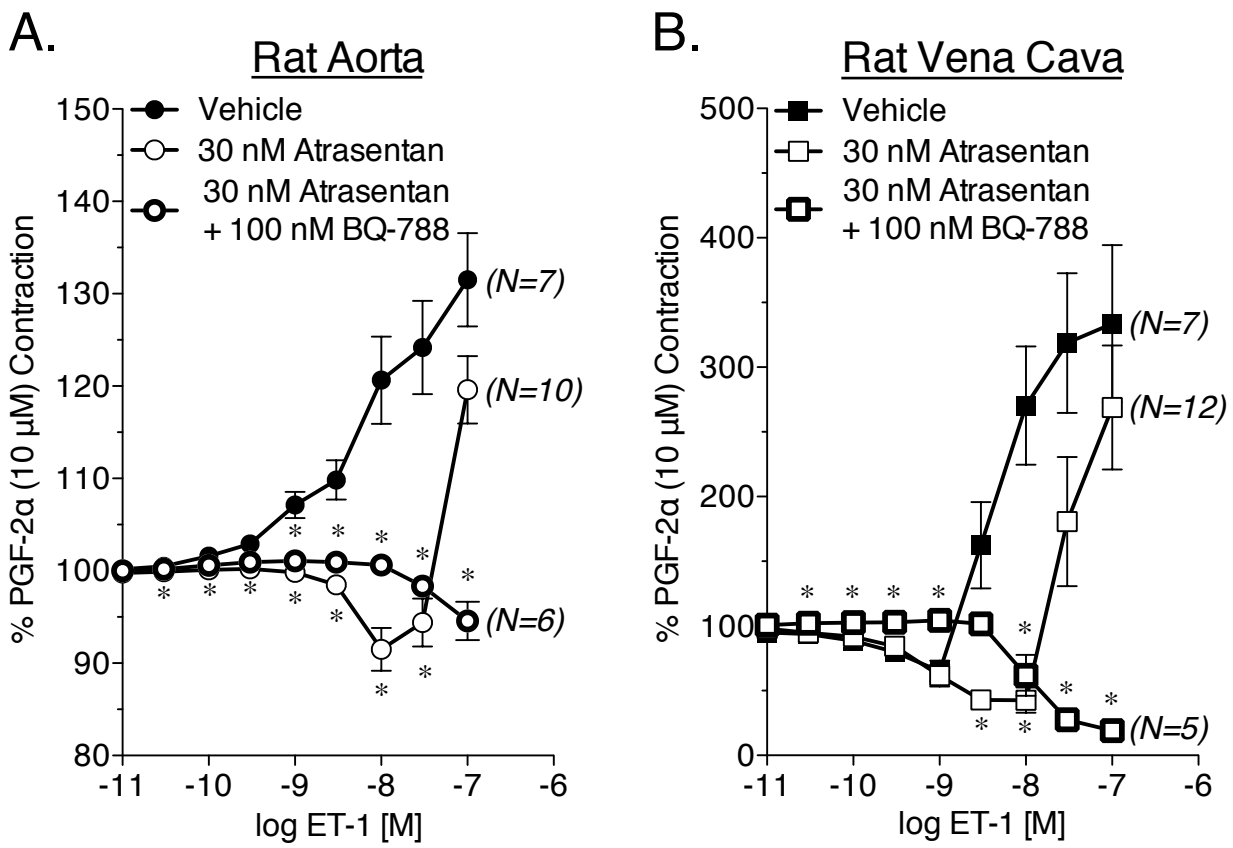

Figure 49. Measurement of endothelin-1-induced responses in PGF-2α (10 μM)-contracted aorta and vena cava, exposed to vehicle, atrasentan (30 nM), or atrasentan (30 nM) with BQ-788 (100 nM). Aorta (A) and vena cava (B) were incubated with vehicle or antagonists for 1h prior to PGF-2α contraction and subsequent ET-1 exposure. Points represent mean ± SEM for the number of animals indicated in parentheses. * = $p<0.05$ *versus* vehicle.

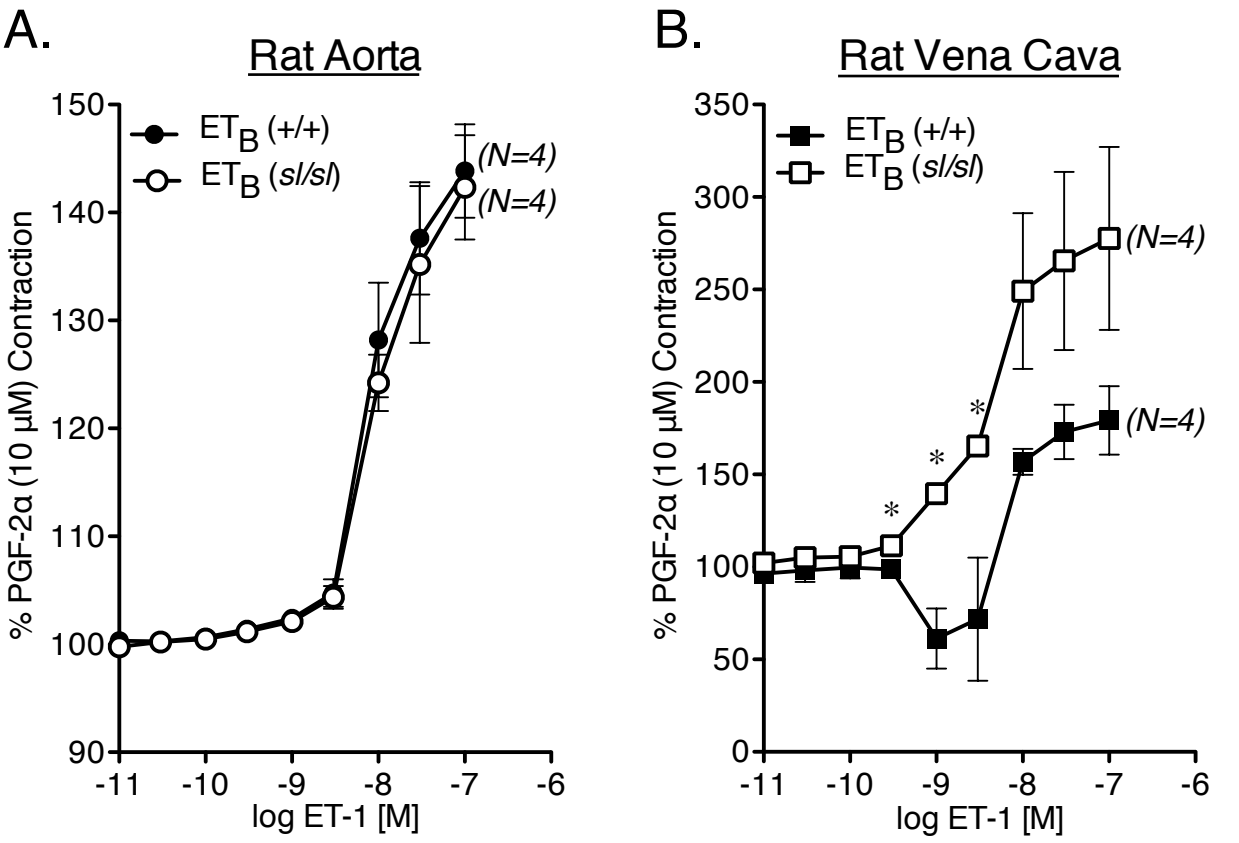

Figure 50. Measurement of endothelin-1-induced responses in PGF-2α (10 μM)-contracted aorta and vena cava from ET_B receptor-deficient rats (*sl/sl*) and their wild-type littermates (+/+). Points represent mean ± SEM for the number of aorta (A) and vena cava (B) indicated in parentheses. * = $p<0.05$ *versus* vehicle.

3. Discussion

3.1. Venous ET_B receptors and vascular function

The main objective of this study was to test if the mechanisms by which ET_B receptors modulate arterial relaxation are the same or different from those that mediate venous relaxation. We also address the idea of whether the ET_B receptor mediating relaxation could be activated by ET-1, the endogenous agonist for this receptor. The data we present here imply not only a different mechanism of endothelial ET_B receptor function between arteries and veins, but the possible existence of an ET_B receptor on venous smooth muscle cells which mediates relaxation. Understanding the mechanisms controlling venous and arterial responses to ET receptor stimulation may help define the roles of ET-1 and veins in regulating blood pressure. Veins can respond differently than arteries when stimulated by the same agonist, including ET-1, in both physiological and pathological conditions [2]. This is important in light of the findings that ET_B receptor stimulation alone causes significant hypertension in rats which is unaffected by ET_A receptor blockade, and may be largely mediated by the venous circulation [235].

3.2. ET_B-mediated relaxation in venous and arterial endothelial and smooth muscle cells

Endothelial cell ET_B receptors in most arterial beds stimulate NO release and relaxation, leading us to postulate that venous relaxation also depended on endothelial eNOS [84]. Even though immunohistochemical analysis confirmed that ET_B receptors are present in

the endothelium of the vena cava, inhibition of eNOS did not totally abolish S6c-induced relaxation. The concentration of LNNA (100 μM) used was adequate to abolish ET_B receptor-mediated relaxation in the aorta, and acetylcholine-induced relaxation in both the aorta and vena cava. This confirms that ET_B receptor-mediated relaxation in the aorta is wholly dependent on NO release, but suggests that venous ET_B receptor-mediated relaxation is only partially dependent on NO release.

When we combine our findings from LNNA-exposed tissues with our findings in endothelium-denuded tissues, they suggest that there is a functional ET_B receptor in venous tissue, as least as revealed by S6c that can regulate relaxation.

3.3. The role of ET_B receptors in regulating responses to ET-1 in contracted aorta and vena cava

Evidence strongly supports the existence of a contractile ET_B receptor in the vena cava. It is unclear, however, if antagonism of both ET_A and ET_B receptors reveals the presence of a contractile ET_B receptor in the aorta. The addition of BQ-788 (100 nM) to atrasentan (30 nM) further reduced ET-1-induced contraction in the aorta, suggesting the presence of an aortic contractile ET_B receptor (**Figure 47**). Other evidence, however, is contradictory to this idea. First, the ET_B agonist S6c (100 nM) did not directly contract isolated aorta, but does contract vena cava (**Figure 44**). Second, experiments with tissues from (*sl/sl*) and (*+/+*) rats revealed that contraction to ET-1 was neither rightward-shifted nor reduced in aorta that lack functional ET_B receptors (**Figure 48a**). These collective results present a mixed conclusion as to the presence of an ET_B

receptor mediating contraction in the aorta. There is, however, no question that a contractile ET_B receptor is present in the vena cava.

Use of ET-1 in testing the presence of relaxant receptors was important, as ET-1 is the endogenous agonist for ET receptors. PGF-2α-contracted vena cava demonstrated a functional ET_B receptor that mediates relaxation when activated by ET-1. This mechanism was not initially apparent in the aorta, since only contraction to ET-1 was observed in aorta controls. Aorta incubated with atrasentan, however, relaxed to ET-1. This implies that a functional and relaxant ET_B receptor exists in the aorta that is revealed by ET_A receptor blockade, and requires a greater concentration of ET-1 than the vein does to activate it. ET-1 induced relaxation has been noted *in vivo* as well, where injection of ET-1 results in a transient drop in blood pressure followed by a prolonged increase in arterial pressure [30].

3.4. Limitations

There are limitations to some of the studies presented here. Making an association between ET receptor function in large conduit vessels the role of the ET receptor in maintaining blood pressure is difficult. Large vessels make for more consistent experiments and more obvious differences between arteries and veins, but small resistance vessels may respond differently than large vessels when taken through the same experimental protocol.

Whenever genetically modified animals are utilized in an experiment, unexpected phenotypical changes caused by the mutation can arise and should be noted. Although there are no outstanding phenotypical changes in (DβH)-ET_B:$ET_B^{(sl/sl)}$ rats that separate them from their DβH-ET_B:$ET_B^{(+/+)}$ male littermates, blood pressure and circulating ET-1 concentrations are slightly elevated [270]. We do not believe this changed our *in vitro* results.

With *en face* immunohistochemical staining, auto-fluorescence is problematic in thick tissues such as the aorta. We tried to locate ET_B receptors in the endothelium of aorta a number of times, using varying concentrations of both primary and secondary antibodies as well as different blocking solutions. We were not able to separate the background fluorescence from the specific staining to provide a clear picture. In this study, we demonstrated a functional response to S6c that was endothelial cell-dependent in aorta (**Figure 47a**). These data provide some confidence in the statement that ET_B receptors are present in the aortic endothelial cell. Moreover, literature reports have located PECAM-1 in *en face* mouse aorta [271], and ET_B receptors in rat aortic endothelial cells [272]. We believe that this information, collectively, is sufficient to state that ET_B receptors are likely present in aortic endothelial cells.

Differing results from endothelium-denuded RVC are another limitation. Whereas treatment with S6c still caused relaxation in denuded RVC, the relaxation caused by ET-1 in denuded RVC was abolished. This does not call into question the existence of a functional ET_B receptor on venous smooth muscle cells, but shows that ET-1 responses are more complex than S6c responses.

3.5. Conclusions

The mechanisms by which ET_B receptors cause relaxation in arteries are different than in veins. We conclude that ET_B receptors in the vena cava regulate relaxation in a manner partially independent of either a functional endothelium or NO release. Importantly, the receptor's endogenous ligand for the ET_B receptor (ET-1) causes relaxation in the vena cava that is not observed in the aorta. We have shown differences in ET_B receptor function in the aorta and vena cava, providing a new understanding of the function of the venous ET receptors. These findings are important in understanding the different ways vascular tone is regulated in the venous and arterial circulation and may help to further understand how veins and arteries interact to maintain blood pressure.

APPENDIX C

Curriculum Vitae

Nathan R. Tykocki

PERSONAL INFORMATION

Name: Nathan Roger Tykocki

Born: 3/28/80 – Detroit, MI

1355 Bogue St. Room B-445

Dept. of Pharmacology and Toxicology

Michigan State University

East Lansing, MI 48824

Phone: (517) 353-3900

Fax: (517) 353-8915

Email: tykockin@msu.edu

EDUCATIONAL BACKGROUND

1998-2002	Michigan State University, East Lansing, MI
	B.S. (Lyman Briggs College, Science and Technology Studies)
2007-present	Michigan State University, East Lansing, MI
	Doctoral Candidate (Pharmacology and Toxicology)

Project Title: *"Endothelin-1-induced calcium signaling in arteries and veins"*

TEACHING ACTIVITIES

2001-2002 Teaching Assistant for Chemistry Lab (LBS 171, LBS 172)
Michigan State University

2009 Teaching Assistant for Pharmacology (PHM 819)
Michigan State University

2010 Tutor for Pharmacology (PHM 350)
Michigan State University

2011 Lecturer, Introduction to Chemical Toxicology (PHM 450)
Renal and Cardiovascular Toxicology sections
Michigan State University

2011 Teaching Assistant for Experimental Design and Analysis (PHM 830)
Michigan State University

RESEARCH TRAINING

2006 **Research Assistant:** Pharmacology Laboratory, Michigan State University. Investigated intracellular signaling mechanisms that regulate smooth muscle contraction and relaxation in hamster cremaster arterioles. Supervisor: Dr. William Jackson.

2007 **Research Rotation:** Cardiovascular Pharmacology Laboratory, Michigan State University. Investigated the role of different calcium channels in regulating responses to ET-1 in rat aorta and vena cava. Supervisor: Dr. Stephanie Watts.

2007-pres. **Doctoral Dissertation Research:** Cardiovascular Pharmacology Laboratory, Michigan State University. Endothelin-1-induced calcium signaling in arteries and veins. Mentors: Dr. Stephanie Watts and Dr. William Jackson.

PROFESSIONAL ACTIVITIES

American Heart Association

American Physiological Society

American Society of Pharmacology and Experimental Therapeutics

Reviewer for *Journal of Vascular Research*

Reviewer for *American Journal of Physiology Heart and Circulatory Physiology*

Reviewer for *Pharmacological Research*

ACADEMIC AND PROFESSIONAL HONORS

2007 Travel Award, 6th Hypertension Summer School

2008 Session Moderator, 35th Annual Pharmacology Research Colloquium

Recipient, Michigan State University Graduate School Summer Research Fellowship

2009 Scholarship, Keystone Symposium –Dissection the Vasculature: Function, Molecular Mechanisms and Malfunction

2011 Third Place in Oral Presentations, 38th Annual Pharmacology Research Colloquium

2012 ASPET Travel Award, Experimental Biology 2012

PRESENTATIONS

Erika M. Boerman, Nathan R. Tykocki, and William F. Jackson. “Ryanodine Receptors and Calcium Activated K^+ Channels are Not Coupled in the Microcirculation". *Poster Presentation; 61st Annual High Blood Pressure Research Conference;* Tucson, AZ (2007).

Nathan R. Tykocki, William F. Jackson, and Stephanie Watts. “Do Different Calcium Entry Mechanisms Mediate Endothelin-1-induced Contraction of Rat Aorta and Vena

Cava?". *Oral Presentation; 35th Annual Pharmacology Research Colloquium;* Ann Arbor, MI (2008).

Nathan R. Tykocki, William F. Jackson, and Stephanie Watts. “Do Different Calcium Entry Mechanisms Mediate Endothelin-1-induced Contraction of Rat Aorta and Vena Cava?”. *Poster Presentation; Experimental Biology Conference*; San Diego, CA (2008).

Nathan R. Tykocki, William F. Jackson, and Stephanie W. Watts. “The Complex Roles of ET_B Receptors in Mediating Venous Tone”. *Poster Presentation; 62nd Annual High Blood Pressure Research Conference*; Atlanta, GA (2008).

Nathan R. Tykocki and Stephanie W. Watts. “Contractile and Relaxant Mechanisms of ET_A and ET_B Receptors in Rat Aorta and Vena Cava”. *Poster Presentation; Keystone Symposium - Dissecting the Vasculature: Function, Molecular Mechanisms, and Malfunction*; Vancouver, BC Canada (2009).

Nathan R. Tykocki and Stephanie W. Watts. “ET_B receptor activation changes ET_B receptor location in venous but not aortic smooth muscle cells”. *Poster Presentation; Experimental Biology Conference*; New Orleans, LA (2009).

Nathan R. Tykocki and Stephanie W. Watts. “Is KB-R7943 a specific inhibitor of reverse-mode NCX in the vasculature?”. *Poster Presentation; Experimental Biology Conference*; Washington, DC (2011).

Nathan R. Tykocki, William F. Jackson and Stephanie W. Watts. “Endothelin-1 increases the frequency of smooth muscle calcium waves in vena cava but not aorta”. *Poster Presentation; Experimental Biology Conference*; Washington, DC (2011).

Nathan R. Tykocki, William F. Jackson and Stephanie W. Watts. “Endothelin-1 increases the frequency and amplitude of calcium waves in rat vena cava”. *Oral Presentation; 38th Annual Pharmacology Research Colloquium;* Toledo, OH (2011).

Nathan R. Tykocki, BinXi Wu, William F. Jackson and Stephanie W. Watts. “Contraction of rat vena cava by endothelin-1 is dependent on phospholipase C, but independent of IP_3 receptor activation”. *Poster Presentation; Experimental Biology Conference;* San Diego, CA (2012).

Nathan R. Tykocki, Robert W. Wiseman, William F. Jackson and Stephanie W. Watts. “An imaging apparatus for simultaneous measurement of isometric contraction and Ca^{2+} fluorescence in large blood vessels of the rat”. *Poster Presentation; Experimental Biology Conference;* San Diego, CA (2012).

PAPERS

Nathan R. Tykocki, William F. Jackson and Stephanie W. Watts (2012) Reverse-mode Na^{+}/Ca^{2+} exchange is an important mediator of venous contraction. *Revised Manuscript submitted.*

Christopher J. Bush, Theodora Szasz, Kyle B. Johnson, Nathan R. Tykocki, Witold K. Surewicz, Ralph E. Watson and Stephanie W. Watts (2011) Expression and potential function of prion protein in the vasculature. *Reinvention: a Journal of Undergraduate Research* [Internet]. Available From: http://www.warwick.ac.uk/go/reinventionjournal/issues/volume4issue2/

Nathan R. Tykocki and Stephanie W. Watts (2010) The Interdependence of Endothelin-1 and Calcium: A Review. *Clinical Science* (119): 361-372.

Nathan R. Tykocki, Cheryl E. Gariepy and Stephanie W. Watts (2009) Endothelin ET_B receptors in arteries and veins: multiple actions in the vein. *J Pharmacol Exp Ther* (329): 875-881.

ABSTRACTS

Nathan R. Tykocki, Robert W. Wiseman, William F. Jackson and Stephanie W. Watts. An imaging apparatus for simultaneous measurement of isometric contraction and Ca^{2+} fluorescence in large blood vessels of the rat [Abstract]. In: Experimental Biology; 2012 Apr 21-25; San Diego, CA. *FASEB J* (26): 870.31

Nathan R. Tykocki, BinXi Wu, William F. Jackson and Stephanie W. Watts. Contraction of rat vena cava by endothelin-1 is dependent on phospholipase C, but independent of IP_3 receptor activation [Abstract]. In: Experimental Biology; 2012 Apr 21-25; San Diego, CA. *FASEB J* (26): 1049.3

Nathan R. Tykocki, William F. Jackson and Stephanie W. Watts. Endothelin-1 increases the frequency of smooth muscle calcium waves in vena cava but not aorta [Abstract]. In: Experimental Biology; 2011 Apr 9-13; Washington, DC. *FASEB J* (25): 1026.2.

Nathan R. Tykocki and Stephanie W. Watts. Is KB-R7943 a specific inhibitor of reverse-mode NCX in the vasculature? [Abstract]. In: Experimental Biology; 2011 Apr 9-13; Washington, DC. *FASEB J* (25): 808.8.

Nathan R. Tykocki and Stephanie W. Watts. ET_B receptor activation changes ET_B receptor location in venous but not aortic smooth muscle cells [Abstract]. In: Experimental Biology; 2009 Apr 18-22; New Orleans, LA. *FASEB J* (23): 945.7.

Nathan R. Tykocki, William F. Jackson, and Stephanie W. Watts. The Complex Roles of ET_B Receptors in Mediating Venous Tone [Abstract]. In: 62nd Annual High Blood Pressure Research Conference; 2008 Sep 17-20; Atlanta, GA. *Hypertension* (52): e109-e110.

Nathan R. Tykocki, William F. Jackson, and Stephanie Watts. Do Different Calcium Entry Mechanisms Mediate Endothelin-1-induced Contraction of Rat Aorta and Vena Cava? [Abstract]. In: Experimental Biology; 2008 Apr 5-9; San Diego, CA. *FASEB J* (22): 744.15.

Erika M. Boerman, Nathan R. Tykocki and William F. Jackson. Ryanodine Receptors and Calcium Activated K^+ Channels are Not Coupled in the Microcirculation [Abstract].

In: 61st Annual High Blood Pressure Research Conference; 2007 Sep 26-29; Tucson, AZ. *Hypertension* (50): e144.

REFERENCES

REFERENCES

[1] Fink GD. Arthur C. Corcoran Memorial Lecture. Sympathetic activity, vascular capacitance, and long-term regulation of arterial pressure. Hypertension 2009;53:307–12.

[2] Thakali K, Fink GD, Watts SW. Arteries and veins desensitize differently to endothelin. J Cardiovasc Pharmacol 2004;43:387–93.

[3] Johnson RJ, Galligan JJ, Fink GD. Effect of an ET(B)-selective and a mixed ET(A/B) endothelin receptor antagonist on venomotor tone in deoxycorticosterone-salt hypertension. J Hypertens 2001;19:431–40.

[4] Cai B-X, Li X-Y, Chen J-H, Tang Y-B, Wang G-L, Zhou J-G, Qui Q-Y, Guan Y-Y. Ginsenoside-Rd, a new voltage-independent Ca^{2+} entry blocker, reverses basilar hypertrophic remodeling in stroke-prone renovascular hypertensive rats. Eur J Pharmacol 2009;606:142–9.

[5] Sokolovsky M. Endothelin receptor subtypes and their role in transmembrane signaling mechanisms. Pharmacol Ther 1995;68:435–71.

[6] Yanagisawa M, Kurihara H, Kimura S, Tomobe Y, Kobayashi M, Mitsui Y, Yazaki Y, Goto K, Masaki T. A novel potent vasoconstrictor peptide produced by vascular endothelial cells. Nature 1988;332:411–5.

[7] Kawanabe Y, Nauli SM. Endothelin. Cell. Mol. Life Sci. 2011;68:195–203.

[8] Ito H, Hirata Y, Adachi S, Tanaka M, Tsujino M, Koike A, Nogami A, Murumo F, Hiroe M. Endothelin-1 is an autocrine/paracrine factor in the mechanism of angiotensin II-induced hypertrophy in cultured rat cardiomyocytes. J Clin Invest 1993;92:398–403.

[9] Ito H, Adachi S, Tamamori M, Fujisaki H, Tanaka M, Lin M, Akimoto H, Marumo F, Hiroe M. Mild hypoxia induces hypertrophy of cultured neonatal rat cardiomyocytes: a possible endogenous endothelin-1-mediated mechanism. J Mol Cell Cardiol 1996;28:1271–7.

[10] Yamazaki T, Komuro I, Kudoh S, Zou Y, Shiojima I, Hiroi Y, Mizuno T, Maemura K, Kurihara H, Aikawa R, Takano H, Yazaki Y. Endothelin-1 is involved in mechanical stress-induced cardiomyocyte hypertrophy. J Biol Chem 1996;271:3221–8.

[11] Davenport AP. International Union of Pharmacology. XXIX. Update on endothelin receptor nomenclature. Pharmacol Rev 2002;54:219–26.

[12] Kitamura K, Shiraishi N, Singer WD, Handlogten ME, Tomita K, Miller RT. Endothelin-B receptors activate Galpha13. Am J Physiol 1999;276:C930–7.

[13] Rubanyi GM, Polokoff MA. Endothelins: molecular biology, biochemistry, pharmacology, physiology, and pathophysiology. Pharmacol Rev 1994;46:325–415.

[14] Mencarelli M, Pecorelli A, Carbotti P, Valacchi G, Grasso G, Muscettola M. Endothelin receptor A expression in human inflammatory cells. Regul Pept 2009;158:1–5.

[15] Motta EM, Chichorro JG, Rae GA. Role of ET(A) and ET(B) endothelin receptors on endothelin-1-induced potentiation of nociceptive and thermal hyperalgesic responses evoked by capsaicin in rats. Neurosci Lett 2009;457:146–50.

[16] Xu D-Y, Wu B, Li Z-Q, Wang Q-P, Zhang Y, Xue F, Ji J-F. Expression of endothelin receptor subtypes in the spiral ganglion neurons of the guinea pig. Int J Pediatr Otorhinolaryngol 2009.

[17] Ali H, Loizidou M, Dashwood M, Savage F, Sheard C, Taylor I. Stimulation of colorectal cancer cell line growth by ET-1 and its inhibition by ET(A) antagonists. Gut 2000;47:685–8.

[18] Fagan KA, McMurtry IF, Rodman DM. Role of endothelin-1 in lung disease. Respir Res 2001;2:90–101.

[19] Khodorova A, Montmayeur J-P, Strichartz G. Endothelin receptors and pain. The Journal of Pain : Official Journal of the American Pain Society 2009;10:4–28.

[20] Ortega Mateo A, de Artiñano AA. Highlights on endothelins: a review. Pharmacol Res 1997;36:339–51.

[21] Pinto-Sietsma SJ, Paul M. A role for endothelin in the pathogenesis of hypertension: fact or fiction? Kidney Int Suppl 1998;67:S115–21.

[22] Cardillo C, Kilcoyne CM, Waclawiw M, Cannon RO, Panza JA. Role of endothelin in the increased vascular tone of patients with essential hypertension. Hypertension 1999;33:753–8.

[23] Pérez-Rivera AA, Fink GD, Galligan JJ. Vascular reactivity of mesenteric arteries and veins to endothelin-1 in a murine model of high blood pressure. Vascul Pharmacol 2005;43:1–10.

[24] Elijovich F, Laffer CL, Amador E, Gavras H, Bresnahan MR, Schiffrin EL. Regulation of plasma endothelin by salt in salt-sensitive hypertension. Circulation 2001;103:263–8.

[25] Jouneaux C, Mallat A, Serradeil-Le Gal C, Goldsmith P, Hanoune J, Lotersztajn S. Coupling of endothelin B receptors to the calcium pump and phospholipase C via Gs and Gq in rat liver. J Biol Chem 1994;269:1845–51.

[26] Luo G, Jamali R, Cao Y-X, Edvinsson L, Xu C-B. Vascular endothelin ET(B) receptor-mediated contraction requires phosphorylation of ERK1/2 proteins. Eur J Pharmacol 2006;538:124–31.

[27] Zeng Q, Li X, Zhong G, Zhang W, Sun C. Endothelin-1 induces intracellular [Ca^{2+}] increase via Ca 2+ influx through the L-type Ca^{2+} channel, Ca 2+ - induced Ca^{2+} release and a pathway involving ET A receptors, PKC, PKA and AT1 receptors in cardiomyocytes. Sci China, C, Life Sci 2009;52:360–70.

[28] Kawanabe Y, Nauli SM. Involvement of extracellular Ca^{2+} influx through voltage-independent Ca^{2+} channels in endothelin-1 function. Cell Signal 2005;17:911–6.

[29] Neylon CB. Vascular biology of endothelin signal transduction. Clin Exp Pharmacol Physiol 1999;26:149–53.

[30] Pollock DM, Keith TL, Highsmith RF. Endothelin receptors and calcium signaling. Faseb J 1995;9:1196–204.

[31] Tykocki NR, Watts SW. The interdependence of endothelin-1 and calcium: a review. Clin Sci 2010;119:361–72.

[32] Parekh AB. Ca^{2+} microdomains near plasma membrane Ca^{2+} channels: impact on cell function. J Physiol (Lond) 2008;586:3043–54.

[33] Leung FP, Yung LM, Yao X, Laher I, Huang Y. Store-operated calcium entry in vascular smooth muscle. Br J Pharmacol 2008;153:846–57.

[34] Dolphin A. A short history of voltage-gated calcium channels. Br J Pharmacol 2006;147 Suppl 1:S56–62.

[35] Bootman MD, Collins TJ, Peppiatt CM, Prothero LS, MacKenzie L, De Smet P, Travers M, Tovey SC, Seo JT, Berridge MJ, Ciccolini F, Lipp P. Calcium signalling--an overview. Semin. Cell Dev. Biol. 2001;12:3–10.

[36] Giorgi C, Romagnoli A, Pinton P, Rizzuto R. Ca^{2+} signaling, mitochondria and cell death. Curr Mol Med 2008;8:119–30.

[37] Catterall WA, Perez-Reyes E, Snutch TP, Striessnig J. International Union of Pharmacology. XLVIII. Nomenclature and structure-function relationships of voltage-gated calcium channels. Pharmacol Rev 2005;57:411–25.

[38] Derkach V, Surprenant A, North R. 5-HT3 receptors are membrane ion channels. Nature 1989;339:706–9.

[39] Noda M, Furutani Y, Takahashi H, Toyosato M, Tanabe T, Shimizu S, Kikyotani S, Kayano T, Hirose T, Inayama S, al E. Cloning and sequence analysis of calf cDNA and human genomic DNA encoding alpha-subunit precursor of muscle acetylcholine receptor. Nature 1983;305:818–23.

[40] Valera S, Hussy N, Evans R, Adami N, North R, Surprenant A, Buell G. A new class of ligand-gated ion channel defined by P2x receptor for extracellular ATP. Nature 1994;371:516–9.

[41] Putney JW. Capacitative calcium entry: from concept to molecules. Immunol Rev 2009;231:10–22.

[42] Taylor CW, Rahman T, Tovey SC, Dedos SG, Taylor EJA, Velamakanni S. IP_3 receptors: some lessons from DT40 cells. Immunol Rev 2009;231:23–44.

[43] Mackrill JJ. Ryanodine receptor calcium channels and their partners as drug targets. Biochem Pharmacol 2010;79:1535–43.

[44] Guerini D. The Ca^{2+} pumps and the Na^{+}/Ca^{2+} exchangers. Biometals 1998;11:319–30.

[45] Wray S, Burdyga T, Noble K. Calcium signalling in smooth muscle. Cell Calcium 2005;38:397–407.

[46] Streb H, Schulz I. Regulation of cytosolic free Ca^{2+} concentration in acinar cells of rat pancreas. Am J Physiol 1983;245:G347–57.

[47] Essin K, Gollasch M. Role of Ryanodine Receptor Subtypes in Initiation and Formation of Calcium Sparks in Arterial Smooth Muscle: Comparison with Striated Muscle. J Biomed Biotechnol 2009;2009:1–16.

[48] Foskett JK, White C, Cheung K-H, Mak D-OD. Inositol trisphosphate receptor Ca^{2+} release channels. Physiol Rev 2007;87:593–658.

[49] Suko J, Maurer-Fogy I, Plank B, Bertel O, Wyskovsky W, Hohenegger M, Hellmann G. Phosphorylation of serine 2843 in ryanodine receptor-calcium release channel of skeletal muscle by cAMP-, cGMP- and CaM-dependent protein kinase. Biochim Biophys Acta 1993;1175:193–206.

[50] Hamada K, Mikoshiba K. Revisiting Channel Allostery: A Coherent Mechanism in IP_3 and Ryanodine Receptors. Science Signaling 2012;5:pe24.

[51] Ochocka A-M, Pawelczyk T. Isozymes delta of phosphoinositide-specific phospholipase C and their role in signal transduction in the cell. Acta Biochim Pol 2003;50:1097–110.

[52] Sureshan KM, Riley AM, Rossi AM, Tovey SC, Dedos SG, Taylor CW, Potter BVL. Activation of IP(3) receptors by synthetic bisphosphate ligands. Chem Commun (Camb) 2009:1204–6.

[53] Hill-Eubanks DC, Werner ME, Heppner TJ, Nelson MT. Calcium signaling in smooth muscle. Cold Spring Harb Perspect Biol 2011;3:a004549.

[54] Rebecchi MJ, Pentyala SN. Structure, function, and control of phosphoinositide-specific phospholipase C. Physiol Rev 2000;80:1291–335.

[55] Clapham DE, Julius D, Montell C, Schultz G. International Union of Pharmacology. XLIX. Nomenclature and structure-function relationships of transient receptor potential channels. Pharmacol Rev 2005;57:427–50.

[56] Endo M. Calcium ion as a second messenger with special reference to excitation-contraction coupling. J Pharmacol Sci 2006;100:519–24.

[57] del Valle-Rodríguez A, López-Barneo J, Ureña J. Ca^{2+} channel-sarcoplasmic reticulum coupling: a mechanism of arterial myocyte contraction without Ca^{2+} influx. Embo J 2003;22:4337–45.

[58] Bolton TB. Calcium events in smooth muscles and their interstitial cells; physiological roles of sparks. J Physiol (Lond) 2006;570:5–11.

[59] Somlyo AV. New roads leading to Ca^{2+} sensitization. Circ Res 2002;91:83–4.

[60] Eto M. Regulation of Cellular Protein Phosphatase-1 (PP1) by Phosphorylation of the CPI-17 Family, C-kinase-activated PP1 Inhibitors. Journal of Biological Chemistry 2009;284:35273–7.

[61] Somlyo AP, Somlyo AV. Ca^{2+} sensitivity of smooth muscle and nonmuscle myosin II: modulated by G proteins, kinases, and myosin phosphatase. Physiol Rev 2003;83:1325–58.

[62] Wang H, Eto M, Steers WD, Somlyo AP, Somlyo AV. RhoA-mediated Ca^{2+} sensitization in erectile function. J Biol Chem 2002;277:30614–21.

[63] O'Brien RF, Robbins RJ, McMurtry IF. Endothelial cells in culture produce a vasoconstrictor substance. J Cell Physiol 1987;132:263–70.

[64] Strait KA, Stricklett PK, Kohan JL, Miller MB, Kohan DE. Calcium regulation of endothelin-1 synthesis in rat inner medullary collecting duct. Am J Physiol Renal Physiol 2007;293:F601–6.

[65] Marsen TA, Simonson MS, Dunn MJ. Roles of calcium and kinases in regulation of thrombin-stimulated preproendothelin-1 transcription. Am J Physiol 1996;271:H1918–25.

[66] Dallas A, Khalil RA. Ca^{2+} antagonist-insensitive coronary smooth muscle contraction involves activation of epsilon-protein kinase C-dependent pathway. Am J Physiol, Cell Physiol 2003;285:C1454–63.

[67] Itoh H, Higuchi H, Hiraoka N, Ito M, Konishi T, Nakano T, Lederis K. Contraction of rat thoracic aorta strips by endothelin-1 in the absence of extracellular Ca2. Br J Pharmacol 1991;104:847–52.

[68] Thorin E, Webb DJ. Endothelium-derived endothelin-1. Pflugers Arch 2009.

[69] Hay DW, Luttmann MA, Muccitelli RM, Goldie RG. Endothelin receptors and calcium translocation pathways in human airways. Naunyn-Schmied Arch Pharmacol 1999;359:404–10.

[70] Elferink JG, de Koster BM. The effect of endothelin-2 (ET-2) on migration and changes in cytosolic free calcium of neutrophils. Naunyn-Schmied Arch Pharmacol 1996;353:130–5.

[71] Kohan DE. Biology of endothelin receptors in the collecting duct. Kidney Int 2009;76:481–6.

[72] Yeung VT, Ho SK, Tsang DS, Nicholls MG, Cockram CS. Endothelin-3 attenuates the cyclic GMP responses to C-type natriuretic peptide in cultured mouse astrocytes. J Neurosci Res 1996;46:686–96.

[73] Toffoli MC, Gabra BH, Teixeira CFP, Sirois P, Jancar S. Endothelins mediate

neutrophil activation, ProMMP-9 release and endothelial cell detachment. Inflammation 2007;30:28–37.

[74] Tokudome T, Horio T, Soeki T, Mori K, Kishimoto I, Suga S-I, Yoshihara F, Kawano Y, Kohno M, Kangawa K. Inhibitory effect of C-type natriuretic peptide (CNP) on cultured cardiac myocyte hypertrophy: interference between CNP and endothelin-1 signaling pathways. Endocrinology 2004;145:2131–40.

[75] Bailey MA, Haton C, Orea V, Sassard J, Bailly C, Unwin RJ, Imbert-Teboul M. ET_A receptor-mediated Ca^{2+} signaling in thin descending limbs of Henle's loop: impairment in genetic hypertension. Kidney Int 2003;63:1276–84.

[76] Dai J, Lee C-H, Poburko D, Szado T, Kuo K-H, van Breemen C. Endothelin-1-mediated wave-like $[Ca^{2+}]i$ oscillations in intact rabbit inferior vena cava. J Vasc Res 2007;44:495–503.

[77] Prasanna G, Krishnamoorthy R, Clark AF, Wordinger RJ, Yorio T. Human optic nerve head astrocytes as a target for endothelin-1. Invest Ophthalmol Vis Sci 2002;43:2704–13.

[78] Someya A, Yuyama H, Fujimori A, Ukai M, Fukushima S, Sasamata M. Effect of YM598, a selective endothelin ET_A receptor antagonist, on endothelin-1-induced bone formation. Eur J Pharmacol 2006;543:14–20.

[79] Chen Y, Tipoe GL, Liong E, Leung S, Lam S-Y, Iwase R, Tjong Y-W, Fung M-L. Chronic hypoxia enhances endothelin-1-induced intracellular calcium elevation in rat carotid body chemoreceptors and up-regulates ET_A receptor expression. Pflugers Arch 2002;443:565–73.

[80] Gouadon E, Meunier N, Grebert D, Durieux D, Baly C, Salesse R, Caillol M, Congar P. Endothelin evokes distinct calcium transients in neuronal and non-neuronal cells of rat olfactory mucosa primary cultures. Neuroscience 2010;165:584–600.

[81] Ge Y, Bagnall A, Stricklett PK, Strait K, Webb DJ, Kotelevtsev Y, Kohan DE. Collecting duct-specific knockout of the endothelin B receptor causes hypertension and sodium retention. Am J Physiol Renal Physiol 2006;291:F1274–80.

[82] Cardozo AM, D'Orléans-Juste P, Yano M, Frank PA, Rae GA. Influence of endothelin ET(A) and ET(B) receptor antagonists on endothelin-induced contractions of the guinea pig isolated gall bladder. Regul Pept 1997;69:15–23.

[83] Bogoni G, Rizzi A, Calo G, Campobasso C, D'Orleans-Juste P, Regoli D. Characterization of endothelin receptors in the human umbilical artery and vein. Br J Pharmacol 1996;119:1600–4.

[84] Tsukahara H, Ende H, Magazine HI, Bahou WF, Goligorsky MS. Molecular and functional characterization of the non-isopeptide-selective ET_B receptor in endothelial cells. Receptor coupling to nitric oxide synthase. J Biol Chem 1994;269:21778–85.

[85] Betts LC, Kozlowski RZ. Electrophysiological effects of endothelin-1 and their relationship to contraction in rat renal arterial smooth muscle. Br J Pharmacol 2000;130:787–96.

[86] Bkaily G, Naik R, D'Orléans-Juste P, Wang S, Fong CN. Endothelin-1 activates the R-type Ca^{2+} channel in vascular smooth-muscle cells. J Cardiovasc Pharmacol 1995;26 Suppl 3:S303–6.

[87] Hirata Y, Yoshimi H, Takata S, Watanabe TX, Kumagai S, Nakajima K, Sakakibara S. Cellular mechanism of action by a novel vasoconstrictor endothelin in cultured rat vascular smooth muscle cells. Biochem Biophys Res Commun 1988;154:868–75.

[88] Kasuya Y, Takuwa Y, Yanagisawa M, Masaki T, Goto K. A pertussis toxin-sensitive mechanism of endothelin action in porcine coronary artery smooth muscle. Br J Pharmacol 1992;107:456–62.

[89] Inoue Y, Oike M, Nakao K, Kitamura K, Kuriyama H. Endothelin augments unitary calcium channel currents on the smooth muscle cell membrane of guinea-pig portal vein. J Physiol (Lond) 1990;423:171–91.

[90] Van Renterghem C, Vigne P, Barhanin J, Schmid-Alliana A, Frelin C, Lazdunski M. Molecular mechanism of action of the vasoconstrictor peptide endothelin. Biochem Biophys Res Commun 1988;157:977–85.

[91] Van Renterghem C, Vigne P, Barhanin J, Schmid-Alliana A, Frelin C, Lazdunski M. Molecular mechanism of endothelin-1 action on aortic cells. J Cardiovasc Pharmacol 1989;13 Suppl 5:S186–7.

[92] Boixel C, Dinanian S, Lang-Lazdunski L, Mercadier JJ, Hatem SN. Characterization of effects of endothelin-1 on the L-type Ca^{2+} current in human atrial myocytes. Am J Physiol Heart Circ Physiol 2001;281:H764–73.

[93] Suzuki T. Endothelin-1-induced depolarization and hyperpolarization in submandibular ganglion neurons. Bull Tokyo Dent Coll 2004;45:189–92.

[94] Hukovic N, Hadziselimovic R. Endothelin 1 action on isolated rat stomach and the role of calcium ions in ET 1 induced depolarization of smooth muscle cells BC3H1. Biochem Mol Biol Int 1998;46:877–86.

[95] Lovenberg W, Miller R. Endothelin: a review of its effects and possible mechanisms of action. Neurochem Res 1990;15:407–17.

[96] Richard S. Vascular effects of calcium channel antagonists: new evidence. Drugs 2005;65 Suppl 2:1–10.

[97] Sudano I, Virdis A, Taddei S, Spieker L, Corti R, Noll G, Salvetti A, Luscher TF. Chronic treatment with long-acting nifedipine reduces vasoconstriction to endothelin-1 in essential hypertension. Hypertension 2007;49:285–90.

[98] Feron O, Salomone S, Godfraind T. Action of the calcium channel blocker lacidipine on cardiac hypertrophy and endothelin-1 gene expression in stroke-prone hypertensive rats. Br J Pharmacol 1996;118:659–64.

[99] Gardner JP, Tokudome G, Tomonari H, Maher E, Hollander D, Aviv A. Endothelin-induced calcium responses in human vascular smooth muscle cells. Am J Physiol 1992;262:C148–55.

[100] Pollock DM, Jenkins JM, Cook AK, Imig JD, Inscho EW. L-type calcium channels in the renal microcirculatory response to endothelin. Am J Physiol Renal Physiol 2005;288:F771–7.

[101] Tanaka Y, Imai T, Igarashi T, Takayanagi K, Otsuka K, Yamaki F, Tanaka H, Shigenobu K. Comparison of the Ca^{2+} entry channels responsible for mechanical responses of guinea-pig aorta to noradrenaline and thapsigargin using SK&F 96365 and LOE 908. Naunyn-Schmied Arch Pharmacol 2000;362:160–8.

[102] Kawanabe Y, Nozaki K, Hashimoto N, Masaki T. Involvement of extracellular Ca^{2+} influx and epidermal growth factor receptor tyrosine kinase transactivation in endothelin-1-induced arachidonic acid release. Br J Pharmacol 2003;139:1516–22.

[103] Ansari HR, Kaddour-Djebbar I, Abdel-Latif AA. Involvement of Ca^{2+} channels in endothelin-1-induced MAP kinase phosphorylation, myosin light chain phosphorylation and contraction in rabbit iris sphincter smooth muscle. Cell Signal 2004;16:609–19.

[104] Miwa S, Iwamuro Y, Zhang XF, Inoki T, Okamoto Y, Okazawa M, Masaki T. Ca^{2+} entry channels in rat thoracic aortic smooth muscle cells activated by endothelin-1. Jpn J Pharmacol 1999;80:281–8.

[105] Guan YY, Kwan CY, He H, Sun JJ, Daniel EE. Effects of Panax notoginseng saponins on receptor-operated Ca^{2+} channels in vascular smooth muscle. Zhongguo Yao Li Xue Bao 1994;15:392–8.

[106] Perez-Zoghbi JF, Sanderson MJ. Endothelin-induced contraction of bronchiole and pulmonary arteriole smooth muscle cells is regulated by intracellular Ca^{2+} oscillations and Ca^{2+} sensitization. Am J Physiol Lung Cell Mol Physiol 2007;293:L1000–11.

[107] Barone F, Genazzani AA, Conti A, Churchill GC, Palombi F, Ziparo E, Sorrentino V, Galione A, Filippini A. A pivotal role for cADPR-mediated Ca^{2+} signaling: regulation of endothelin-induced contraction in peritubular smooth muscle cells. Faseb J 2002;16:697–705.

[108] Guse AH, Lee HC. NAADP: a universal Ca^{2+} trigger. Science Signaling 2008;1:re10.

[109] Poburko D, Liao C-H, van Breemen C, Demaurex N. Mitochondrial regulation

of sarcoplasmic reticulum Ca^{2+} content in vascular smooth muscle cells. Circ Res 2009;104:104–12.

[110] Tostes RC, Wilde DW, Bendhack LM, Webb RC. Calcium handling by vascular myocytes in hypertension. Braz J Med Biol Res 1997;30:315–23.

[111] Schiffrin EL. Intracellular signal transduction for vasoactive peptides in hypertension. Can J Physiol Pharmacol 1994;72:954–62.

[112] Bkaily G, Choufani S, Avedanian L, Ahmarani L, Nader M, Jacques D, D'Orléans-Juste P, Khoury Al J. Nonpeptidic antagonists of ET_A and ET_B receptors reverse the ET-1-induced sustained increase of cytosolic and nuclear calcium in human aortic vascular smooth muscle cells. Can J Physiol Pharmacol 2008;86:546–56.

[113] Bkaily G, Nader M, Avedanian L, Choufani S, Jacques D, D'Orléans-Juste P, Gobeil F, Chemtob S, Khoury Al J. G-protein-coupled receptors, channels, and Na^+-H^+ exchanger in nuclear membranes of heart, hepatic, vascular endothelial, and smooth muscle cells. Can J Physiol Pharmacol 2006;84:431–41.

[114] Bkaily G, Avedanian L, Jacques D. Nuclear membrane receptors and channels as targets for drug development in cardiovascular diseases. Can J Physiol Pharmacol 2009;87:108–19.

[115] Bkaily G, Pothier P, D'Orléans-Juste P, Simaan M, Jacques D, Jaalouk D, Belzile F, Hassan G, Boutin C, Haddad G, Neugebauer W. The use of confocal microscopy in the investigation of cell structure and function in the heart, vascular endothelium and smooth muscle cells. Mol Cell Biochem 1997;172:171–94.

[116] Booz G, Conrad K, Hess A, Singer H, Baker K. Angiotensin-II-binding sites on hepatocyte nuclei. Endocrinology 1992;130:3641–9.

[117] Pendergrass KD, Gwathmey TM, Michalek RD, Grayson JM, Chappell MC. The angiotensin II-AT1 receptor stimulates reactive oxygen species within the cell nucleus. Biochem Biophys Res Commun 2009;384:149–54.

[118] Brini M, Carafoli E. Calcium pumps in health and disease. Physiol Rev 2009;89:1341–78.

[119] Yokomori H, Oda M, Ogi M, Yoshimura K, Nomura M, Fujimaki K, Kamegaya Y, Tsukada N, Ishii H. Endothelin-1 suppresses plasma membrane Ca++-ATPase, concomitant with contraction of hepatic sinusoidal endothelial fenestrae. Am J Pathol 2003;162:557–66.

[120] Lytton J. Na^+/Ca^{2+} exchangers: three mammalian gene families control Ca^{2+} transport. Biochem J 2007;406:365–82.

[121] Schulze DH, Muqhal M, Lederer WJ, Ruknudin AM. Sodium/calcium exchanger (NCX1) macromolecular complex. J Biol Chem 2003;278:28849–55.

[122] Dyck C, Omelchenko A, Elias CL, Quednau BD, Philipson KD, Hnatowich M, Hryshko LV. Ionic regulatory properties of brain and kidney splice variants of the NCX1 Na(+)-Ca(2+) exchanger. J Gen Physiol 1999;114:701–11.

[123] Poburko D, Fameli N, Kuo K-H, van Breemen C. Ca^{2+} signaling in smooth muscle: TRPC6, NCX and LNats in nanodomains. Channels (Austin) 2008;2:10–2.

[124] Fameli N, Kuo K-H, van Breemen C. A model for the generation of localized transient $[Na^+]$ elevations in vascular smooth muscle. Biochem Biophys Res Commun 2009;389:461–5.

[125] Blaustein MP, Charpentier TH, Weber DJ. Getting a grip on calcium regulation. Proc Natl Acad Sci USA 2007;104:18349–50.

[126] Li X, Zima AV, Sheikh F, Blatter LA, Chen J. Endothelin-1-induced arrhythmogenic Ca^{2+} signaling is abolished in atrial myocytes of inositol-1,4,5-trisphosphate(IP_3)-receptor type 2-deficient mice. Circ Res 2005;96:1274–81.

[127] Aiello EA, Villa-Abrille MC, Dulce RA, Cingolani HE, Pérez NG. Endothelin-1 stimulates the Na^+/Ca^{2+} exchanger reverse mode through intracellular Na^+ (Na^+i)-dependent and Na^+i-independent pathways. Hypertension 2005;45:288–93.

[128] Hilge M, Aelen J, Vuister GW. Ca^{2+} regulation in the Na^{+}/Ca^{2+} exchanger involves two markedly different Ca^{2+} sensors. Mol Cell 2006;22:15–25.

[129] Rothe CF. Physiology of Venous Return: An Unappreciated Boost to the Heart. Arch Intern Med 1986;146:977–82.

[130] Gao Y, Raj J. Role of veins in regulation of pulmonary circulation. Am J Physiol Lung Cell Mol Physiol 2005;288:L213–26.

[131] Grisk O, Rettig R. Renal transplantation studies in genetic hypertension. News Physiol Sci 2001;16:262–5.

[132] Beretta-Piccoli C, Weidmann P. Circulatory volume in essential hypertension. Relationships with age, blood pressure, exchangeable sodium, renin, aldosterone and catecholamines. Miner Electrolyte Metab 1984;10:292–300.

[133] Johnson R, Herrera-Acosta J, Schreiner G, Rodriguez-Iturbe B. Subtle acquired renal injury as a mechanism of salt-sensitive hypertension. N Engl J Med 2002;346:913–23.

[134] Lifton R, Gharavi A, Geller D. Molecular mechanisms of human hypertension. Cell 2001;104:545–56.

[135] Brengelmann GL. A critical analysis of the view that right atrial pressure determines venous return. J Appl Physiol 2003;94:849–59.

[136] Safar ME, London GM, Weiss YA, Milliez PL. Altered blood volume regulation in sustained essential hypertension: a hemodynamic study. Kidney Int 1975;8:42–7.

[137] Safar ME, London GM. Arterial and venous compliance in sustained essential hypertension. Hypertension 1987;10:133–9.

[138] Xu H, Kandlikar SS, Westcott EB, Fink GD, Galligan JJ. Requirement for functional BK channels in maintaining oscillation in venomotor tone revealed by species differences in expression of the β1 accessory subunits. J Cardiovasc Pharmacol 2012;59:29–36.

[139] Pérez-Rivera AA, Fink GD, Galligan JJ. Increased reactivity of murine mesenteric veins to adrenergic agonists: functional evidence supporting increased alpha1-adrenoceptor reserve in veins compared with arteries. J Pharmacol Exp Ther 2004;308:350–7.

[140] Pérez-Rivera AA, Hlavacova A, Rosario-Colón LA, Fink GD, Galligan JJ. Differential contributions of alpha-1 and alpha-2 adrenoceptors to vasoconstriction in mesenteric arteries and veins of normal and hypertensive mice. Vascul Pharmacol 2007;46:373–82.

[141] Galligan JJ, Miller SB, Katki K, Supowit S, DiPette D, Fink GD. Increased substance P content in nerve fibers associated with mesenteric veins from deoxycorticosterone acetate (DOCA)-salt hypertensive rats. Regul Pept 2006;133:97–104.

[142] Szasz T, Thakali K, Fink GD, Watts SW. A comparison of arteries and veins in oxidative stress: producers, destroyers, function, and disease. Exp Biol Med (Maywood) 2007;232:27–37.

[143] Szasz T, Thompson JM, Watts SW. A comparison of reactive oxygen species metabolism in the rat aorta and vena cava: focus on xanthine oxidase. Am J Physiol Heart Circ Physiol 2008;295:H1341–50.

[144] Rondelli CM, Szasz IT, Kayal A, Thakali K, Watson RE, Rovner AS, Eddinger TJ, Fink GD, Watts SW. Preferential myosin heavy chain isoform B Expression may contribute to the faster velocity of contraction in veins versus arteries. J Vasc Res 2007;44:264–72.

[145] Watts SW, Thakali K, Smark C, Rondelli C, Fink GD. Big ET-1 processing into vasoactive peptides in arteries and veins. Vascul Pharmacol 2007;47:302–12.

[146] Thakali K, Galligan JJ, Fink GD, Gariepy CE, Watts SW. Pharmacological endothelin receptor interaction does not occur in veins from ET(B) receptor deficient rats. Vascul Pharmacol 2008;49:6–13.

[147] Sumner MJ, Cannon TR, Mundin JW, White DG, Watts IS. Endothelin ET_A and ET_B receptors mediate vascular smooth muscle contraction. Br J Pharmacol 1992;107:858–60.

[148] Tykocki NR, Gariepy CE, Watts SW. Endothelin ET(B) receptors in arteries and veins: multiple actions in the vein. J Pharmacol Exp Ther 2009;329:875–81.

[149] Watts SW, Fink GD, Northcott CA, Galligan JJ. Endothelin-1-induced venous contraction is maintained in DOCA-salt hypertension; studies with receptor agonists. Br J Pharmacol 2002;137:69–79.

[150] National Research Council. Guide for the Care and Use of Laboratory Animals: Eighth Edition. The National Academies Press; 2011.

[151] Hamilton S. Ryanodine receptors. Cell Calcium 2005;38:253–60.

[152] Vaithianathan T, Narayanan D, Asuncion-Chin MT, Jeyakumar LH, Liu J, Fleischer S, Jaggar JH, Dopico AM. Subtype identification and functional characterization of ryanodine receptors in rat cerebral artery myocytes. Am J Physiol, Cell Physiol 2010;299:C264–78.

[153] Watts SW, Webb RC. Mechanism of ergonovine-induced contraction in the mesenteric artery from deoxycorticosterone acetate-salt hypertensive rat. J Pharmacol Exp Ther 1994;269:617–25.

[154] Zhang J, Ren C, Chen L, Navedo MF, Antos LK, Kinsey SP, Iwamoto T, Philipson KD, Kotlikoff MI, Santana LF, Wier WG, Matteson DR, Blaustein MP. Knockout of Na^{+}/Ca^{2+} exchanger in smooth muscle attenuates vasoconstriction and L-type Ca^{2+} channel current and lowers blood pressure. Am J Physiol Heart Circ Physiol 2010;298:H1472–83.

[155] Grynkiewicz G, Poenie M, Tsien RY. A new generation of Ca^{2+} indicators with greatly improved fluorescence properties. J Biol Chem 1985;260:3440–50.

[156] Gee K, Brown K, Chen W, Bishop-Stewart J, Gray D, Johnson I. Chemical and physiological characterization of fluo-4 Ca(2+)-indicator dyes. Cell Calcium 2000;27:97–106.

[157] Davis RP, Pattison J, Thompson JM, Tiniakov R, Scrogin KE, Watts SW. 5-hydroxytryptamine (5-HT) reduces total peripheral resistance during chronic infusion: direct arterial mesenteric relaxation is not involved. BMC Pharmacol

2012;12:4.

[158] Blaustein MP, Lederer WJ. Sodium/calcium exchange: its physiological implications. Physiol Rev 1999;79:763–854.

[159] Iwamoto T, Pan Y, Wakabayashi S, Imagawa T, Yamanaka HI, Shigekawa M. Phosphorylation-dependent regulation of cardiac Na^+/Ca^{2+} exchanger via protein kinase C. J Biol Chem 1996;271:13609–15.

[160] Blaustein MP. Sodium ions, calcium ions, blood pressure regulation, and hypertension: a reassessment and a hypothesis. Am J Physiol 1977;232:C165–73.

[161] Iwamoto T, Kita S, Zhang J, Blaustein MP, Arai Y, Yoshida S, Wakimoto K, Komuro I, Katsuragi T. Salt-sensitive hypertension is triggered by Ca^{2+} entry via Na^+/Ca^{2+} exchanger type-1 in vascular smooth muscle. Nat Med 2004;10:1193–9.

[162] Davis KA, Samson SE, Hammel KE, Kiss L, Fulop F, Grover AK. Functional linkage of Na^+-Ca^{2+}-exchanger to sarco/endoplasmic reticulum Ca^{2+} pump in coronary artery: comparison of smooth muscle and endothelial cells. J Cell Mol Med 2009;13:1775–83.

[163] Fameli N, van Breemen C, Kuo K-H. A quantitative model for linking Na^+/Ca^{2+} exchanger to SERCA during refilling of the sarcoplasmic reticulum to sustain $[Ca^{2+}]$ oscillations in vascular smooth muscle. Cell Calcium 2007;42:565–75.

[164] Poburko D, Liao C-H, Lemos VS, Lin E, Maruyama Y, Cole WC, van Breemen C. Transient receptor potential channel 6-mediated, localized cytosolic $[Na^+]$ transients drive Na^+/Ca^{2+} exchanger-mediated Ca^{2+} entry in purinergically stimulated aorta smooth muscle cells. Circ Res 2007;101:1030–8.

[165] Ashida T, Blaustein MP. Regulation of cell calcium and contractility in mammalian arterial smooth muscle: the role of sodium-calcium exchange. J Physiol (Lond) 1987;392:617–35.

[166] Fort A, Cordaillat M, Thollon C, Salazar G, Mechaly I, Villeneuve N, Vilaine J-P, Richard S, Virsolvy A. New insights in the contribution of voltage-gated Na(v)

channels to rat aorta contraction. PLoS ONE 2009;4:e7360.

[167] Wolf SC, Brodbeck C, Sauter G, Risler T, Brehm BR. Endothelin-1 regulates protein kinase C isoforms differently in smooth muscle cells and in cardiomyocytes. J Cardiovasc Pharmacol 2004;44 Suppl 1:S301–3.

[168] Kita S, Katsuragi T, Iwamoto T. Endothelin-1 enhances the activity of Na+/Ca^{2+} exchanger type 1 in renal epithelial cells. J Cardiovasc Pharmacol 2004;44 Suppl 1:S239–43.

[169] Kraft R. The Na^+/Ca^{2+} exchange inhibitor KB-R7943 potently blocks TRPC channels. Biochem Biophys Res Commun 2007;361:230–6.

[170] Liang GH, Kim JA, Seol GH, Choi S, Suh SH. The Na^+/Ca^{2+} exchanger inhibitor KB-R7943 activates large-conductance Ca^{2+}-activated K^+ channels in endothelial and vascular smooth muscle cells. Eur J Pharmacol 2008;582:35–41.

[171] Cheng H, Smith GL, Hancox JC, Orchard CH. Inhibition of spontaneous activity of rabbit atrioventricular node cells by KB-R7943 and inhibitors of sarcoplasmic reticulum Ca^{2+} ATPase. Cell Calcium 2011;49:56–65.

[172] Barrientos G, Bose DD, Feng W, Padilla I, Pessah IN. The Na^+/Ca^{2+} exchange inhibitor 2-(2-(4-(4-nitrobenzyloxy)phenyl)ethyl)isothiourea methanesulfonate (KB-R7943) also blocks ryanodine receptors type 1 (RyR1) and type 2 (RyR2) channels. Mol Pharmacol 2009;76:560–8.

[173] Levitsky DO. Three types of muscles express three sodium-calcium exchanger isoforms. Ann N Y Acad Sci 2007;1099:221–5.

[174] Hurtado C, Prociuk M, Maddaford TG, Dibrov E, Mesaeli N, Hryshko LV, Pierce GN. Cells expressing unique Na^+/Ca^{2+} exchange (NCX1) splice variants exhibit different susceptibilities to Ca^{2+} overload. Am J Physiol Heart Circ Physiol 2006;290:H2155–62.

[175] Zheng Y-M, Wang Y-X. Sodium-calcium exchanger in pulmonary artery smooth muscle cells. Ann N Y Acad Sci 2007;1099:427–35.

[176] Amran MS, Homma N, Hashimoto K. Pharmacology of KB-R7943: a Na^{+}-Ca^{2+} exchange inhibitor. Cardiovascular Drug Reviews 2003;21:255–76.

[177] Iwamoto T. Forefront of Na^{+}/Ca^{2+} exchanger studies: molecular pharmacology of Na^{+}/Ca^{2+} exchange inhibitors. J Pharmacol Sci 2004;96:27–32.

[178] Rosker C, Graziani A, Lukas M, Eder P, Zhu MX, Romanin C, Groschner K. Ca^{2+} signaling by TRPC3 involves Na^{+} entry and local coupling to the Na^{+}/Ca^{2+} exchanger. J Biol Chem 2004;279:13696–704.

[179] Lemos VS, Poburko D, Liao C-H, Cole WC, van Breemen C. Na^{+} entry via TRPC6 causes Ca^{2+} entry via NCX reversal in ATP stimulated smooth muscle cells. Biochem Biophys Res Commun 2007;352:130–4.

[180] Teubl M, Groschner K, Kohlwein SD, Mayer B, Schmidt K. Na(+)/Ca(2+) exchange facilitates Ca(2+)-dependent activation of endothelial nitric-oxide synthase. J Biol Chem 1999;274:29529–35.

[181] Schneider J-C, Kebir El D, Chéreau C, Mercier J-C, Dall'Ava-Santucci J, Dinh-Xuan AT. Involvement of Na(+)/Ca(2+) exchanger in endothelial NO production and endothelium-dependent relaxation. Am J Physiol Heart Circ Physiol 2002;283:H837–44.

[182] Ji G, Feldman ME, Greene KS, Sorrentino V, Xin H-B, Kotlikoff MI. RYR2 proteins contribute to the formation of Ca(2+) sparks in smooth muscle. J Gen Physiol 2004;123:377–86.

[183] Nelson MT, Cheng H, Rubart M, Santana LF, Bonev AD, Knot HJ, Lederer WJ. Relaxation of arterial smooth muscle by calcium sparks. Science 1995;270:633–7.

[184] Ruehlmann DO, Lee CH, Poburko D, van Breemen C. Asynchronous Ca(2+) waves in intact venous smooth muscle. Circ Res 2000;86:E72–9.

[185] Xia Y, Khalil RA. Sex-related decrease in $[Ca^{2+}]i$ signaling and Ca^{2+}-dependent contraction in inferior vena cava of female rat. Am J Physiol Regul Integr Comp Physiol 2010;298:R15–24.

[186] Lehnart SE, Wehrens XHT, Laitinen PJ, Reiken SR, Deng S-X, Cheng Z, Landry DW, Kontula K, Swan H, Marks AR. Sudden death in familial polymorphic ventricular tachycardia associated with calcium release channel (ryanodine receptor) leak. Circulation 2004;109:3208–14.

[187] Duan DD. A leakage leads to failure: roles of sarcoplasmic reticulum Ca^{2+} leak via RyR2 in heart failure progression. Hypertension 2010;55:849–51.

[188] Manjarrés IM, Alonso MT, García-Sancho J. Calcium entry-calcium refilling (CECR) coupling between store-operated Ca(2+) entry and sarco/endoplasmic reticulum Ca(2+)-ATPase. Cell Calcium 2011;49:153–61.

[189] Hamilton SL, Serysheva II. Ryanodine receptor structure: progress and challenges. J Biol Chem 2009;284:4047–51.

[190] Kurien BT, Scofield RH. A brief review of other notable protein blotting methods. Methods Mol Biol 2009;536:367–84.

[191] McPherson PS, Campbell KP. Characterization of the major brain form of the ryanodine receptor/Ca^{2+} release channel. J Biol Chem 1993;268:19785–90.

[192] Jones PP, Meng X, Xiao B, Cai S, Bolstad J, Wagenknecht T, Liu Z, Chen SRW. Localization of PKA phosphorylation site, Ser(2030), in the three-dimensional structure of cardiac ryanodine receptor. Biochem J 2008;410:261–70.

[193] Meli AC, Refaat MM, Dura M, Reiken S, Wronska A, Wojciak J, Carroll J, Scheinman MM, Marks AR. A novel ryanodine receptor mutation linked to sudden death increases sensitivity to cytosolic calcium. Circ Res 2011;109:281–90.

[194] Macmillan D, Currie S, McCarron JG. FK506-binding protein (FKBP12) regulates ryanodine receptor-evoked Ca^{2+} release in colonic but not aortic smooth muscle. Cell Calcium 2008;43:539–49.

[195] Zucchi R, Ronca-Testoni S. The sarcoplasmic reticulum Ca^{2+} channel/ryanodine receptor: modulation by endogenous effectors, drugs and disease states. Pharmacol Rev 1997;49:1–51.

[196] Fill M, Copello JA. Ryanodine receptor calcium release channels. Physiol Rev 2002;82:893–922.

[197] Raffetto JD, Ross RL, Khalil RA. Matrix metalloproteinase 2-induced venous dilation via hyperpolarization and activation of K^+ channels: relevance to varicose vein formation. J. Vasc. Surg. 2007;45:373–80.

[198] Kupittayanant S, Luckas MJM, Wray S. Effect of inhibiting the sarcoplasmic reticulum on spontaneous and oxytocin-induced contractions of human myometrium. Bjog 2002;109:289–96.

[199] Taggart MJ, Wray S. Contribution of sarcoplasmic reticular calcium to smooth muscle contractile activation: gestational dependence in isolated rat uterus. J Physiol (Lond) 1998;511 (Pt 1):133–44.

[200] Dabertrand F, Fritz N, Mironneau J, Macrez N, Morel J-L. Role of RYR3 splice variants in calcium signaling in mouse nonpregnant and pregnant myometrium. Am J Physiol, Cell Physiol 2007;293:C848–54.

[201] Westcott EB, Jackson WF. Heterogeneous function of ryanodine receptors, but not IP_3 receptors, in hamster cremaster muscle feed arteries and arterioles. Am J Physiol Heart Circ Physiol 2011;300:H1616–30.

[202] Westcott EB, Goodwin EL, Segal SS, Jackson WF. Function and expression of ryanodine receptors and inositol 1,4,5-trisphosphate receptors in smooth muscle cells of murine feed arteries and arterioles. J Physiol (Lond) 2012;590:1849–69.

[203] Jaggar JH. Intravascular pressure regulates local and global Ca(2+) signaling in cerebral artery smooth muscle cells. Am J Physiol, Cell Physiol 2001;281:C439–48.

[204] Agapitov AV, Haynes WG. Role of endothelin in cardiovascular disease. J Renin Angiotensin Aldosterone Syst 2002;3:1.

[205] Sudjarwo SA, Hori M, Tanaka T, Matsuda Y, Okada T, Karaki H. Subtypes of endothelin ET_A and ET_B receptors mediating venous smooth muscle contraction. Biochem Biophys Res Commun 1994;200:627–33.

[206] Kawanabe Y, Okamoto Y, Hashimoto N, Masaki T. Molecular mechanisms for activation of voltage-independent Ca^{2+} channels by endothelin-1/endothelin-A receptors. J Cardiovasc Pharmacol 2004;44 Suppl 1:S219–23.

[207] Tumelty J, Hinds K, Bankhead P, McGeown NJ, Scholfield CN, Curtis TM, McGeown JG. Endothelin 1 stimulates Ca^{2+}-sparks and oscillations in retinal arteriolar myocytes via IP_3R and RyR-dependent Ca^{2+} release. Invest Ophthalmol Vis Sci 2011;52:3874–9.

[208] Jaffe LF. Fast calcium waves. Cell Calcium 2010;48:102–13.

[209] Jacobsen JCB, Aalkjaer C, Nilsson H, Matchkov VV, Freiberg J, Holstein-Rathlou N-H. A model of smooth muscle cell synchronization in the arterial wall. Am J Physiol Heart Circ Physiol 2007;293:H229–37.

[210] Perez JF, Sanderson MJ. The frequency of calcium oscillations induced by 5-HT, ACH, and KCl determine the contraction of smooth muscle cells of intrapulmonary bronchioles. J Gen Physiol 2005;125:535–53.

[211] Koenigsberger M, Sauser R, Lamboley M, Bény J-L, Meister J-J. Ca^{2+} dynamics in a population of smooth muscle cells: modeling the recruitment and synchronization. Biophys J 2004;87:92–104.

[212] Horowitz LF, Hirdes W, Suh B-C, Hilgemann DW, Mackie K, Hille B. Phospholipase C in living cells: activation, inhibition, Ca^{2+} requirement, and regulation of M current. J Gen Physiol 2005;126:243–62.

[213] Kukkonen JP. A ménage à trois made in heaven: G-protein-coupled receptors, lipids and TRP channels. Cell Calcium 2011;50:9–26.

[214] Antigny F, Jousset H, König S, Frieden M. Thapsigargin activates Ca(2+) entry both by store-dependent, STIM1/Orai1-mediated, and store-independent, TRPC3/PLC/PKC-mediated pathways in human endothelial cells. Cell Calcium 2011;49:115–27.

[215] Wynne BM, Chiao C-W, Webb RC. Vascular Smooth Muscle Cell Signaling Mechanisms for Contraction to Angiotensin II and Endothelin-1. J Am Soc Hypertens 2009;3:84–95.

[216] DURBIN RP, JENKINSON DH. The effect of carbachol on the permeability of depolarized smooth muscle to inorganic ions. J Physiol (Lond) 1961;157:74–89.

[217] Bozler E. Role of calcium in initiation of activity of smooth muscle. Am J Physiol 1969;216:671–4.

[218] Thakali K, Demel SL, Fink GD, Watts SW. Endothelin-1-induced contraction in veins is independent of hydrogen peroxide. Am J Physiol Heart Circ Physiol 2005;289:H1115–22.

[219] Johnson RJ, Galligan JJ, Fink GD. Factors affecting endothelin-induced venous tone in conscious rats. J Cardiovasc Pharmacol 2001;37:187–95.

[220] Zhang XF, Iwamuro Y, Enoki T, Okazawa M, Lee K, Komuro T, Minowa T, Okamoto Y, Hasegawa H, Furutani H, Miwa S, Masaki T. Pharmacological characterization of Ca^{2+} entry channels in endothelin-1-induced contraction of rat aorta using LOE 908 and SK&F 96365. Br J Pharmacol 1999;127:1388–98.

[221] Watano T, Kimura J. Calcium-dependent inhibition of the sodium-calcium exchange current by KB-R7943. The Canadian Journal of Cardiology 1998;14:259–62.

[222] Xu S-Z, Boulay G, Flemming R, Beech DJ. E3-targeted anti-TRPC5 antibody inhibits store-operated calcium entry in freshly isolated pial arterioles. Am J Physiol Heart Circ Physiol 2006;291:H2653–9.

[223] Guibert C, Ducret T, Savineau J-P. Expression and Physiological Roles of TRP Channels in Smooth Muscle Cells. Adv Exp Med Biol 2011;704:687–706.

[224] Goel M, Zuo C-D, Sinkins WG, Schilling WP. TRPC3 channels colocalize with Na^{+}/Ca^{2+} exchanger and Na^{+} pump in axial component of transverse-axial tubular system of rat ventricle. Am J Physiol Heart Circ Physiol 2007;292:H874–83.

[225] Thai TL, Arendshorst WJ. ADP-ribosyl cyclase and ryanodine receptors mediate endothelin ET_A and ET_B receptor-induced renal vasoconstriction in vivo. Am J Physiol Renal Physiol 2008;295:F360–8.

[226] Neylon CB, Richards SM, Larsen MA, Agrotis A, Bobik A. Multiple types of ryanodine receptor/Ca^{2+} release channels are expressed in vascular smooth muscle. Biochem Biophys Res Commun 1995;215:814–21.

[227] Maruyama T, Kanaji T, Nakade S, Kanno T, Mikoshiba K. 2APB, 2-aminoethoxydiphenyl borate, a membrane-penetrable modulator of Ins(1,4,5)P3-induced Ca^{2+} release. J Biochem 1997;122:498–505.

[228] Amberg GC, Earley S, Glapa SA. Local Regulation of Arterial L-Type Calcium Channels by Reactive Oxygen Species. Circ Res 2010.

[229] Jaggar JH, Nelson MT. Differential regulation of Ca(2+) sparks and Ca(2+) waves by UTP in rat cerebral artery smooth muscle cells. Am J Physiol, Cell Physiol 2000;279:C1528–39.

[230] Harper MT, Molkentin JD, Poole AW. Protein kinase C alpha enhances sodium-calcium exchange during store-operated calcium entry in mouse platelets. Cell Calcium 2010;48:333–40.

[231] Hirano K. Current topics in the regulatory mechanism underlying the Ca^{2+} sensitization of the contractile apparatus in vascular smooth muscle. J Pharmacol Sci 2007;104:109–15.

[232] Meves H. Arachidonic acid and ion channels: an update. Br J Pharmacol 2008;155:4–16.

[233] Tsui JC, Shi-Wen X. Endothelin-1 in peripheral arterial disease: A potential role in muscle damage. Pharmacol Res 2011;63:473–6.

[234] Deacon K, Knox AJ. Endothelin-1 (ET-1) increases the expression of remodeling genes in vascular smooth muscle through linked calcium and cAMP pathways: role of a phospholipase A(2)(cPLA(2))/cyclooxygenase-2 (COX-2)/prostacyclin receptor-dependent autocrine loop. Journal of Biological Chemistry 2010;285:25913–27.

[235] Fink G, Li M, Lau Y, Osborn J, Watts S. Chronic activation of endothelin B receptors: new model of experimental hypertension. Hypertension 2007;50:512–8.

[236] Marinissen MJ, Gutkind JS. G-protein-coupled receptors and signaling networks: emerging paradigms. Trends Pharmacol Sci 2001;22:368–76.

[237] Minneman KP. Heterodimerization and surface localization of G protein coupled receptors. Biochem Pharmacol 2007;73:1043–50.

[238] Panetta R, Greenwood MT. Physiological relevance of GPCR oligomerization and its impact on drug discovery. Drug Discov Today 2008;13:1059–66.

[239] Dai X, Galligan JJ. Differential trafficking and desensitization of human ET(A) and ET(B) receptors expressed in HEK 293 cells. Exp Biol Med (Maywood) 2006;231:746–51.

[240] Fukuroda T, Ozaki S, Ihara M, Ishikawa K, Yano M, Miyauchi T, Ishikawa S, Onizuka M, Goto K, Nishikibe M. Necessity of dual blockade of endothelin ET_A and ET_B receptor subtypes for antagonism of endothelin-1-induced contraction in human bronchi. Br J Pharmacol 1996;117:995–9.

[241] Pate M, Chester A, Brown T, Roach A, YACOUB M. Atypical antagonism observed with BQ-123 in human saphenous vein. J Cardiovasc Pharmacol 1998;31 Suppl 1:S172–4.

[242] Malik R, Vlasicova K, Sedo A. Functional cross-talk of Ca^{2+}-mobilizing endothelin receptors in C6 glioma cells. Physiol Res 2002;51:73–8.

[243] Sexton P, Morfis M, Tilakaratne N, Hay D, Udawela M, Christopoulos G, Christopoulos A. Complexing receptor pharmacology: modulation of family B G protein-coupled receptor function by RAMPs. Ann N Y Acad Sci 2006;1070:90–104.

[244] Evans NJ, Walker JW. Endothelin receptor dimers evaluated by FRET, ligand binding, and calcium mobilization. Biophys J 2008;95:483–92.

[245] Evans NJ, Walker JW. Sustained Ca^{2+} signaling and delayed internalization associated with endothelin receptor heterodimers linked through a PDZ finger. Can J Physiol Pharmacol 2008;86:526–35.

[246] Miao L, Dai Y, Zhang J. Mechanism of RhoA/Rho kinase activation in endothelin-1- induced contraction in rabbit basilar artery. Am J Physiol Heart Circ Physiol 2002;283:H983–9.

[247] Cho Y-E, Ahn D-S, Morgan KG, Lee Y-H. Enhanced contractility and myosin phosphorylation induced by Ca(2+)-independent MLCK activity in hypertensive rats. Cardiovasc Res 2011;91:162–70.

[248] Manyari DE, Rose S, Tyberg JV, Sheldon RS. Abnormal reflex venous function in patients with neuromediated syncope. J. Am. Coll. Cardiol. 1996;27:1730–5.

[249] Gross BA, Du R. Hemorrhage from arteriovenous malformations during pregnancy. Neurosurgery 2012;71:349–56.

[250] Bonanno FG. Physiopathology of shock. J Emerg Trauma Shock 2011;4:222–32.

[251] Wilson TE, Tollund C, Yoshiga CC, Dawson EA, Nissen P, Secher NH, Crandall CG. Effects of heat and cold stress on central vascular pressure relationships during orthostasis in humans. J Physiol (Lond) 2007;585:279–85.

[252] Braam B, Cupples WA, Joles JA, Gaillard C. Systemic arterial and venous determinants of renal hemodynamics in congestive heart failure. Heart Fail Rev 2012;17:161–75.

[253] Frumkin LR. The pharmacological treatment of pulmonary arterial hypertension. Pharmacol Rev 2012;64:583–620.

[254] Iglarz M, Binkert C, Morrison K, Fischli W, Gatfield J, Treiber A, Weller T, Bolli MH, Boss C, Buchmann S, Capeleto B, Hess P, Qiu C, Clozel M. Pharmacology of macitentan, an orally active tissue-targeting dual endothelin receptor antagonist. J Pharmacol Exp Ther 2008;327:736–45.

[255] Magee WP, Deshmukh G, Deninno MP, Sutt JC, Chapman JG, Tracey WR. Differing cardioprotective efficacy of the Na^{+}/Ca^{2+} exchanger inhibitors SEA0400 and KB-R7943. Am J Physiol Heart Circ Physiol 2003;284:H903–10.

[256] Ander BP, Hurtado C, Raposo CS, Maddaford TG, Deniset JF, Hryshko LV, Pierce GN, Lukas A. Differential sensitivities of the NCX1.1 and NCX1.3 isoforms of the Na^{+}-Ca^{2+} exchanger to alpha-linolenic acid. Cardiovasc Res 2007;73:395–403.

[257] Nielsen-Kudsk F, Poulsen B, Ryom C, Nielsen-Kudsk JE. A strain-gauge myograph for isometric measurements of tension in isolated small blood vessels and other muscle preparations. J Pharmacol Methods 1986;16:215–25.

[258] Schiffrin EL. State-of-the-Art lecture. Role of endothelin-1 in hypertension. Hypertension 1999;34:876–81.

[259] Böhm F, Pernow J. The importance of endothelin-1 for vascular dysfunction in cardiovascular disease. Cardiovasc Res 2007;76:8–18.

[260] Fukuroda T, Fujikawa T, Ozaki S, Ishikawa K, Yano M, Nishikibe M. Clearance of circulating endothelin-1 by ET_B receptors in rats. Biochem Biophys Res Commun 1994;199:1461–5.

[261] Zellers TM, McCormick J, Wu Y. Interaction among ET-1, endothelium-derived nitric oxide, and prostacyclin in pulmonary arteries and veins. Am J Physiol 1994;267:H139–47.

[262] White DG, Cannon TR, Garratt H, Mundin JW, Sumner MJ, Watts IS. Endothelin ET_A and ET_B receptors mediate vascular smooth-muscle contraction. J Cardiovasc Pharmacol 1993;22 Suppl 8:S144–8.

[263] Caló G, Gratton JP, Télémaque S, D'Orléans-Juste P, Regoli D. Pharmacology of endothelins: vascular preparations for studying ET_A and ET_B receptors. Mol Cell Biochem 1996;154:31–7.

[264] Bax WA, Aghai Z, van Tricht CL, Wassenaar C, Saxena PR. Different endothelin receptors involved in endothelin-1- and sarafotoxin S6B-induced contractions of the human isolated coronary artery. Br J Pharmacol 1994;113:1471–9.

[265] Montagnani M, Vulpis V, Nazzaro P, Potenza MA, Rinaldi R, Nacci C, De Salvia MA, Siro Brigiani G, Pirrelli A, Mitolo-Chieppa D. Endothelin-1-receptor-

mediated responses in resistance vessels of young and adult spontaneously hypertensive rats. J Hypertens 2000;18:893–900.

[266] Teerlink JR, Breu V, Sprecher U, Clozel M, Clozel JP. Potent vasoconstriction mediated by endothelin ET_B receptors in canine coronary arteries. Circ Res 1994;74:105–14.

[267] Warner TD, Allcock GH, Corder R, Vane JR. Use of the endothelin antagonists BQ-123 and PD 142893 to reveal three endothelin receptors mediating smooth muscle contraction and the release of EDRF. Br J Pharmacol 1993;110:777–82.

[268] D'Orléans-Juste P, Claing A, Warner TD, Yano M, Télémaque S. Characterization of receptors for endothelins in the perfused arterial and venous mesenteric vasculatures of the rat. Br J Pharmacol 1993;110:687–92.

[269] Eguchi D, Nishimura J, Kobayashi S, Komori K, Sugimachi K, Kanaide H. Down-regulation of endothelin B receptors in autogenous saphenous veins grafted into the arterial circulation. Cardiovasc Res 1997;35:360–7.

[270] Hocher B, Dembowski C, Slowinski T, Friese ST, Schwarz A, Siren AL, Neumayer HH, Thöne-Reineke C, Bauer C, Nafz B, Ehrenreich H. Impaired sodium excretion, decreased glomerular filtration rate and elevated blood pressure in endothelin receptor type B deficient rats. J Mol Med 2001;78:633–41.

[271] Dusserre N, L'Heureux N, Bell KS, Stevens HY, Yeh J, Otte LA, Loufrani L, Frangos JA. PECAM-1 interacts with nitric oxide synthase in human endothelial cells: implication for flow-induced nitric oxide synthase activation. Arterioscler Thromb Vasc Biol 2004;24:1796–802.

[272] Shichiri M, Marumo F, Hirata Y. Endothelin-B receptor-mediated suppression of endothelial apoptosis. J Cardiovasc Pharmacol 1998;31 Suppl 1:S138–41.